THE STRUCTURAL BEHAVIOUR OF CASTELLATED ROLLED STEEL BEAMS.

William McLaren Jenkins B.Sc.

A thesis submitted to the University of Glasgow
for the degree of
Doctor of Philosophy.

The composition of this thesis and the research which is described herein were carried out by myself.

The theoretical treatment, except where specifically stated, is original.

24th September, 1957.

PREFACE

The work which forms the subject of this thesis extended over a period of four years between the autumns of 1953 and 1957. The problem of the behaviour of the castellated (or "expanded") beam came to the author's attention whilst working as a student civil engineer with the Appleby-Frodingham Steel Company between the years 1944 and 1949 but it was not until four years later that an opportunity arose to carry out some research on the problem.

After graduating B.Sc., in civil engineering in the University of Glasgow in 1953 the author was appointed Assistant in Civil Engineering in that University and registered in October 1953 as a research student of the University. The problem selected for research was the one forming the subject of this thesis.

The work was carried out in Glasgow until September 1955 when the author was appointed Lecturer in Civil Engineering in the University of London, King's College. The Engineering Faculty in Glasgow then sanctioned the continuation of the work in London.

The author is indebted to his supervisor Professor W.T. Marshall of the Regius Chair of Civil Engineering in the University of Glasgow for his helpful criticism and encouragement throughout the work. The author is also indebted to the United Steel Structural Company Limited, of Scunthorpe, Lincs., who supplied all the beams for testing and made available some unpublished test results. He also wishes to express his gratitude to Dr. J.E. Gibson formerly Lecturer in Civil Engineering at Glasgow now Senior Lecturer in Civil Engineering in the University of Manchester for his help during the first two years of the research.

The help of the technical staffs of the engineering departments of the University of Glasgow and of King's College London is also gratefully acknowledged.

Finally the author is indebted to the Faculties of Engineering at Glasgow and King's College for making available laboratory space and equipment for carrying out the work.

King's College,
London.

September 1957.

CONTENTS

CHAPTER 1

Method of manufacture of the beams.

Statement of the problem.

Existing design methods.

Proposed investigations.

Previous work.

When a rolled steel joist is used as a beam there is a certain span, for given loading conditions, at which the bending stresses in the flanges become critical. For shorter spans than the critical the criterion for design is based on the shearing resistance of the web. At and above the critical span bending stresses and the stiffness of the section are the important factors and the maximum resistance to shear of the web is no longer fully utilised.

A certain economy could therefore be achieved by reducing the amount of material in the web by cutting holes and so reducing the dead weight of the member. Such a system, however, would lead to wastage of the material cut out, and moreover, the saving in dead weight of the member would be small due to the thinness of the web.

An alternative means of achieving some economy of web material would be to increase the depth of the beam and hence its stiffness, without changing its weight and thereby producing no wastage Such a system has been developed and given various names such as " castellated beams", "expanded beams" or "open-web beams". The term "expanded beam" is more common in the U.S.A. whereas in this country the term "castellated beam" is generally adopted.

The idea of increasing the stiffness of a beam by expansion is not new. It is claimed (1) to have been first used about 1910 by H.E. Horton of the Chicago Bridge and Ironworks. The use of such beams in this country appears to have been originated by G.M. Boyd in 1938 and then developed by the Appleby-Frodingham Steel Company under British patent (2).

Short descriptive notes on the method appeared in"the Engineer" in September 1949 (3) and in "Engineering" in October 1949 (4).

Method of manufacture of the beams.

In making a castellated beam the original rolled steel joist is cut along the web by an oxy-acetylene cutting machine using a template. The cutting profile is shown by the dotted line in fig. 1.1 (a). To prevent undue distortion a joist is clamped to either flange of the beam being cut and a small distance, usually about 3", is left uncut at intervals along the beam. These portions are then cut manually to allow the two pieces to be separated, as shown in fig. 1.1 (b). One half of the beam is then moved lengthwise relative to the other, or turned end for end, until the crests of the undulations meet. The junctions of the two halves of the beam are then deep penetration welded and the resulting beam is shown in fig. 1.1 (c).

A certain amount of waste material occurs at the ends of the beam due to the relative displacement of the two parts but this will be small in long beams.

Fig. 1.2 shows the final geometry of the castellated beam and it will be seen that the process has increased the depth of the beam by 50%. A row of hexagonal holes is left in the web but the final overall weight per unit length of the beam is unchanged. The chosen profile allows a radius at the top and bottom corners of the hexagon but this is at the expense of the material at the centre of the web. This sharp corner is normally filled with weld metal during the welding process.

The geometry of the expanded beams as used in the U.S.A. (1) is

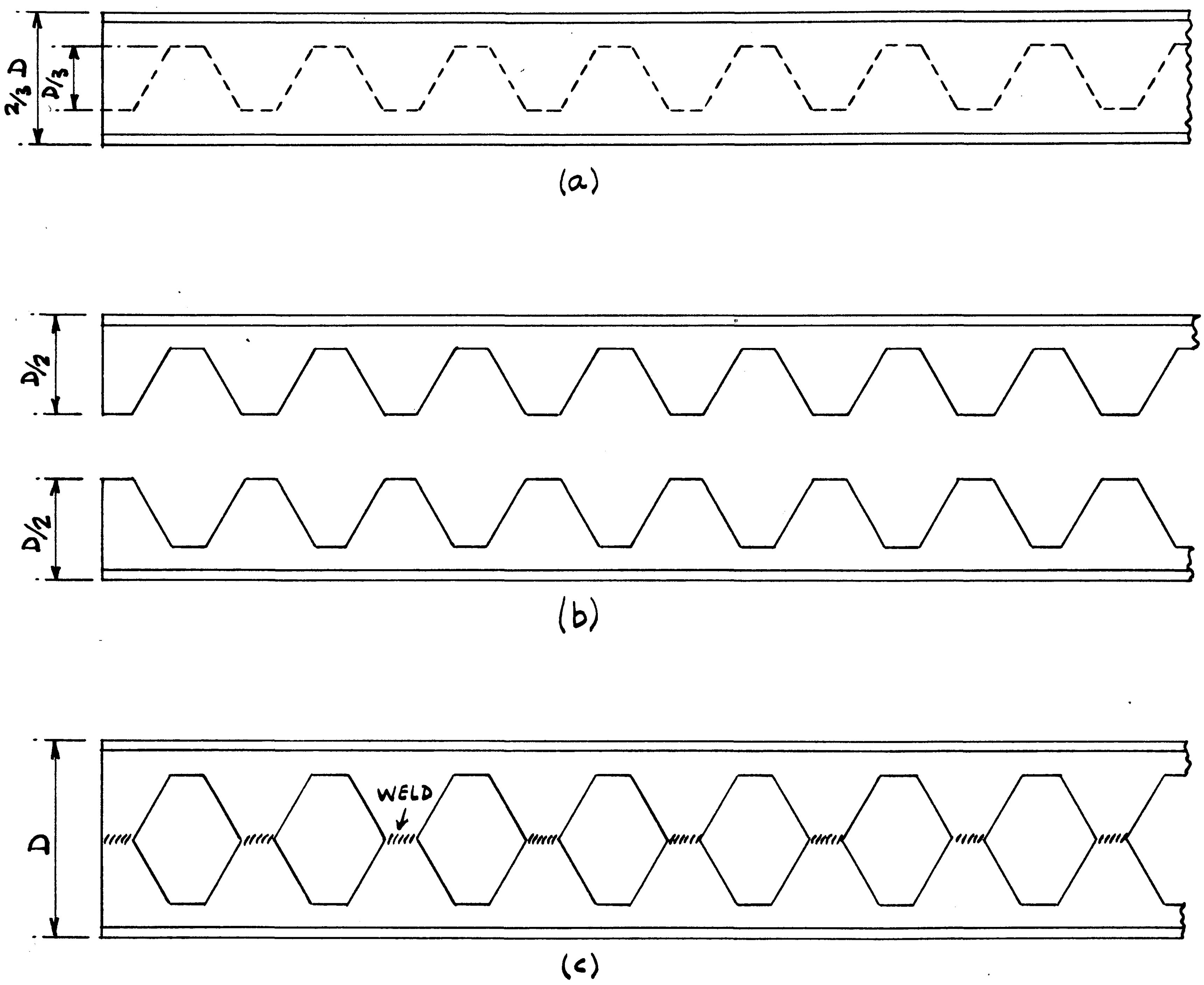

FIG. 1. 1.

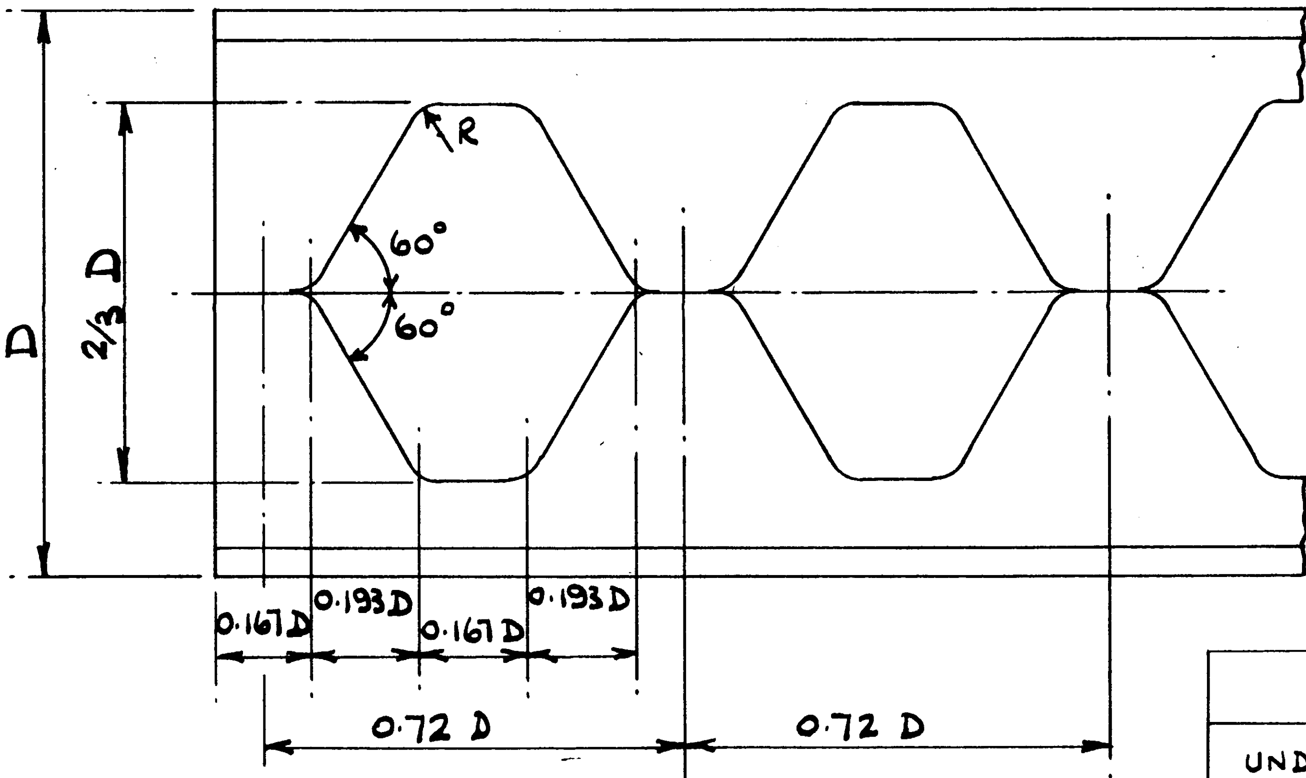

D	R
UNDER 12"	3/8"
12" TO UNDER 18"	1/2"
18" AND OVER	1"

FIG. 1.2.

somewhat different. The angle of slope of the cut is 45° to the centre-line of the beam as against 60° in this country. Many variations are possible in choosing the geometry of the resulting beam but only the one shown in fig. 1.2 as used in this country will be considered in this work although some reference will be made to the problem of the most economical outline in the discussion in chapter 6.

The increase in depth of section of 50% increases the second moment of area of the cross-section by approximately 135% (2) and the stiffness is increased accordingly. Thus it is clear that the main structural advantage is to be found with light loads on long spans where the stiffness of the section is the governing factor and not the shearing resistance of the web.

Statement of the problem.

In relation to the use of castellated or expanded beams some of the questions that naturally arise are,

1) What are the deflection characteristics of the castellated beam?
2) How is the flange stress distribution affected by castellation?
3) What will be the magnitude of the stresses occuring in the web?
4) What will be the buckling value of the web under concentrated loads or reactions?

1) is important for long spans where deflection is the design criterion; 2) and 3) are relevant to intermediate spans and 3) and 4) are of importance for short spans.

The use of the beams necessitates some attempt at a design procedure which answers some, if not all, of the above queries. Moreover any proposed analytical approach would be expected to have support from experimental evidence.

At the outset of the work the author could find no report of theoretical or experimental investigations into the behaviour of the beams apart from some unpublished test data communicated to him by the Appleby-Frodingham Steel Co. There seemed a clear case therefore of the need for a fairly thorough investigation into the behaviour of the beams in order that their design could be given a rational basis and the above mentioned questions given answers substantiated by experimental work.

Existing design method.

The present basis of design is given by the Appleby-Frodingham Steel Co., and the United Steel Structural Co., in their brochure (2) and handbook (5) in the form of safe load tables and graphs. A typical safe load diagram is shown in fig. 1.3. The safe loads are quoted as uniformly distributed on simply-supported spans with the compression flange laterally supported. This eliminates any considerations of lateral or torsional instability and the design is then covered by three criteria depending on the span required.

Referring to fig. 1.3 curve BD represents the safe distributed loads which can be carried by the beam in question without violating the maximum deflection of 1/325 span specified by BS 449 (1948) clause 34. On reducing the span when point B is reached the maximum extreme fibre stress of 10 tons/sq.in. in bending becomes critical and curve AB represents safe loads based on this criterion. The maximum value of load carried is taken to be controlled by the buckling value of the web at a support. The neck width of the castellation is constant for each beam and equal to D/6 where D is the

FIG. 1.3.

TYPICAL SAFE LOAD DIAGRAM.
LOADS UNIFORMLY DISTRIBUTED
COMPRESSION FLANGE LATERALLY
SUPPORTED.

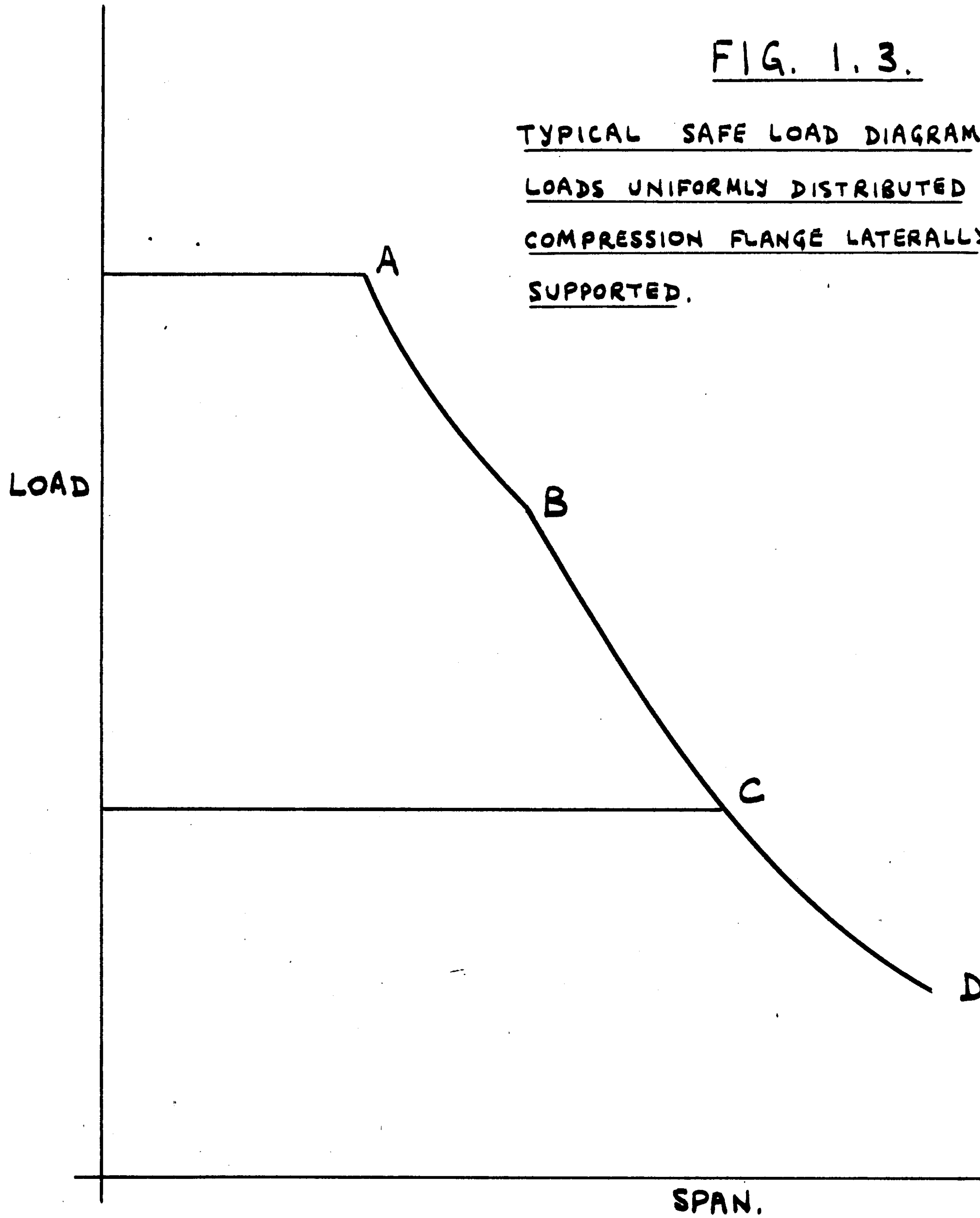

overall depth of the finished section. The safe value of reaction is obtained from BS 449 Cl. 47a using a slenderness ratio of $\frac{d\sqrt{3}}{t}$ where, d = the clear depth of the web and t = the web thickness, as defined in the specification, and computing the maximum safe concentrated load or reaction from,

$$W = F_a.t.l \qquad \text{.............................} (1.1)$$

where, W = max. safe reaction,

F_a = axial stress for a strut of slenderness ratio $\frac{d\sqrt{3}}{t}$ from table 7 of BS 449.

t = web thickness, and,

l = D/6.

For a beam with intact web l would be equal to the length of the stiff bearing plus D/2 in accordance with BS 449. In other words the axial stress F_a for a strut of slenderness ratio $\frac{d\sqrt{3}}{t}$ is applied to a member of cross-sectional area equal to that of the neck of the castellation to determine the maximum safe value of reaction. The safe load corresponding to the value of reaction so found is indicated by point C on fig. 1.3.

The maximum permissible load may be increased by "filling-in" the end castellation. This process is adopted when it is required to carry heavier loads than those given by point C. The end holes of the beam are filled by welding in a plate cut to the shape of the hole. The maximum safe reaction in this case is obtained in a similar way to that used for normal rolled sections. A stiff bearing length of 1" is adopted for beams over $13\frac{1}{2}$" x 4" x 21 lb. and $\frac{1}{2}$" for other beams. Point A on fig. 1.3 corresponds to the lesser of the web buckling and web bearing loads. In the latter case a permissible bearing stress of 12 tons/sq.in. is used in accordance with clause 21 of BS 449.

In this country the practice of filling in the end castellation seems to be preferred to the use of stiffeners whereas Altfillisch, Cooke and Toprac (1) recommend the use of stiffeners and the beams they tested had orthodox stiffeners at the supports and in some cases at the loads points as well.

Proposed investigations.

It is clear that the existing design methods, whilst given some basis from BS 449, are inadequate in a number of respects. The calculations of deflections based on the second moment of area of the minimum cross-section take account of simple bending only and neglect the shearing deformations across the panels and the bending of the web members themselves. These effects will presumably be small for long spans but some attempt should be made to take account of them and establish the lower limit of span/depth ratio at which they can be neglected if at all.

The flange stress criterion (curve AB of fig. 1.3) is also based on simple beam theory and it may well be that higher stresses occur along the boundaries of the web members. Moreover the flange stresses may be underestimated to a considerable extent by neglecting the secondary bending of the flanges over the holes and it would seem desirable to obtain some actual distributions of flange stress in order that this effect may be observed.

The use of the slenderness ratio of $\frac{d\sqrt{3}}{t}$ for the end web member of a castellated beam is distinctly questionable. This ratio is intended for rolled beams and is based on a strut assumed to have an effective length equal to one-half the depth of the web and a thickness equal to the web thickness (6). The action of the end web member of a castellated beam will clearly be different from that of the web of a normal rolled beam. In addition to an axial thrust coming from the bearing the member will be subjected to end moments in the plane of the web due to the rigidity of its connections with the flanges. The behaviour of this part of the beam will be studied in some detail. The proposed investigations can be summarized as follows;

a) Experimental determination of stress distributions in flanges and web of simply-supported beams. It was proposed to use vibrating wire strain gauges for this purpose in order that a more continuous set of strain readings could be taken. This will be of importance in regions of high strain gradient and demountable gauges would have the advantage of enabling a more complete exploration of the stress distribution to be made in these regions.

This part of the work was to be accompanied by a photo-elastic investigation designed to give a complete picture of the stress distribution throughout the beams. The photo-elastic work was carried out and gave precisely the same kind of distribution as that obtained from the steel specimens and it is not intended to include a report of the work in this thesis. No new points of interest were brought to light and in the interests of space it was decided to include the test results from the steel beams in some detail whilst omitting all the photo-elastic work.

b) Experimental determination of the deflection characteristics of the beams. These experiments were to be carried out along with those under a) using standard dial gauges in the usual way.

c) The effect of stiffeners. It was decided to investigate the effect of stiffeners in a limited way by testing two beams one with stiffeners and one without, the beams being identical in all other respects, and comparing the stresses occuring in the two beams at the same load. The two tests would be continued to ultimate collapse and the collapse loads compared.

d) Web stability. This investigation was to be conducted mainly on short lengths of beams having the compression flanges supported laterally to prevent torsional instability and to induce the web buckling mode of failure. It was intended to explore the stress distribution in the end web member and eventually increase the load until collapse occured.

All the investigations were to be accompanied by theoretical considerations and some attempt made to predict the behaviour of the beams in theory.

The subject of web stability is dealt with in isolation in chapter 5. All other experimental work is described in chapter 3 and the results, both theoretical and experimental presented in chapter 4. Theoretical work on methods of analysis for stress distribution and deflection is confined to chapter 2.

Previous work.

At the outset of the research very little work could be found which had any real bearing on the problem. The case of the single circular hole in a rectangular beam subjected to pure bending had been considered by Tuzi (7) using a stress function analysis to predict the stresses on the boundary of the hole. As a subsidiary part of the present research, and following along similar lines to those adopted by Tuzi the author considered the same problem for a beam subjected to bending with shear, again using a stress function analysis, and published the results in The Structural Engineer in December 1956 (8).

Previously the problem of the beam containing a row of circular holes subjected to bending with shear had been tackled by R.C.J. Howland (9) using biharmonic analysis. S.R. Heller (10) had also considered the problem of a single hole in a beam subjected to non-uniform bending. The case he selected for analysis was the cantilever of rectangular cross-section subjected to a concentrated load at the free end and containing a single hole of ovaloid form.

The first paper discovered to have any real bearing on the subject was that published by Miss Letitia Chitty (11) dealing with the problem of the cantilever composed of parallel beams inter-connected by cross members. In this paper a solution is proposed which replaces the discrete cross members by a hypothetical continuous web medium. By this means it is possible to write down expressions for the curvature, slope and deflection of the beams in continuous form. This latter work was followed in 1952 by Professor Pippard's book "Studies in Elastic Structures" (12) of which chapter 8 is devoted to the analysis of open-panel structures Professor Pippard's methods follow closely on Miss Chitty's but he develops the analysis to cover a variety of loading and support conditions and applies the method to the problems of wind loads on building frames and the determination of the critical load for a battened column.

On studying these latter works it became clear that in modified and extended form they might give a suitable solution to the present problems, in particular that of the deflections of castellated beams. In chapter 2 a solution will be proposed on these lines when more detailed mention will be made of the method.

M. Smolira in his book "Analysis of Structures" 1955 (13) gives an example of what is virtually a slope-deflection analysis of a castellated beam. He deals with an 8 - panel beam symmetrically loaded and treats it as a vierendeel girder. Twelve equations of equilibrium are set out and solved in terms of the bending moments acting on the ends of the flanges in each panel of the beam. It is seen that points of inflexion occur very nearly at the mid-points of the chord members of each panel. If it is assumed that points of inflexion actually occur at the mid-points of the chord members then the girder can be analysed by statical principles alone. If this method is applied to the example cited by Smolira (fig. 1.4) then the resulting end bending moments on the chords are as set out in table 1.1 along with those obtained by Smolira.

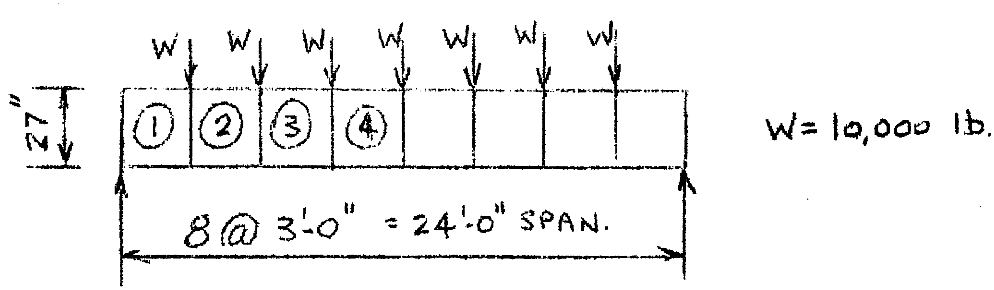

FIG. 1.4.

TABLE 1.1.

End moments on chord members (lb.ft)

Panel		Smolira	Simplified statical analysis assuming points of inflexion at mid-points of chords.
1	left	27,150	26,200
	right	25,350	"
2	left	18,380	18,700
	right	19,120	"
3	left	9,890	11,300
	right	12,610	"
4	left	3,360	3,750
	right	4,140	"

It is clear that the differences are not serious but the amount of work involved in the simplified solution is very much less than that needed to produce Smolira's figures. This kind of analysis will be mentioned in more detail in chapter 2.

The work of Altfillisch, Cooke and Toprac at the University of Texas (1) came to the author's attention when most of the theoretical work for this thesis was completed. The paper appeared in February 1957 and describes the testing of three "expanded" beams all originally $9\frac{7}{8}$" deep and measuring after expansion 13", $14\frac{3}{4}$" and $16\frac{1}{4}$" deep. The different depths were got by varying the cutting profile although a slope of 45° to the longitudinal axis was used throughout. All three beams were 17' - 0" long and were supplied with stiffeners at the supports. One specimen was fitted with full depth stiffeners at the load points, one with short stiffeners just under the compression flange, and the third specimen had no stiffeners at the load points.

All tests were carried out under symmetrical two-point loading and the beams were laterally supported at intervals along the compression flange by means of wire braces and turnbuckles.

The specimens were whitewashed with slaked lime to aid the detection of yield.

The stress analysis proposed by Altfillisch, Cooke and Toprac follows similar lines to that which will be described in chapter 2. The normal flexural stresses are considered uniform across the tee sections of the panels and the vertical shear is taken to be resisted equally by the top and bottom tee sections for any panel. Further, secondary bending stresses are taken to be induced by these shears acting at assumed points of inflexion at the centres of the chord members.

Considerations of buckling and web bearing stresses follow identical lines to those used in the existing design method already outlined and the same criticisms apply.

The evaluation of deflections is done in stages;

a) Obtain deflection as if beam were solid throughout, y_s

b) Increase y_s to take account of increased stresses existing at the tee sections as follows,

$$y = y_s \times \left(\frac{f + f_n}{2\,f} \right)$$

where, f = max. fibre stress at solid section,

f_n = max. fibre stress at the throat section.

c) Add the shearing deflection across each panel. This is done taking into account the varying cross section of the chord members by a summation process using the Area-Moment theorems.

An example of deflection calculations is given. The process is fairly lengthy but gives good agreement with experimental results.

A comparison of the actual and predicted loads to produce first signs of yield in the beams does not show good agreement. The use of a slaked lime coating to aid the observation of yield lines would seem to give qualitative rather than quantitative information.

As a result of the different geometry of finished beam chosen by the authors the holes are more elongated than those in the beams tested in this present investigation. The result of this is to increase the secondary bending stresses in the tee sections but make the buckling of the web members less critical. In fact web buckling was barely studied by the authors as stiffeners were introduced at critical sections.

Further reference will be made to the effect of varying the geometry of the castellated beam in chapter 6.

CHAPTER 2

Methods of analysis :

1) Simple beam theory.

2) Vierendeel girder theory.

3) Continuous web medium theory.

The type of analysis carried out by the author and Dr. J.E. Gibson(8) on the stress distribution in a beam with a single circular hole using stress functions is not suitable for application to castellated beams. The use of stress functions for single internal contours is relatively straight forward but their application to a multi-connected region is extremely complicated particularly when the internal contours are rectilineal. It would appear that a simpler, more approximate, treatment would be more suitable in this case.

The structural behaviour of the beams will clearly lie somewhere between that of a simple beam with intact web and that of an open panel rigid frame. Just where the behaviour will lie between these two extremes will depend primarily on the span/depth ratio r since this will automatically govern the number of panels in the beam. It is to be expected that as r increases the behaviour will tend to that of the simple beam without holes, and as r decreases the beam will tend to behave more as a rigid frame. This effect is borne out in the results which will be presented later.

In seeking an analytical solution for the stresses and deflections occuring in the beams the author considered a number of methods, adapting them where necessary to the problem in hand. These methods will now be given, the less successful ones will be only briefly outlined.

1) Simple beam theory with relaxation.

In this method the critical stresses are taken to be the bending stresses given by simple bending theory and the deflections found by integration of the M/EI diagram along the beam by a simple summation method or by relaxation. The deflections are taken to be caused by flexure alone and the M/EI diagram taken to be composed of straight lines between the centres of the verticals and the centres of the holes, sections AA and BB of fig. 2.1.

Using a simple one-dimensional relaxation method as outlined by Allen (14) the deflected form of the beam corresponding to a given bending moment diagram can be obtained. The deflections produced by this method lie between those computed by simple bending theory for beams of uniform sections AA and BB of fig. 2.1.
In fact the experimental results have shown that the deflections are always greater than those computed by simple bending theory based on the minimum cross-section of the beam BB.

The method does not take into account the shearing deformations across the panels and it would seem that it will be necessary to take account of these if a more accurate prediction of deflection is to be made.

2) Treatment as a vierendeel girder.

Any of the so called "exact" methods of analysis of vierendeel girders(13), (15) may be applied to castellated beams but the work is laborious and it is difficult to see how a general solution could be obtained applicable to all beams and loading arrangements.
In the majority of cases where castellated beams are used the number of panels, and hence the number of redundancies to be evaluated, is large and the amount of work involved in producing a solution would be correspondingly great.

Figs. 2.1 to 2.3

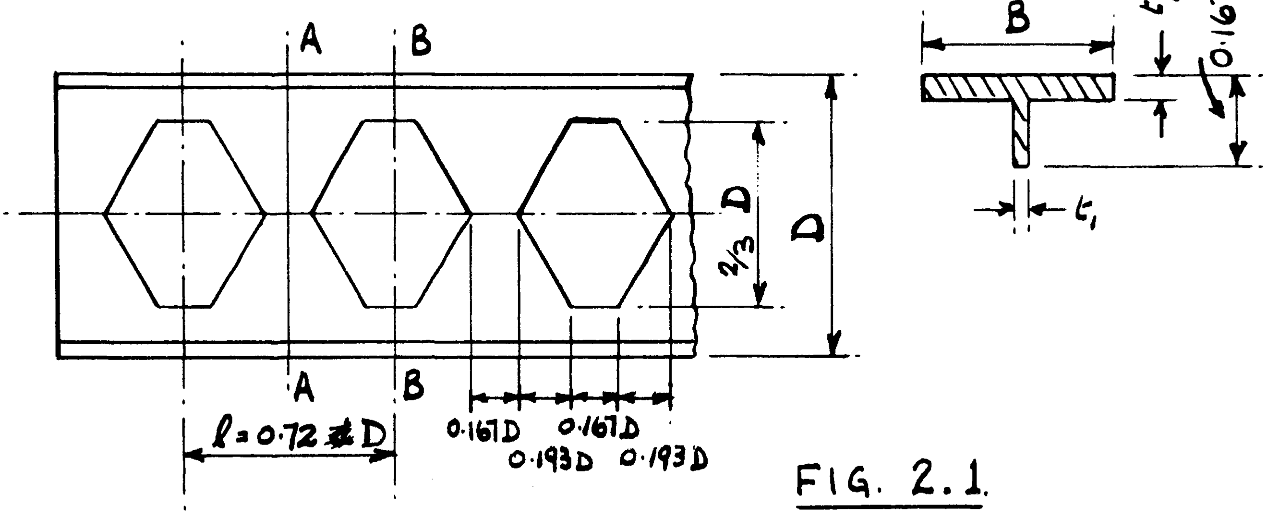

FIG. 2.1.

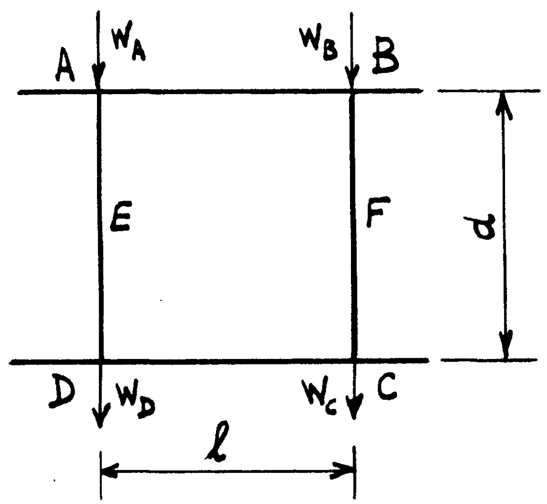

FIG. 2.2.

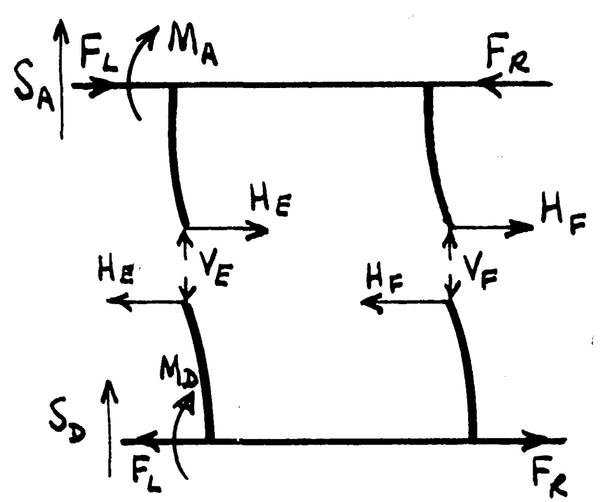

FIG. 2.3.

Moreover, the usual methods for vierendeel girders take no account of deformations due to axial forces and with large numbers of panels this effect becomes marked.

In the case of a symmetrical girder with the loads applied at the nodes only, the bending moment and shearing force distributions are alike in the upper and lower chords and points of inflexion occur at the mid-heights of the vertical members. If it is assumed that this is so in the case of the castellated beam, whatever the loading arrangement, then a simple solution can be obtained along the lines proposed by Salmon (16). Consider a typical panel ABCD fig. 2.2. AB, BC, etc., representing the centre lines of the members forming the panel. The panel spacing is ℓ and the panel depth (between centroids) d. It is assumed that points of inflexion occur at E and F the mid-points of the verticals AD and BC. The loads are taken to be concentrated at the panel points A,B,C and D as shown in fig. 2.2. The force actions imposed on the panel by the adjacent portions of the beam are shown in fig. 2.3. Salmon's method is to equate the distance EF in terms of H_E and H_F for the upper and lower halves of the panel and obtain a relationship between H_E and H_F. This relationship is applied successively to each panel until the value of H for each vertical is found. Other forces and moments then follow from statical considerations. Bending deformations only are considered and the result can be expressed as follows,

$$(H_{n+1} - H_n)\frac{d^2}{I_W} = \frac{6\ell}{I_c}\left(d\sum_{1}^{n} H - M_{n+1/2}\right) \quad \ldots\ldots\ldots\ldots\ldots(2.1)$$

ℓ

where, H_n = horizontal force at mid-point of nth vertical from one end of the beam.

H_{n+1} = Ditto of (n+1)th vertical,

I_W = 2nd moment of area of web members

I_C = Ditto of chord members

$M_{n+\frac{1}{2}}$ = External applied bending moment midway between the nth and the (n + 1)th verticals.

In the foregoing it is assumed that the members are of uniform section and some correction must now be introduced to make allowance for the varying cross-section of the verticals. Referring to fig. 2.4. consider the upper half of a typical web member and let I_W represent the 2nd moment of area of the equivalent uniform section. I_W must be so chosen to make the horizontal deflection at O due to H the same for the tapered and uniform sections. The geometry of the web member is such that the width of the member at x = 0 is D/6 where D represents the overall depth of the section. It will be convenient to take this dimension as d/6 where d is the distance between the centroids of the chords. The loss in accuracy will not be serious being of the order of $t_2/3$ where t_2 is the flange thickness.

The 2nd moment of area of the tapered section is,

$$I = \frac{t_1}{12}\left(\frac{d}{6} + \frac{2x}{\sqrt{3}}\right)^3 \qquad \ldots\ldots\ldots\ldots\ldots\ldots(2.2)$$

where t_1 = web thickness.

The horizontal deflection at x = 0 due to H is,

$$\Delta_H = \frac{1}{E}\int_0^{d/2} \frac{Mx}{I}\,dx \qquad \ldots\ldots\ldots\ldots\ldots\ldots(2.3)$$

Putting d/6 = a and $d/\sqrt{3}$ = b and M = Hx, (2.3) becomes,

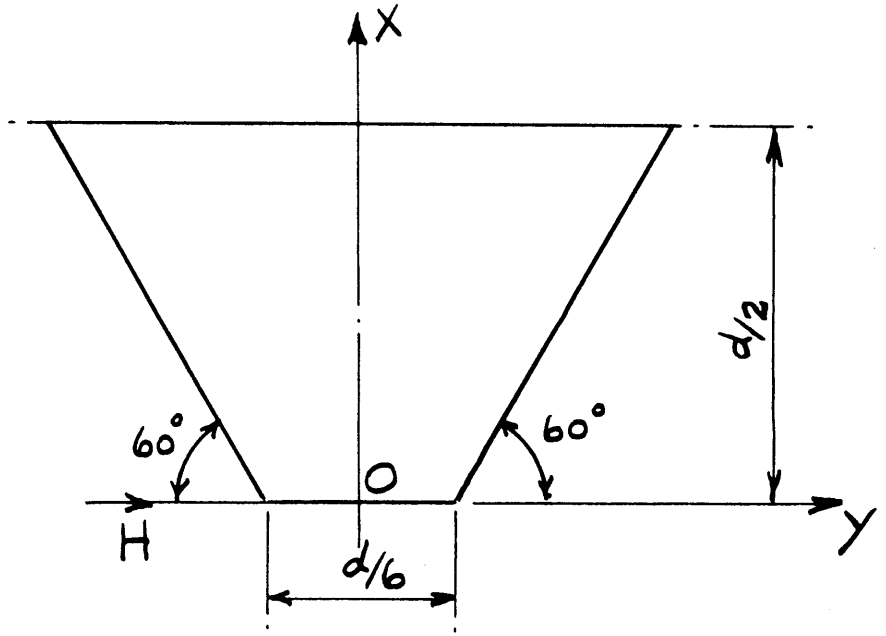

FIG. 2.4.

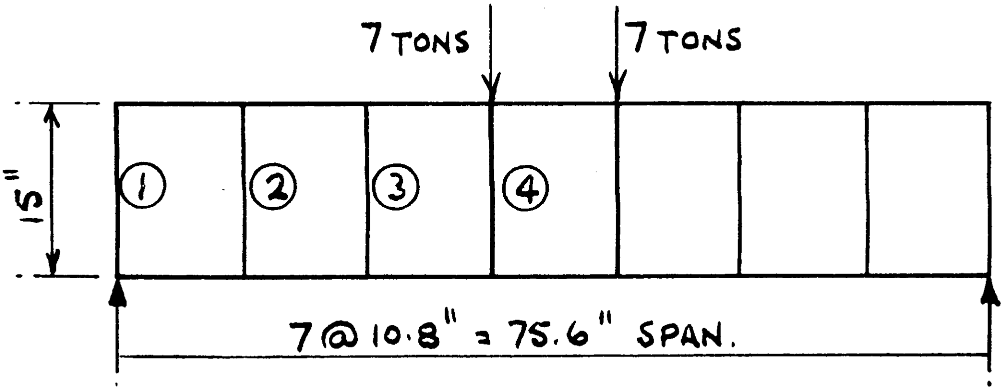

FIG. 2.5.

$$\Delta_H = \frac{12\,H}{t_1 E}\int_0^{d/2} \frac{x^2\,dx}{\left(a + \frac{2bx}{d}\right)^3} \qquad \text{.............(2.4)}$$

Integrating (2.4) using partial fractions the following expression results,

$$\Delta_H = \frac{3\,H\,d^3}{2E t_1 b^2}\left[\frac{1}{b}\log_e\left(\frac{a+b}{a}\right) - \frac{2a+3b}{2(a+b)^2}\right] \qquad \text{........(2.5)}$$

Hence the equivalent 2nd moment of area I_W of the tapered section is given by,

$$\frac{3EI_W\Delta_H}{(d/2)^2} = \frac{Hd}{2}$$

whence, $$\frac{1}{I_W} = \frac{36}{t_1 b^2}\left[\frac{1}{b}\log_e\left(\frac{a+b}{a}\right) - \frac{2a+3b}{2(a+b)^2}\right]$$

This latter expression may be simplified if it is re-written in terms of d observing that $a = d/6$ and $b = d/\sqrt{3}$, the result is,

$$I_W = \frac{t_1 d^3}{79} \qquad \text{...............(2.6)}$$

The 2nd moment of area of the chord I_c at section BB (fig.2.1) can be obtained by assuming that the cross-section is a regular T as shown is fig. 2.1. It is found in most cases that the centroid of this tee section is located, very nearly, at a depth below the outer face of the flange equal to the flange thickness. With this approximation the 2nd moment of area of the chord is,

$$I_c = \frac{B t_2^3}{3} + \frac{t_1}{3}\left(0.167\,D - t_2\right)^3 \qquad \text{...............(2.7)}$$

and the cross-sectional area of the chord is,

$$A = B t_2 + t_1\left(0.167\,D - t_2\right) \qquad \text{..............(2.8)}$$

Equations (2.1), (2.6) and (2.7) enable the horizontal forces acting at the mid-points of the vertical members to be computed. The forces and bending moments acting in all members can then be found from statical considerations.

When applying equation (2.1) a good deal of accuracy is required with the arithmetic since the resulting equations representing the values of H are ill-conditioned. This difficulty can be avoided and an approximate answer obtained quickly if the following procedure is used.

In equation (2.1) put $\frac{6 l I_W}{d I_c} = k$ the equation then becomes,

$$H_{n+1} - H_n = k \sum_{1}^{n} H - \frac{k}{d} M_{n+1/2} \qquad \text{.................(2.9)}$$

Now for values of k large enough to make k + 1 ≑ k it can readily be shown that,

$$H_n = \frac{H_{n+1}}{k} + \frac{1}{d}\left\{ M_{n+1/2} - M_{n-1/2} \right\} \qquad \text{..............(2.10)}$$

Further, if the value of k is large enough to make the first term in the right hand side of (2.10) negligible in comparison with the second then,

$$H_n = \frac{1}{d}\left(M_{n+1/2} - M_{n-1/2} \right) \qquad \text{............(2.11)}$$

Equation (2.11) could also be derived by assuming points of inflexion to exist at the mid-points of the chord members.

In the case of castellated beams the value of k will be about 30 and the approximations mentioned may well be acceptable.

Using equation (2.11) a rapid evaluation of the forces and moments acting in the various members can be made.

Consider a 15" x 6" beam having 7 panels loaded as shown in fig. 2.5. This was one of the beams tested and was in fact prepared from a 15" x 6" x 45 lb. R.S.J., the holes being flame cut out of the web without expanding the original depth. The test results relevant to this particular beam will be given later but some of the calculations will be considered at this stage in order to illustrate the foregoing theory. Values of horizontal thrust at the mid-points of the verticals 1 to 4 (fig.2.5) were calculated using equations(2.9) and(2.11) and are given in table 2.1 below,

TABLE 2.1.

Vertical	Value of H (tons) by Vierendeel eqn. (2.9)	Value of H (tons) by approximate relationship (2.11).
1	2.5641	2.52
2	4.9978	5.04
3	5.1019	5.04
4	2.3704	2.52

As mentioned before it is necessary to work accurately when using equation(2.9) and the values of H quoted were obtained using a desk calculating machine to four decimal places.

It is clear that equations(2.9)and(2.11) produce virtually the same solution and in view of the substantially greater amount of work required in using (2.9) its use for castellated beams does not appear to be justified.

The stress analysis of a castellated beam on the basis of equation (2.11) is very straightforward. Examples are shown in figs. 2.6 and 2.7 where a five-panel beam is analysed for single

Fig. 2.6

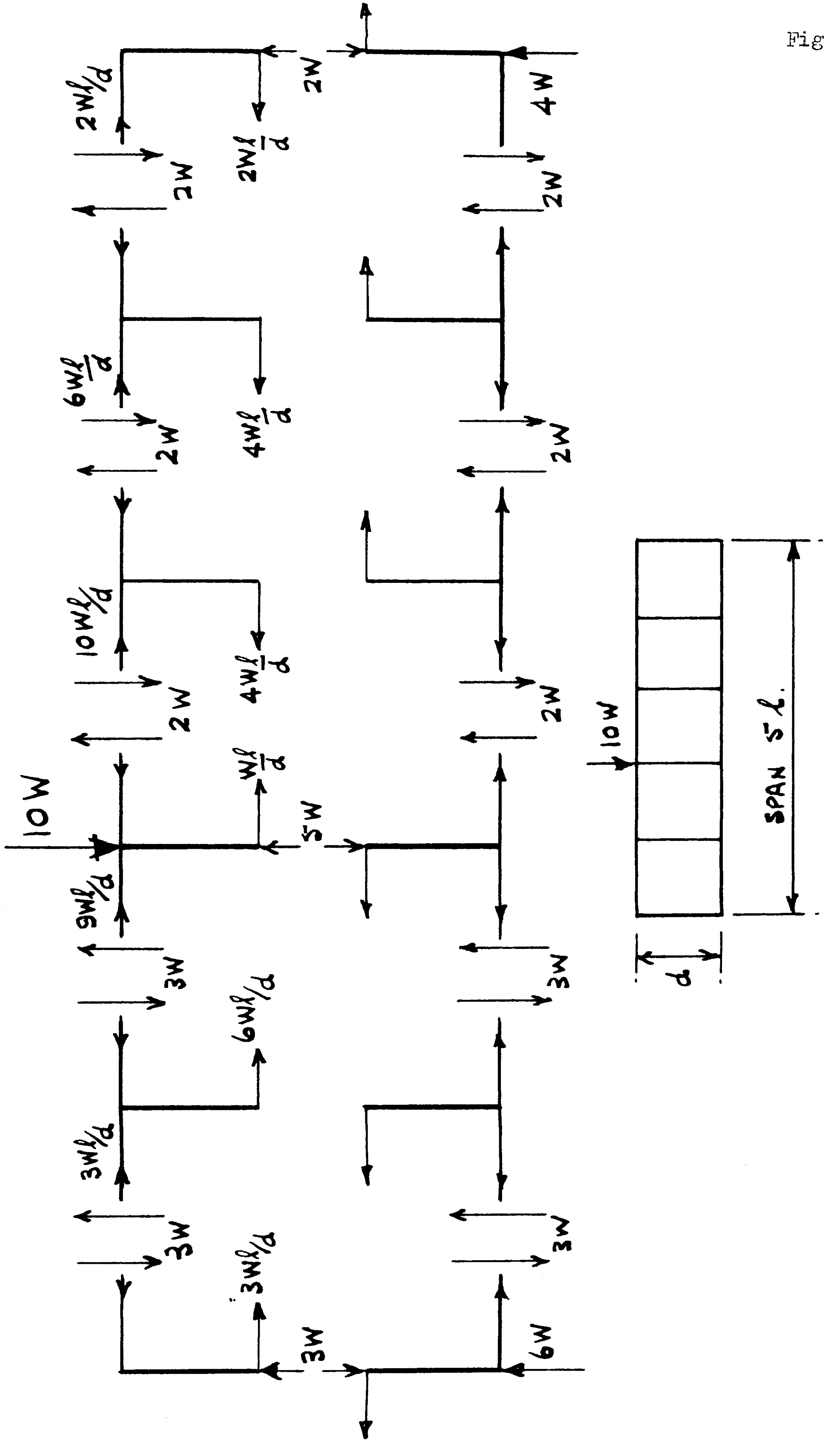

FIG. 2.6.

Fig. 2.7

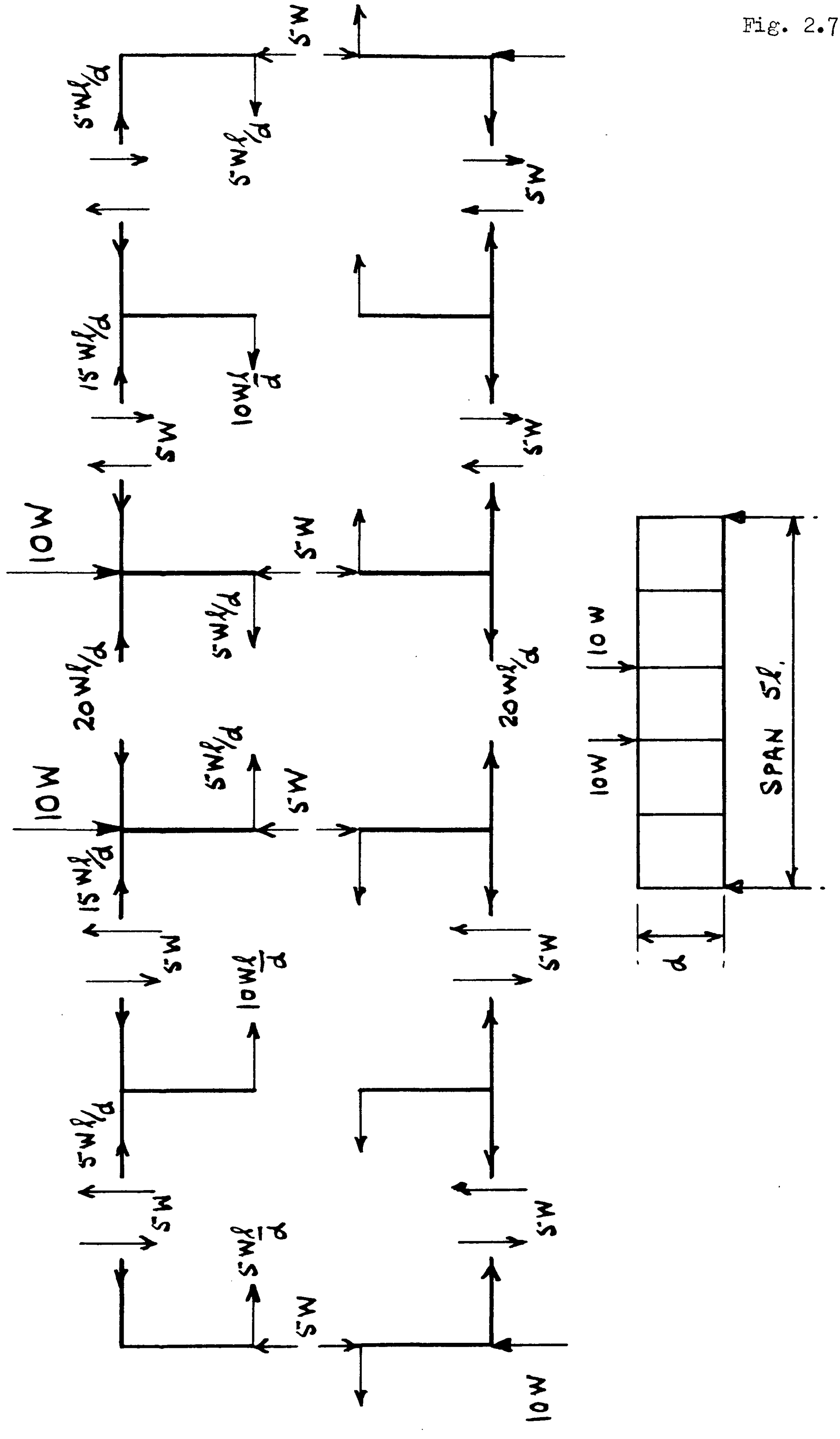
10W
10W
20Wl/d
20Wl/d
15Wl/d
15Wl/d
5Wl/d
5Wl/d
10Wl/d
10Wl/d
5W
10 W
10 W
SPAN 5l
d

FIG. 2.7.

unsymmetrical one-point loading and symmetrical two-point loading respectively. The forces shown are those acting at the assumed points of contraflexure and it will be noticed that the top and bottom chord members share the shear force across each panel equally and that a vertical member carries thrust only if some external applied force acts at its panel points.

Comparisons of the stresses produced by the forces shown in figs. 2.6 and 2.7 with those actually occuring will be made later.

The calculation of deflections will be discussed in the next method of analysis.

3) Analysis based on the conception of a continuous web medium.

This method of analysis is an adapted form of that used by Chitty (11) and Pippard (12) for open-panel structures. The method follows closely on that of Pippard except in the treatment of the term covering the bending of the web members and in the addition of a term to allow for the distortions caused by the secondary bending of the chords.

The method is an approximate one and consists in replacing the perforated web by a continuous medium which is designed to transmit actions to the flanges similar to those of the original web. The actions from the perforated web are simplified to those of moment and thrust at discrete points in the flanges. An expression is obtained for the slope of a flange at a typical panel point and this is transformed into a continuous expression in terms of the actions from the hypothetical web. The solution proceeds for the hypothetical case and the results are then applied, in an approximate way, to the actual beam.

As will be seen the solutions are produced in continuous form, unlike those of the preceding method, and this is a very desirable feature particularly when dealing with long span cases where the number of panels is large.

For simplification it is assumed that the upper and lower chords take up identical deflected forms. This will imply points of inflexion at the mid-heights of the web members and also that these members do not shorten under axial thrust.

The analysis will be restricted to the purely elastic behaviour of the beams.

Referring to fig. 2.8, consider a typical web member AB and let the bending moments in this at A and B be M_W, a point of inflexion occuring midway between A and B. The corresponding chord forces will be $\frac{2\,M_W}{d}$ where d is the distance between the centroids of the chords.

If it is assumed that the chord and web members are rigidly connected then the slope of the chord at A and at B will be given by $\theta + \phi$ where θ represents the rotation of AB due to the end moments M_W and ϕ represents the slope produced by the changes in length of the chords.

If it is further assumed that the moment M_W is shared equally by the chord members meeting at A and at B, then the deflection due to the bending of the chord members, corresponding to the angle β may also be expressed in terms of M_W.

Consider now a simply-supported beam of span 2L and take origin

Figs. 2.8 & 2.9

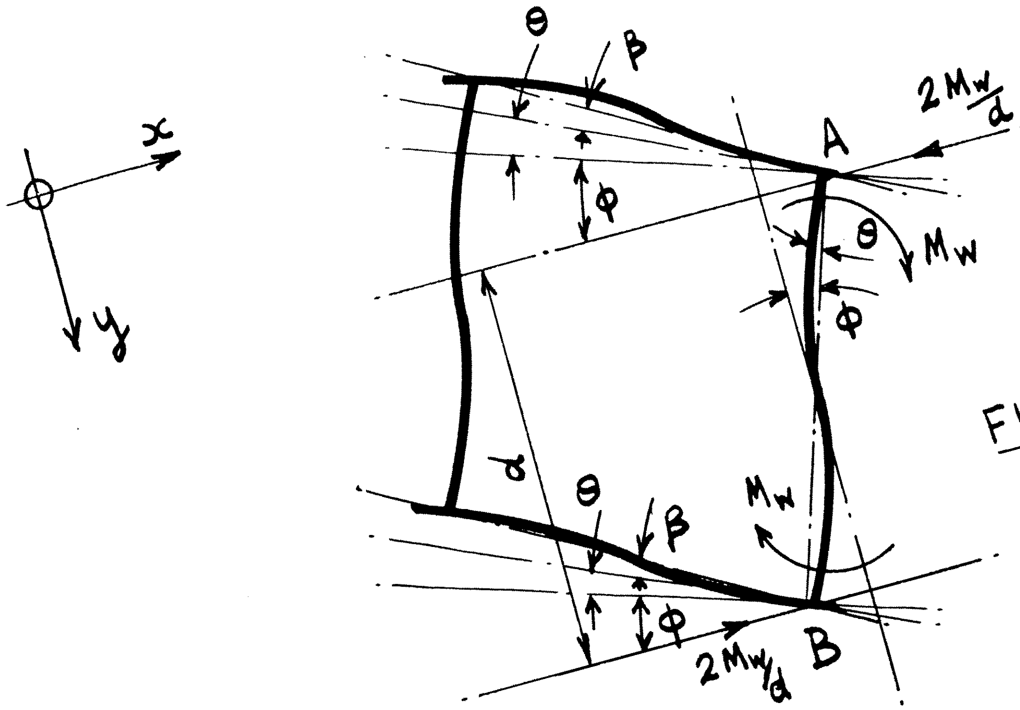

FIG. 2.8.

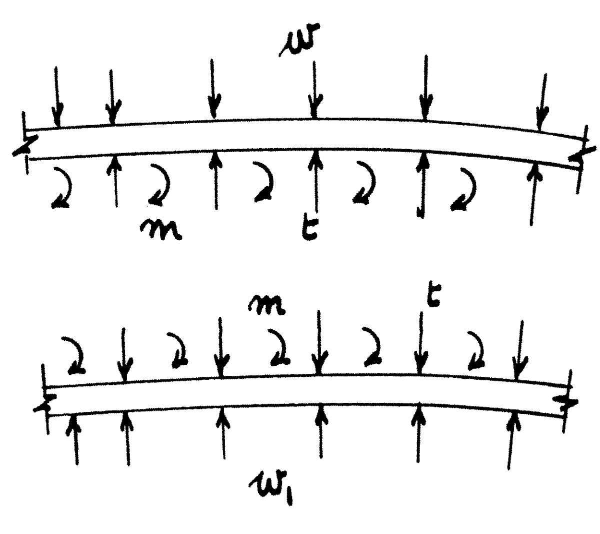

FIG. 2.9.

at the left-hand support with x positive along the beam and y positive downwards. The slope of the deflection curve for the beam is given by,

$$dy/dx = \theta + \phi + \beta \qquad \text{..................(2.12)}$$

Suppose a continuous medium to replace the web of the beam applying continuous actions to the chords as follows; a variable moment m per unit length of the beam and a variable distributed load t per unit length as shown in fig. 2.9.

Determination of ϕ

Now the total chord force P_c at any point x along the beam is given by, $$P_c = \sum_0^x 2\frac{M_w}{d} \qquad \text{.........(2.13)}$$

and the total change in length of the chord due to this,

$$= \int_x^L \sum_0^x \frac{2M_w}{dAE}\,dx$$

where A = the cross-sectional area of the chord.

In the hypothetical case the total chord force at x is

$$P_c = \int_0^x \frac{2m}{d}\,dx \qquad \text{....................(2.14)}$$

If the hypothetical web is to transmit actions similar to those of the original web then equations (2.13) and (2.14) must give the same value of P_c.

Now, $$\phi = \frac{2}{d}\int_x^L \sum_0^x \frac{2M_w}{dAE}\,dx$$

Hence, $$\phi = \frac{4}{d^2AE}\int_x^L\int_0^x m\,dx\,.dx \qquad \text{....................(2.15)}$$

Determination of θ

It is convenient to express θ in terms of m as, $\theta = K_1 m$ where K_1 is a constant which depends on the geometry of the web member.

Referring to equation (2.6) the 2nd moment of area of the equivalent uniform section web member is given by $I_w = \frac{t_1 d^3}{79}$

Now $K_1 = \frac{\theta}{m}$, and in terms of I_w,

$$\theta = \frac{M_w d}{6 E I_w} \qquad \text{..........................(2.16)}$$

Further, $M_w \doteq m\ell$

whence, $K_1 = \frac{d\ell}{6 E I_w} = \frac{d \times 0.72d \times 79}{6 \times E \times t_1 d^3}$

$$\text{or, } K_1 = \frac{9.5}{d E t_1} \qquad \text{..(2.17)}$$

<u>Determination of β</u>

Again it is convenient to write $\beta = K_2 m$ and determine K_2 having regard to the geometry of the chord. The solution is greatly simplified if it is assumed that all parts other than those of minimum cross-section (i.e. the "bridge" of the castellation) have infinite flexural rigidity, and that the moment M_w is shared equally by the parts of the chord meeting at the panel point considered. It is further assumed, for the purposes of obtaining an expression for β that the moment M_w does not change appreciably from one vertical to the next. The contribution of β to the slope of the beam will always be small compared with that due to $\theta + \phi$ Fig. 2.10 shows the M/I diagram for a typical chord member subject to the foregoing assumptions. Applying the Area-Moment theorem it is easily seen that, $\beta = \frac{0.00054 \, d^2 m}{E I_c}$

where I_c = the 2nd moment of area of the chord at the minimum cross-section, and $K_2 = \frac{\beta}{m}$ whence,

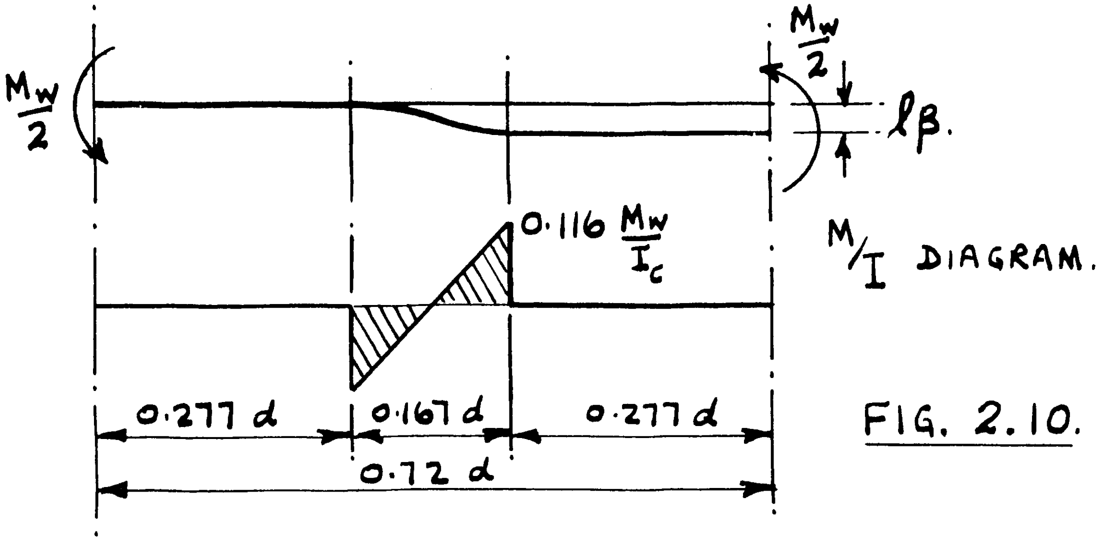

FIG. 2.10.

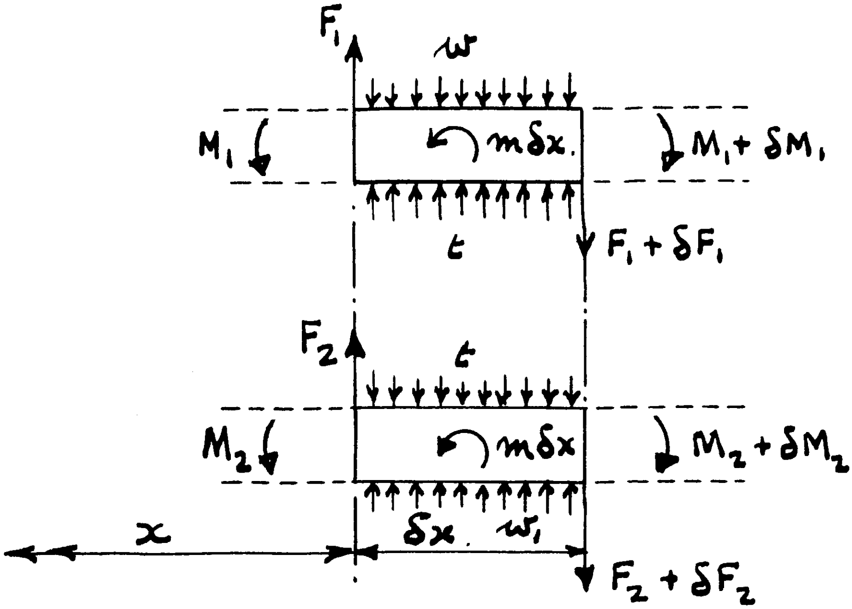

FIG 2.11.

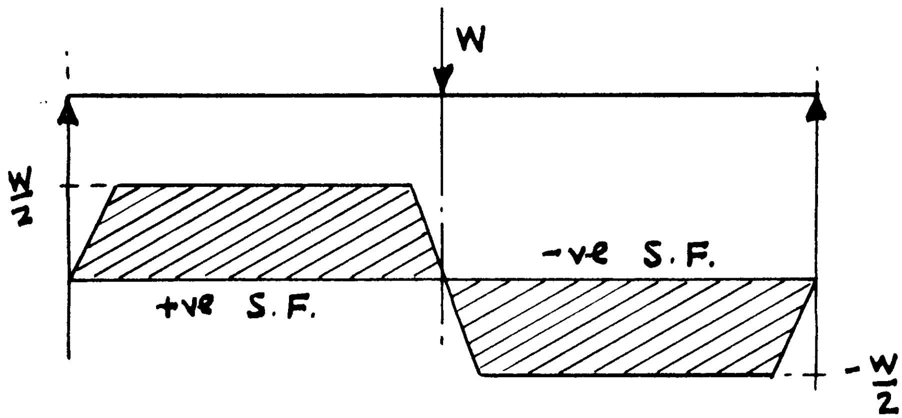

FIG. 2.12.

$$K_2 = \frac{54 \times 10^{-5} d^2}{E I_c} \qquad \ldots\ldots\ldots\ldots\ldots\ldots\ldots(2.18)$$

Now equation (2.12) states that, $dy/dx = \theta + \phi + \beta$

and putting $\theta + \beta = Km$ where $K = K_1 + K_2$

and substituting the value of ϕ from equation (2.15),

$$\left.\begin{aligned} dy/dx &= Km + \frac{4}{d^2 AE}\int_x^L \int_0^x m\, dx\, dx \\ \& \; d^2y/dx^2 &= K\frac{dm}{dx} - \frac{4}{d^2 AE}\int_0^x m\, dx \end{aligned}\right\} \qquad \ldots\ldots(2.19)$$

$$\text{Further, } d^3y/dx^3 = K\frac{d^2m}{dx^2} - \frac{4m}{d^2 AE} \qquad \ldots\ldots\ldots\ldots(2.20)$$

Now consider elemental lengths of the chords in the hypothetical case as shown in fig. 2.11. The external applied load is denoted by w, m and t represent the continuous actions from the hypothetical web, w_1 represents the reactive force from a typical support (w_1 will vanish over the greater length of the beam) and the other symbols have their usual meanings. With the choice of origin and co-ordinate axes made M will be positive if acting as shown. The other forces will be taken as positive if acting in the directions indicated.

Considering the equilibrium of the elements,

$$\left.\begin{aligned} &\delta F_1 + (w - t)\,\delta x = 0 && \text{(a)} \\ &\delta F_2 + (t - w_1)\,\delta x = 0 && \text{(b)} \\ &\delta M_1 - m\,\delta x + F_1\,\delta x - (w-t)\frac{(\delta x)^2}{2} = 0 && \text{(c)} \\ &\delta M_2 - m\,\delta x + F_2\,\delta x - (t-w_1)\frac{(\delta x)^2}{2} = 0 && \text{(d)} \end{aligned}\right\} \qquad \ldots\ldots(2.21)$$

Neglecting infinitesimals of the second order and observing that

$F_1 + F_2 = F$ (the total shear force at the section) and that

$M_1 + M_2 = M$ (the total bending moment acting at the section) then,

$$\frac{dM_1}{dx} + \frac{dM_2}{dx} = 2m - F$$

and, $M_1 = M_2 = EI_c\, d^2y/dx^2$

then, $2EI_c\, d^3y/dx^3 - 2m + F = 0$ ....(2.22)

Substituting for d^3y/dx^3 from (2.20), (2.22) becomes,

$$K\, d^2m/dx^2 - \frac{4m}{d^2AE} = \frac{m}{EI_c} - \frac{F}{2EI_c}$$

or, $K\, d^2m/dx^2 - m\left(\frac{4}{d^2AE} + \frac{1}{EI_c}\right) + \frac{F}{2EI_c} = 0$

or, $\frac{d^2m}{dx^2} - \mu^2 m + \lambda^2 F = 0$ ....(2.23)

where, $\mu^2 = \frac{1}{K}\left(\frac{4}{d^2AE} + \frac{1}{EI_c}\right)$

and, $\lambda^2 = \frac{1}{2KEI_c}$ ....(2.24)

The solution of equation (2.23) is,

$$m = A\cosh\mu x + B\sinh\mu x + \frac{\lambda^2 F}{\mu^2} \quad \text{.............(2.25)}$$

The constants A and B are to be determined from the terminal conditions of the beam and at this stage the analysis will be restricted to simply-supported spans 2L, symmetrically loaded.

<u>Central Concentrated load W on simply-supported span 2L</u>

For this case,

$dy/dx = 0$ when $x = L$

$\left.\begin{array}{l} y = 0 \\ M/EI_c = d^2y/dx^2 = 0 \end{array}\right\}$ when $x = 0$ ....(2.26)

Applying these conditions to equations (2.19),

$$\left.\begin{array}{l} m = 0, \text{ when } x = L \\ \frac{dm}{dx} = 0 \quad \text{when } x = 0 \end{array}\right\} \qquad \ldots\ldots\ldots\ldots (2.27)$$

Applying conditions (2.27) to equation (2.25),

$$B = 0, \text{ and } A = -\frac{W\lambda^2}{2\mu^2}\frac{1}{\cosh\mu L}$$

$$\text{whence, } m = \frac{W\lambda^2}{2\mu^2}\left(1 - \frac{\cosh\mu x}{\cosh\mu L}\right) \qquad \ldots\ldots\ldots (2.28)$$

Differentiating this last expression twice with respect to x,

$$\frac{d^2m}{dx^2} = -\frac{W\lambda^2}{2}\frac{\cosh\mu x}{\cosh\mu L}$$

and substituting this value of $\frac{d^2m}{dx^2}$ and the value of m from (2.28) in (2.20),

$$d^3y/dx^3 = -\frac{W\lambda^2}{2}\left\{\frac{4}{\mu^2 d^2 AE} + \left(K - \frac{4}{\mu^2 d^2 AE}\right)\frac{\cosh\mu x}{\cosh\mu L}\right\}$$

Now put, $Q = \frac{4}{\mu^2 d^2 AE}$ and integrate this latter equation having regard to conditions (2.26),

$$d^2y/dx^2 = -\frac{W\lambda^2}{2}\left\{Qx + (K-Q)\frac{1}{\mu}\frac{\sinh\mu x}{\cosh\mu L} + C_1\right\}$$

and this vanishes for x = 0, hence $C_1 = 0$,

$$\text{Again, } dy/dx = -\frac{W\lambda^2}{2}\left\{\frac{Qx^2}{2} + (K-Q)\frac{1}{\mu^2}\frac{\cosh\mu x}{\cosh\mu L} + C_2\right\}$$

and this vanishes for x = L, hence $C_2 = -\frac{QL^2}{2} - \frac{(K-Q)}{\mu^2}$

$$\text{Therefore } dy/dx = -\frac{W\lambda^2}{2}\left\{\frac{Q}{2}(x^2 - L^2) + \frac{(K-Q)}{\mu^2}\left(\frac{\cosh\mu x}{\cosh\mu L} - 1\right)\right\}$$

$$\text{and } y = -\frac{W\lambda^2}{2}\left\{\frac{Q}{2}\left(\frac{x^3}{3} - L^2x\right) + \left(\frac{K-Q}{\mu^2}\right)\left(\frac{\sinh\mu x}{\mu\cosh\mu L} - x\right) + C_3\right\}$$

= 0 for x = 0, hence $C_3 = 0$.

whence, $y = \frac{W\lambda^2}{2}\left\{\frac{Q}{2}\left(L^2x - \frac{x^3}{3}\right) + \frac{K-Q}{\mu^2}\left(x - \frac{\sinh\mu x}{\mu\cosh\mu L}\right)\right\}$ ....(2.29)

Equation (2.29) gives the deflected form of the beam for $0 \leqslant x \leqslant L$.
The maximum deflection occurs at x = L, and, noting that $\tanh\mu L$ tends to unity and that $\frac{1}{\mu}$ is small in comparison with L, this is given by,

$$y_{max.} = \frac{W\lambda^2}{2}\left\{\frac{QL^3}{3} + \frac{(K-Q)L}{\mu^2}\right\} \qquad \text{..............(2.30)}$$

Referring again to fig. 2.11.

$$\delta F_2 = (w_1 - t)\,\delta x \qquad \text{or,} \quad \frac{dF_2}{dx} = (w_1 - t)$$

Also, $\delta M_2 = m\,\delta x - F_2\,\delta x$

or, $\frac{dM_2}{dx} = m - F_2$

whence, $\frac{d^2M_2}{dx^2} = \frac{dm}{dx} - (w_1 - t)$

or, $(t - w_1) = EI_c\, d^4y/dx^4 - \frac{dm}{dx}$ ....(2.31)

Now, differentiating (2.20) and substituting for $\frac{d^4y}{dx^4}$ in (2.31),

$$(t - w_1) = EI_c\left(K\, d^3m/dx^3 - \frac{4}{d^2AE}\frac{dm}{dx}\right) - \frac{dm}{dx}$$
$$= -KEI_c\left(\mu^2\, dm/dx - d^3m/dx^3\right)$$

whence, on substitution from (2.23),

$$(t - w_1) = -KEI_c\,\lambda^2\, dF/dx$$

$$\text{or,}\quad t = w_1 - \frac{1}{2}\frac{dF}{dx} \qquad \text{.........................(2.32)}$$

Thus in the case of a concentrated load system t = 0 everywhere providing the loads are "point" loads. If on the other hand the loads and reactions are taken to be uniformly distributed over short lengths equal to the width of the web member, then the shear force diagram will be typified by that shown in fig. 2.12. It is easily seen that the thrust T_W in a web member is then one-half of the force (R) applied at its panel point, this result being in agreement with that obtained by method 2.

i.e., $T_W = R/_2$ ....(2.32a)

Now the chord force at any point x is given by (2.14) as,

$$P_c = \int_0^x \frac{2m}{d}\,dx$$

and substituting for m from (2.28),

$$P_c = \frac{2}{d}\int_0^x \frac{W\lambda^2}{2\mu^2}\left(1 - \frac{\cosh\mu x}{\cosh\mu L}\right)dx$$

i.e., $P_c = \frac{W\lambda^2}{\mu^2 d}\left(x - \frac{\sinh\mu x}{\mu\cosh\mu L}\right)$ ....(2.33)

and, since $\frac{\sinh\mu x}{\mu\cosh\mu L}$ can be neglected in comparison with x in the range $0 \leqslant x \leqslant L$,

$$P_c = \frac{W\lambda^2 x}{\mu^2 d}$$

Now, from (2.24), $\frac{\lambda^2}{\mu^2} = \frac{1}{2EI_c\left(\frac{4}{d^2AE} + \frac{1}{EI_c}\right)}$

and $\frac{4}{d^2A}$ is small in comparison with $1/I_c$ so P_c is given approximately by,

$P_c = \frac{Wx}{2d}$ ....(2.34)

If it is further assumed that the value of M_W at any panel point is given by the integral of m between the adjacent mid-panel points

then, $M_W = \int_{x-\ell/2}^{x+\ell/2} m\,dx = \frac{W\lambda^2}{2\mu^2}\left[x - \frac{\sinh\mu x}{\mu\cosh\mu L}\right]_{x-\ell/2}^{x+\ell/2}$

i.e., $M_W = \frac{W\lambda^2}{2\mu^2}\left[\ell - \frac{2\cosh\mu x\,\sinh\mu\,\ell/2}{\mu\cosh\mu L}\right]$ ....(2.35)

Equation (2.35) holds for $0 \leqslant x \leqslant (L - \frac{\ell}{2})$ since the range of validity of (2.28) is $0 \leqslant x \leqslant L$. An examination of equation (2.35) shows that $M_W = \frac{W\lambda^2\ell}{2\mu^2}$ for all values of x until x approaches

L when M_W quickly reduces to zero. This is more readily seen from equation (2.28), from (2.28),

$$\frac{dm}{dx} = -\frac{W\lambda^2}{2\mu}\,\frac{\sinh \mu x}{\cosh \mu L}$$

Since for castellated beams μ always takes a value of the order of unity then $\frac{dm}{dx}$ can be taken as zero until x is very nearly equal to L the half-span.

Hence in the case of the simply-supported beam with central concentrated load the following holds approximately,

$$M_W = \frac{Wl}{4} \qquad \text{..........................(2.36)}$$

(since $\frac{\lambda^2}{\mu^2} \doteqdot \frac{1}{2}$) and again it may be noted that this corresponds to the solution given by method 2.

For convenience the equations needed to analyse a beam with central concentrated load will now be summarized;

the central deflection is given by,

$$y_{max} = \frac{W\lambda^2}{2}\left\{\frac{QL^3}{3} + \frac{(K-Q)\,L}{\mu^2}\right\} \qquad \text{........(2.30)}$$

$$\left.\begin{aligned} \text{where, } \mu^2 &= \frac{1}{K}\left(\frac{4}{d^2AE} + \frac{1}{EI_c}\right) \\ \lambda^2 &= \frac{1}{2KEI_c} \end{aligned}\right\} \qquad \text{..............(2.24)}$$

$$K = K_1 + K_2 = \frac{9.5}{dEt_1} + 54 \times 10^{-5}\frac{d^2}{EI_c} \qquad \text{..(2.17)\&(2.18)}$$

$$Q = \frac{4}{\mu^2 d^2 AE}$$

The thrust in a web member is given by,

$$T_W = R/2 \qquad \text{.....................(2.32a)}$$

The chord force is,

$$P_c = \frac{Wx}{2d} \qquad \text{................(2.34)}$$

and the end moments acting on the web members are,

$$M_w = \frac{wl}{4} \qquad \text{.........................(2.36)}$$

Consider now the case of a simply-supported span carrying a uniformly distributed load.

<u>Simply-supported span 2L with uniformly distributed load w.</u>

The solution continues from equation (2.25)

$$m = A\cosh\mu x + B\sinh\mu x + \frac{\lambda^2 F}{\mu^2} \qquad \text{.............(2.25)}$$

The terminal conditions are still given by (2.26) and (2.27).
Applying conditions (2.27) to equation (2.25) and observing that $F = 0$ for $x = L$ and $dF/dx = -w$ for $x = 0$,

$$m = \frac{w\lambda^2}{\mu^3}\left(\sinh\mu x - \tanh\mu L\cosh\mu x\right) + \frac{\lambda^2 F}{\mu^2} \qquad \text{.....(2.37)}$$

Now adopting a similar procedure to that used for the beam with concentrated load the following expression can be deduced for the central deflection,

$$y_{max} = w\lambda^2\left\{\frac{5}{24}QL^4 + \frac{(K-Q)L^2}{2\mu^2}\right\} \qquad \text{............(2.38)}$$

Further, $t = w_1 - \frac{1}{2}\frac{dF}{dx}$

Hence the thrust in each web member other than those over the supports is $\frac{wl}{2}$ and again it is seen that this thrust is to all intents and purposes one-half of the total concentrated force applied at its panel point if the distributed load is applied as uniform concentrated loads at the panel points.

Thus for the intermediate web members,

$$T_w = \frac{wl}{2} \qquad \text{......................(2.39)}$$

and for the end web members,

$$T_w = \frac{w}{4}\left(2L + l\right) \qquad \text{.............(2.40)}$$

The value of M_W will be given very nearly by,

$$M_W = m\ell = \frac{w\lambda^2\ell}{\mu^2}\left\{\frac{\sinh\mu x - \cosh\mu x}{\mu} + \frac{1}{2}(L - x)\right\}$$

In the range $0 \leqslant x \leqslant L$ $(\sinh\mu x - \cosh\mu x)$ varies from -unity to zero and can thus be neglected, whence,

$$M_W = \frac{w\ell}{4}(L - x) \quad \text{.......................(2.41)}$$

This result can be expressed more conveniently in terms of the moment M_{wn} acting at the ends of the nth vertical as,

$$M_{wn} = \frac{w\ell}{4}\left\{L - (n-1)\ell\right\} \quad \text{..................(2.42)}$$

The chord force P_{cn} in the nth panel is given by,

$$P_{cn} = \sum_0^n \frac{2M_w}{d}$$

whence, $$P_{cn} = \frac{w\ell}{2d}\left\{nL - \frac{n}{2}(n-1)\ell\right\} \quad \text{................(2.43)}$$

The deflection equation (2.38) could also be obtained by observing that equation (2.29) with W = unity represents the influence line for central deflection. If this equation is integrated from 0 to L and the result multiplied by 2w equation (2.38) results.

When dealing with other loading systems it would seem convenient to use (2.29) as the expression for the influence line for central deflection and obtain the central deflection due to other loading systems from it.

i.e., central deflection y_c for a load system is,

$$y_c = \sum W\frac{\lambda^2}{2}\left\{\frac{Q}{2}\left(L^2x - x^3/3\right) + \frac{K-Q}{\mu^2}\left(x - \frac{\sinh\mu x}{\mu\cosh\mu L}\right)\right\} \quad \text{........(2.44)}$$

Before leaving this method of analysis it is interesting to examine the variation of maximum deflection with changing span/depth ratio (r) in the two cases of central concentrated load and uniformly distributed load.

Variation of y_{max} with span/depth ratio (r)

a) Central concentrated load W

$$y_{max} = \frac{W\lambda^2}{2}\left\{\frac{QL^3}{3} + \frac{(K-Q)L}{\mu^2}\right\} \qquad \ldots\ldots\ldots\ldots(2.30)$$

Now $\mu^2 \doteq 2\lambda^2$

and $Q = \dfrac{4}{\mu^2 d^2 A E}$

whence (2.30) becomes,

$$y_{max} = \frac{WL^3}{3d^2AE} + \frac{W}{4}(K-Q)L \qquad \ldots\ldots\ldots\ldots(2.45)$$

Putting $I_{min.} = Ad^2/2$, (2.45) becomes,

$$y_{max} = \frac{WL^3}{6EI_{min}} + \frac{W}{4}(K-Q)L \qquad \ldots\ldots\ldots\ldots(2.46)$$

and the first term of (2.46) represents the deflection given by simple bending theory based on the 2nd moment of area of the minimum cross-section of the beam (I_{min}).

Putting $y_c = \dfrac{W L^3}{6 E I_{min}}$, $\dfrac{y_{max}}{y_c}$ is shown plotted against r in fig. (2.13) for the case of a 15" x 4½" castellated beam.

b) Uniformly distributed load.

In a similar way it can be shown that,

$$y_{max} = \frac{5}{24}\frac{wL^4}{EI_{min}} + \frac{wL^2}{4}(K-Q) \qquad \ldots\ldots\ldots\ldots\ldots\ldots(2.47)$$

Now the first term of (2.47) represents the central deflection given by simple bending theory, and with $y_c = \dfrac{5\ w\ L^4}{24\ E\ I_{min}}$, $\dfrac{y_{max}}{y_c}$ is shown plotted against r in fig (2.13), again for the case of a 15" x $4\frac{1}{2}$" castellated beam. It is seen immediately that as the span of a particular beam increases the error involved in taking the deflection as that given by simple bending theory becomes less. For example if r is of the order of 20 (representing a span of 25 ft.) the error involved is somewhat less than 5 %.

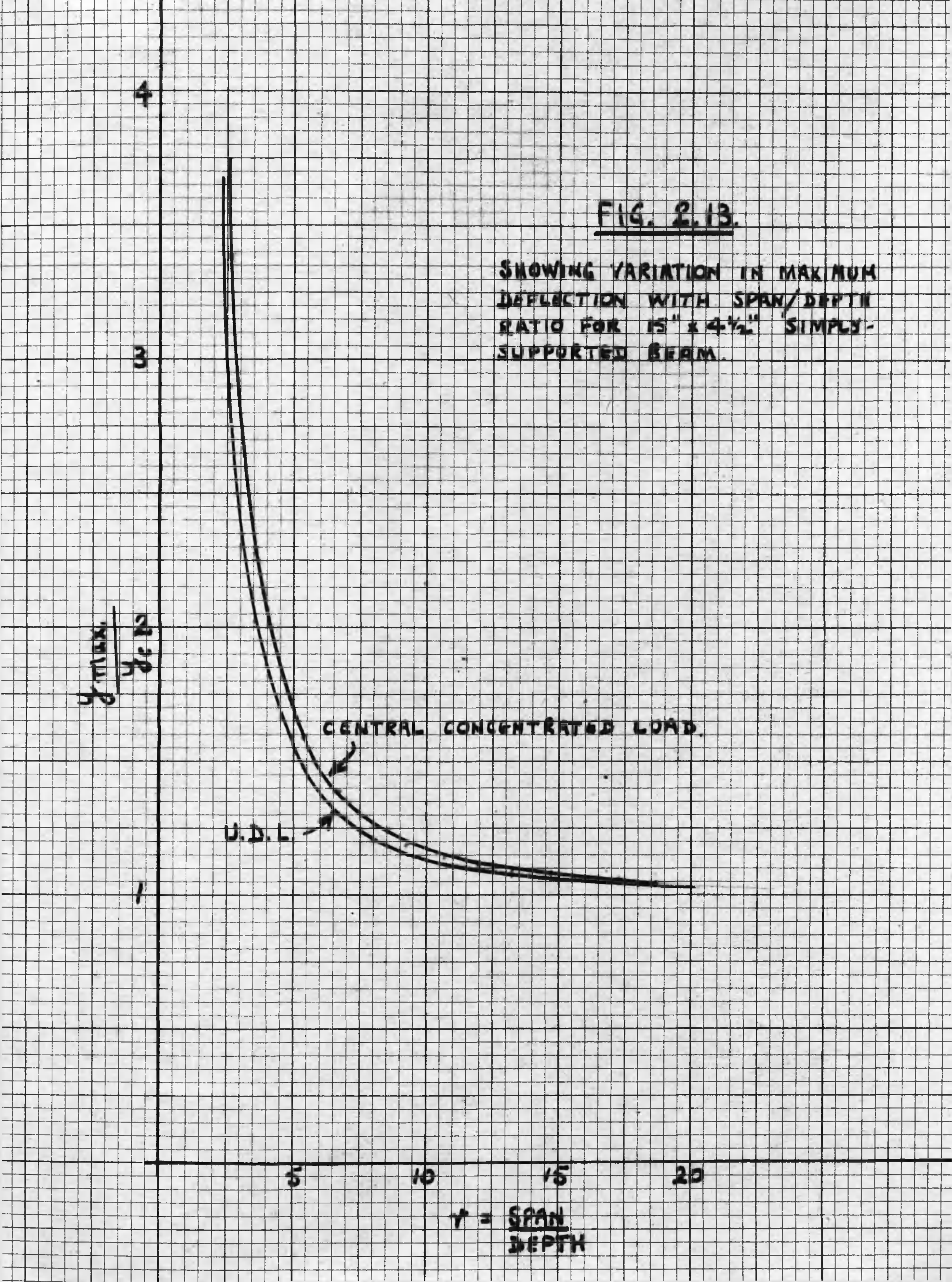

FIG. 2.13.

SHOWING VARIATION IN MAXIMUM DEFLECTION WITH SPAN/DEPTH RATIO FOR 15" x 4½" SIMPLY-SUPPORTED BEAM.

CHAPTER 3

Description of experimental work and equipment.

The bulk of the experimental work on stress distribution and deflection was carried out in the engineering laboratories of the University of Glasgow. A beam testing frame was already available in the laboratory and this was modified and added to in order to make it more suitable for testing castellated beams. The testing frame was basically an 18" x 6" R.S.J. supported at the ends through mild steel rounds bearing on latticed columns and equipped with adjustable hangers for testing simply-supported beams. The method of loading a test beam was to insert a screw jack between the 18" x 6" beam and the test beam and register the load on a pressure capsule of suitable capacity. Thus the live load was carried by the test beam, the 18" x 6" beam and the hangers only, and only dead load was transmitted to the floor of the laboratory. No provision was made in the basic frame for giving lateral support to the test beam.

In order to make the frame suitable for testing castellated beams the height of the 18" x 6" beam above floor level was increased by extending the latticed columns and new hangers were designed which would give lateral support to the test beams at their ends.

The modified testing frame is shown, with a beam under test, in fig. 3.1. The overall length of the testing frame was 22 ft., and the frame was capable of accepting spans up to 16 ft. For the purpose of testing castellated beams the frame was equipped with two 25 tons capacity Tangye hydraulic jacks and two 20 tons Macklow-Smith pressure capsules. As the jacks were to be used in the inverted position they were fitted by the makers with helical springs which would return the ram on release of the load.

Fig. 3.1

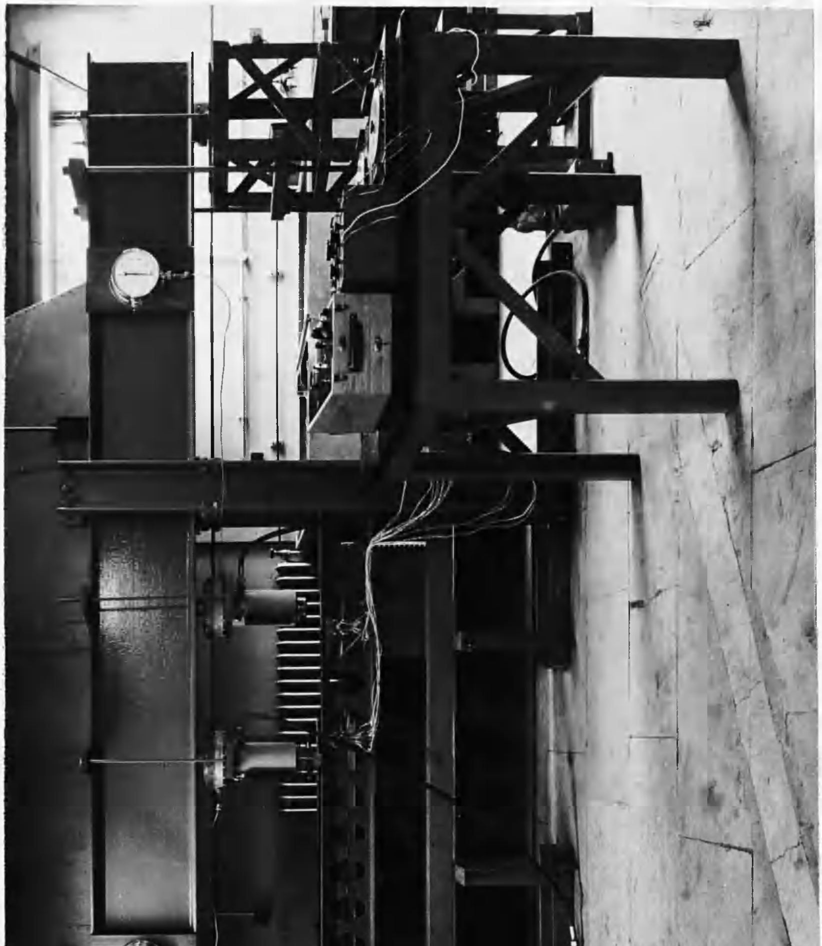

FIG. 3.1. BEAM TESTING FRAME, GLASGOW.

50

FIG. 3.2

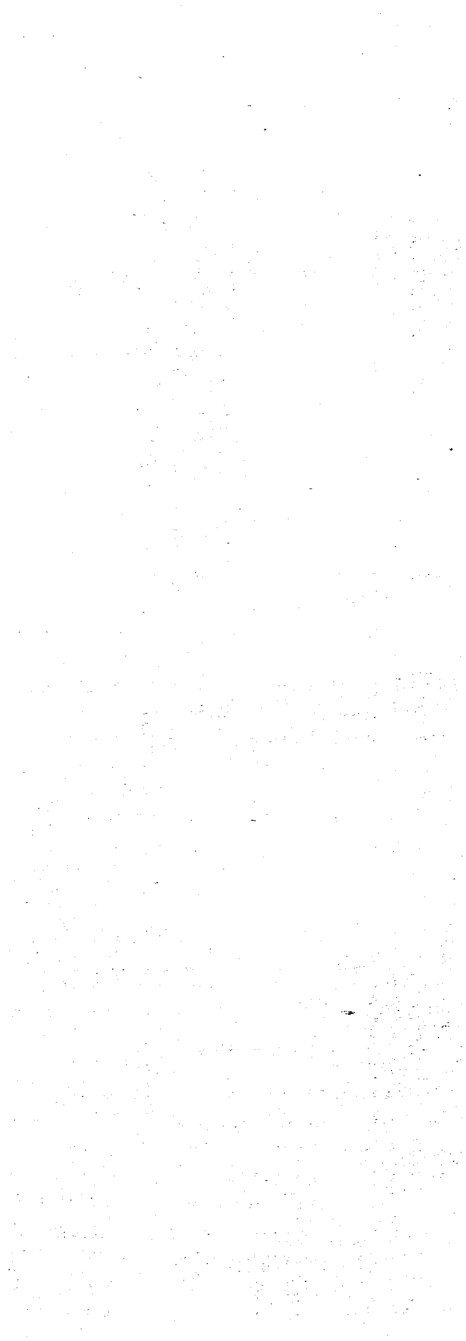

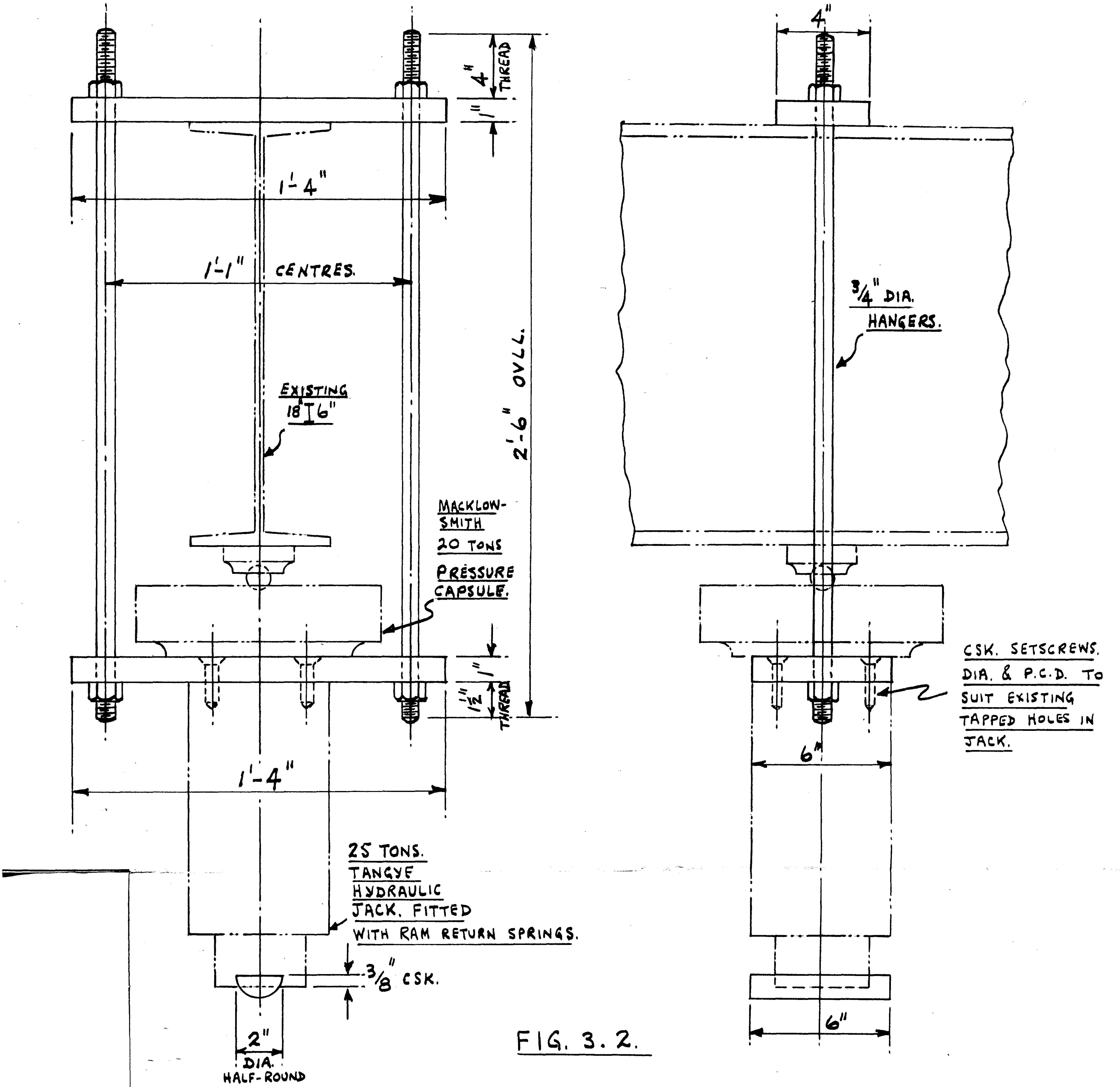

FIG. 3.2.

HANGERS FOR JACKS & PRESSURE CAPSULES - BEAM TESTING FRAME

2 OFF - MILD STEEL.

SCALE 3" = 1'-0". DATE 30.12.54.

DEPARTMENT OF CIVIL ENGINEERING.
UNIVERSITY OF GLASGOW.

WmG.

The arrangement and details of the hangers for the jacks and pressure capsules are shown in fig. 3.2 and again in fig. 3.1.

The load was transmitted to the test beam through a 2" dia. half round of mild steel countersunk to fit over the ram of the jack. On tightening the hangers shown in fig. 3.2 some load was registered by the pressure capsule. This was kept to a round figure of $\frac{1}{2}$ ton throughout the tests and used as a datum from which actual loads were measured.

On receipt from the makers the calibration of the pressure capsules was compared with that of a 30 tons Avery machine and found to be satisfactory. The dial gauges used with the capsules were calibrated from 0 to 20 tons in 0.1 ton intervals.

The combined hanger and lateral supporting device is shown in detail in fig. 3.3 and again in fig. 3.1. It was composed of vertical 8" x $3\frac{1}{2}$" R.S. channels arranged to straddle another 8" x $3\frac{1}{2}$" channel bolted to the concrete floor of the laboratory. The bolted coonections of the hanger were designed to transmit safely a maximum load of 25 tons. The channel fixed to the floor gave no restraint in the longitudinal direction of the beam under test but provided lateral restraint at the supports.

When it was desired to load a beam to collapse steel wedges were inserted between the top flange of the test beam and the inside faces of the vertical channels, the dimensions of the wedges depending on the flange width under test. The device was found to work well in practice but of course lateral restraint was effective only at the supports. The jacks gave some lateral restraint at the load points due to the nature of their connection with the

FIG. 3.3.

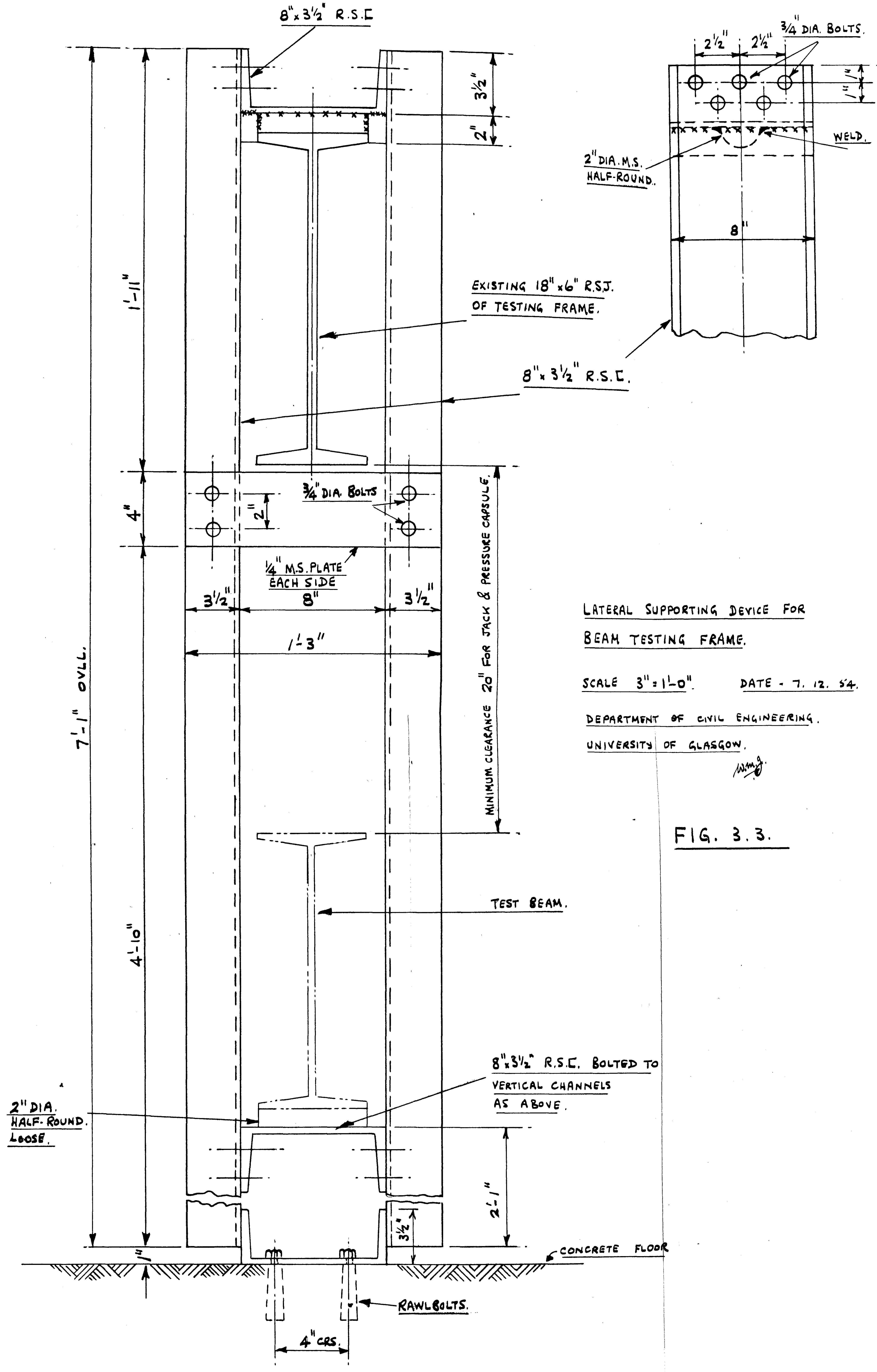

LATERAL SUPPORTING DEVICE FOR BEAM TESTING FRAME.

SCALE 3" = 1'-0". DATE - 7. 12. 54.

DEPARTMENT OF CIVIL ENGINEERING.
UNIVERSITY OF GLASGOW.

W.M.G.

FIG. 3.3.

testing frame but this was inadequate and in cases where lateral instability occured the beams were seen to have rotated considerably at the load points carrying the jacks with them.

As seen in fig. 3.1 the hand pumps for the hydraulic jacks were located at either end of the testing frame. These pumps were equipped with 25 tons pressure gauges of doubtful accuracy. The pressure gauge readings were not used except in cases where it was desired to take the jack loads above 20 tons when the pressure capsules were isolated and the pump pressure gauge readings used.

The measurement of deflections was carried out using Mercer dial gauges reading to 0.0001". The gauges were clamped to a horizontal channel supported on angle brackets attached to the floor channels already mentioned. The arrangement is shown in fig. 3.1. In all cases dial gauges were positioned immediately under the hangers so that the deflections of the hangers could be ascertained and subtracted from the other readings.

Strain measurements were made with Mai-hak vibrating wire strain gauges. A gauge length of 20 mm. (the smallest gauge made by Mai-hak) was adopted for all the web stress readings and all flange stress readings except for the flange stresses of the 15" x 4½" beams where a 50 mm. gauge length was employed.

The gauges behaved extremely well after the author had become familiar with their use. The 20 mm. gauges were a little troublesome at the outset as they are small and require delicate handling. The following procedure was found to work reasonably well and produce fairly rapid results.

1) Prepare the surface on which strain readings are to be made by removing all mill scale and loose material. If the surface is badly pitted a grinder should be used. The amount of work expended on the surface need not be excessive but the surface should be reasonably smooth and free from pits.

2) Ensure that the screw controlling the tension in the gauge wire is slack. This is important for the wire may be broken if the gauge is clamped to the specimen with it tight.

3) Position the gauges carefully ensuring as far as possible that all knife edges bear with equal pressure on the surface of the specimen. The gauges are equipped with a pair of knife edges at the fixed end and a single knife edge at the hinged end. The importance of a smooth surface is now apparent. If one of the knife edges is located over a pit in the surface difficulty will be experienced in getting the gauge to function correctly.

4) Tighten the gauge wire until a suitable initial reading is obtained at the receiver.

5) If it is found difficult to get a reading from the gauge, taking off and re-setting in a slightly different position usually succeeds. It was thought that surface pits were responsible for this phenomenen.

The major difficulty in using Mai-hak gauges is in the designing of a suitable clamp for holding the gauge on to the specimen. For the readings of strain in the web it was desirable to have a clamp which would hold two gauges, one on either side of the web, in order that transverse bending strains could be eliminated. After some experimenting with various forms of clamp the one shown in fig. 3.4 was adopted and proved very satisfactory. The clamp holds two 20 mm. gauges each free to slide in a slot machined in the body of the clamp. The gauges are held in position in the clamp by means of the springs shown. A threaded screw is used to tighten the gauges on to the specimen, the head of the screw being located on the pressure cap on the top of the nearer gauge. A steel centre at the other end of the clamp located the second gauge. With this type of clamp the clamp and gauges could be held in place with one hand whilst using the other for tightening the screw.

The hard steel pins which can be seen projecting from either gauge in fig. 3.4 are used to locate the movable knife edge in the body of the gauge. These pins are removed once the gauges are secured in position and before any readings are taken.

The clamp holding the gauges can be seen positioned on a specimen in fig. 3.5 along with another, less successful, form of clamp.

Strain readings were also taken on the outer faces of the flanges, the gauges being located in the centre of the flanges.

The vibrating wire strain gauges are supplied by the makers with a calibration constant for each gauge. The measuring range of the gauges in conjunction with the receiver varies slightly from one gauge to the next but is generally of the order of 10 to 11 tons/sq.in. for mild steel. This range is generally adequate when dealing with strains in steel specimens but it can be

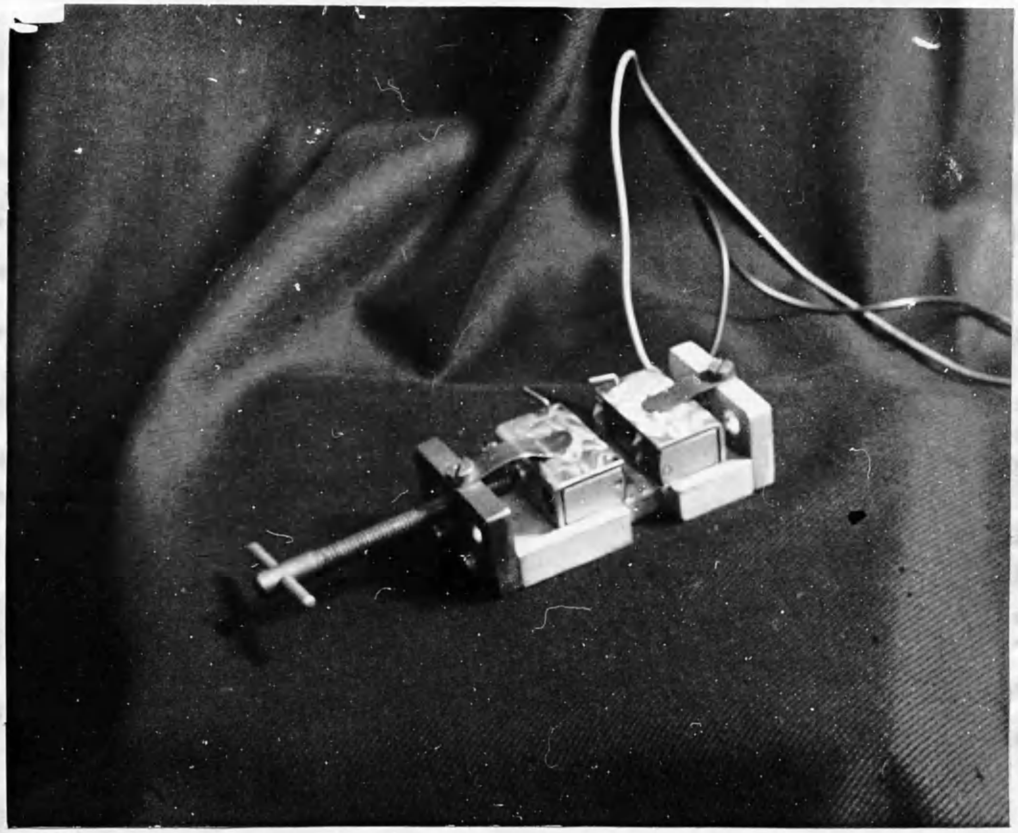

Figure 3.4

Clamp holding two 20 mm. gauge length Mai-hak vibrating wire strain gauges.

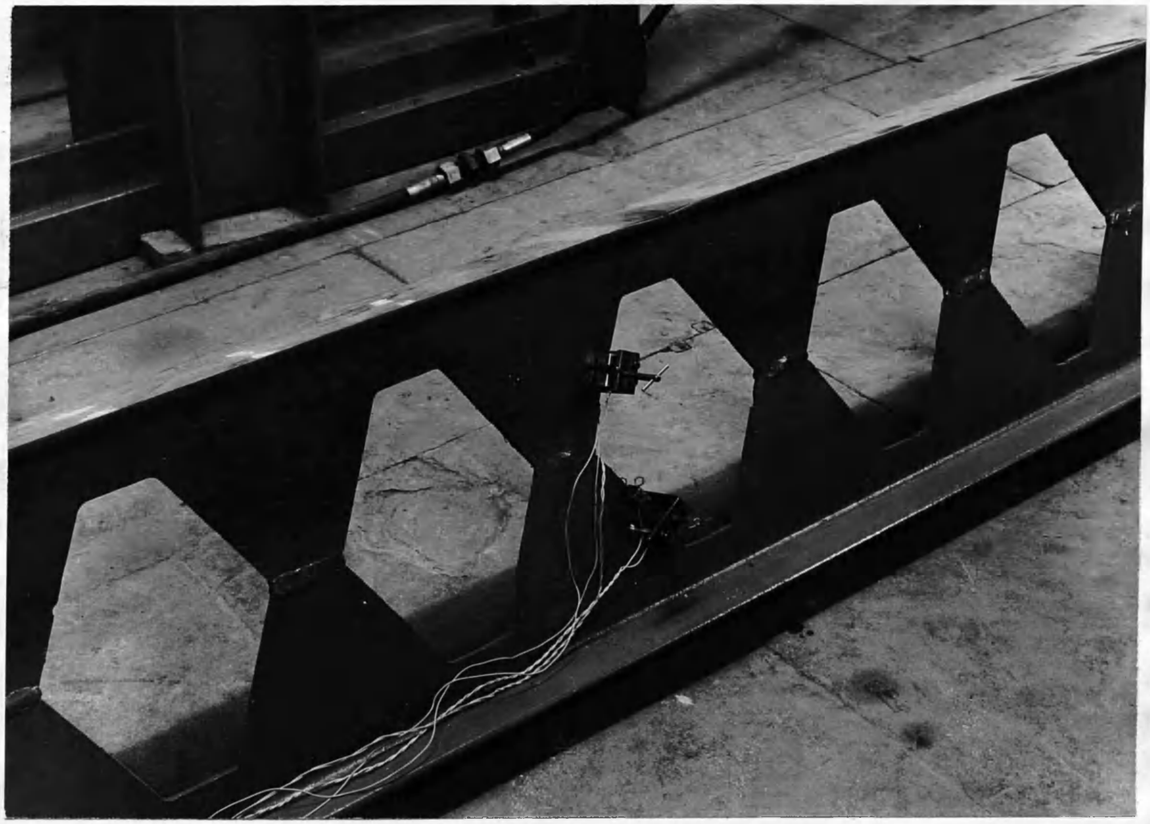

Figure 3.5

Showing strain gauges in position. The local crippling of the top flange at the centre hole can also be seen.

extended if required by a procedure which will be outline in chapter 5.

All the tests on stress distribution in the beams except the one on the $7\frac{1}{2}$" x 3" beam (fig. 4.14) were carried out in the Civil Engineering laboratory in Glasgow. The deflection tests on 15" x $4\frac{1}{2}$" and 9" x 3" beams for deflected form (fig. 4.7) were also carried out in Glasgow. The remainder of the deflection tests were carried out in London.

Of the tests on web buckling the ones on the 15" x 6" beams were carried out in Glasgow and the remainder in London.

The work in London was conducted in much the same way as that already described. In this case the testing frame used was the space frame in the structures laboratory in King's College. This frame is shown in chapter 5 fig. 5.16 and is described there in connection with its use for web buckling tests.

Throughout the tests advantage was taken of symmetrical conditions wherever possible but in all cases sufficient readings were taken on both halves of the beam to justify the assumption.

Values of Young's Modulus and yield stress for the beams.

A value of E of 13,400 tons/sq.in. was used throughout in converting the strain readings and in evaluating theoretical deflections. Tensile stress-strain tests were conducted on two specimens cut from the flanges of two of the beams tested. The specimens were taken from the flanges of beams which had been subjected to low loads only and were cut from low-strain regions of these beams. The results of the tests are shown in table 3.1 below.

3.1

TABLE 3.1. Stress-strain tensile tests.

Specimen	Young's Modulus tons/sq. in.	tensile yield stress tons/sq. in.
1	13,800	17.2
2	13,600	17.8

CHAPTER 4

Calculations and results. Comparisons of experimental and theoretical results.

For convenience the theoretical and experimental results will be considered under two headings, deflections and stress distributions.

Deflections.

In order to facilitate the calculations the constants associated with each section tested are listed in table 4.1. The constants for any other section could readily be obtained using the expressions given in chapter 2.

Using the relevant equation of (2.29), (2.30) or (2.44) an expression for the deflected form or the central deflection of any castellated beam can easily be deduced. To take an example, consider a $4\frac{1}{2}''$ x $1\frac{1}{2}''$ beam with 28 castellations, centrally loaded. The half-span $L = 0.72 \times 4\frac{1}{2} \times 14 = 45.36''$. Using the values of the relevant constants from table 4.1 and substituting in equation (2.30) the following expression results for the central deflection y_c,

$$y_c = 0.314 \text{ W ins. where W = central load (tons).}$$

In a similar way the deflected form of a 9" x 3" beam with 15 castellations carrying a central load of 1 ton is obtained from equation (2.29) as,

$$y = 10^{-4}(8.90 x - 0.00129 x^3) \text{ ins.} \quad (x \text{ in inch units from nearest support})$$

A summary of the tests on deflection with references to the figures in which the results appear, along with theoretical results, is given in table 4.2 below.

Table 4.1

PROPERTIES OF SECTIONS TABLE 4.1.

SECTION D" × B"	t_1 INS. (WEB)	t_2 INS. (FLANGE)	d INS.	A INS.^{2}	I_c INS.^{4}	$K_1 = \frac{9.5}{d E t_1}$	$K_2 = \frac{54 \times 10^{-5} d^2}{E I_c}$	$K = K_1 + K_2$	$\lambda^2 = \frac{1}{2KEI_c}$	$\mu^2 \doteqdot 2\lambda^2$	μ	$Q = \frac{4}{\mu^2 d^2 A E}$
15 × 6 (EX. 15"×6" R.S.J.)	0.38	0.655	13.94	4.63	1.26	$\frac{1.79}{E}$	$\frac{0.083}{E}$	$\frac{1.873}{E}$	0.211	0.422	0.65	$\frac{0.0105}{E}$
15 × 6	0.36	0.709	14.0	4.88	1.23	$\frac{1.89}{E}$	$\frac{0.086}{E}$	$\frac{1.976}{E}$	0.206	0.412	0.641	$\frac{0.0101}{E}$
15 × 4½	0.30	0.505	14.0	2.85	1.00	$\frac{2.26}{E}$	$\frac{0.106}{E}$	$\frac{2.366}{E}$	0.211	0.422	0.65	$\frac{0.0169}{E}$
9 × 3	0.23	0.377	8.34	1.39	0.16	$\frac{4.96}{E}$	$\frac{0.235}{E}$	$\frac{5.195}{E}$	0.60	1.20	1.10	$\frac{0.0345}{E}$
7½ × 3	0.22	0.376	6.95	1.32	0.085	$\frac{6.22}{E}$	$\frac{0.307}{E}$	$\frac{6.527}{E}$	0.90	1.80	1.34	$\frac{0.0348}{E}$
6 × 3	0.24	0.347	5.52	1.20	0.050	$\frac{7.18}{E}$	$\frac{0.33}{E}$	$\frac{7.51}{E}$	1.33	2.66	1.63	$\frac{0.0412}{E}$
4½ × 1½	0.16	0.249	4.12	0.454	0.013	$\frac{14.4}{E}$	$\frac{0.71}{E}$	$\frac{15.11}{E}$	2.54	5.08	2.25	$\frac{0.102}{E}$

TABLE 4.2. Summary of deflection tests.

Section	Span/depth ratio (r)	Results shown in fig.	Test carried out.
$7\frac{1}{2}$" x 3" x 5 castellations.	3.6	4.1	Central deflection, Concentrated load not at centre.
9"x 3"x 14 castellations.	10.1	4.2	Central deflection, central load.
$7\frac{1}{2}$"x 3"x 18 castellations	13.0	4.3	Do.
6"x 3"x 22 castellations	15.8	4.4	Do.
$4\frac{1}{2}$"x $1\frac{1}{2}$"x 28 castellations	20.1	4.5	Do.
9"x 3"x 5 castellations	3.6	4.6	Central deflection. Two-point loading to collapse.
15"x $4\frac{1}{2}$"x 12 castellations	8.6	4.7	Deflected form. Central load.
9"x 3"x 15 castellations	10.8	4.7	Do.

In each case the theoretical curve shown is that obtained from the relevant expression in the continuous web medium theory of chapter 2. In the case of the deflected forms of fig. 4.7 those obtained using simple bending theory are plotted also for purposes of comparison.

An examination of the results shows that the theory under-estimates the deflections for low span/depth ratios but when the span/depth ratio is increased to 20.1 (fig. 4.5) the actual deflections are slightly less than the theoretical. For the particular case of r = 20.1 (beam $4\frac{1}{2}$" x $1\frac{1}{2}$" x 28 castellations) the

Fig. 4.1

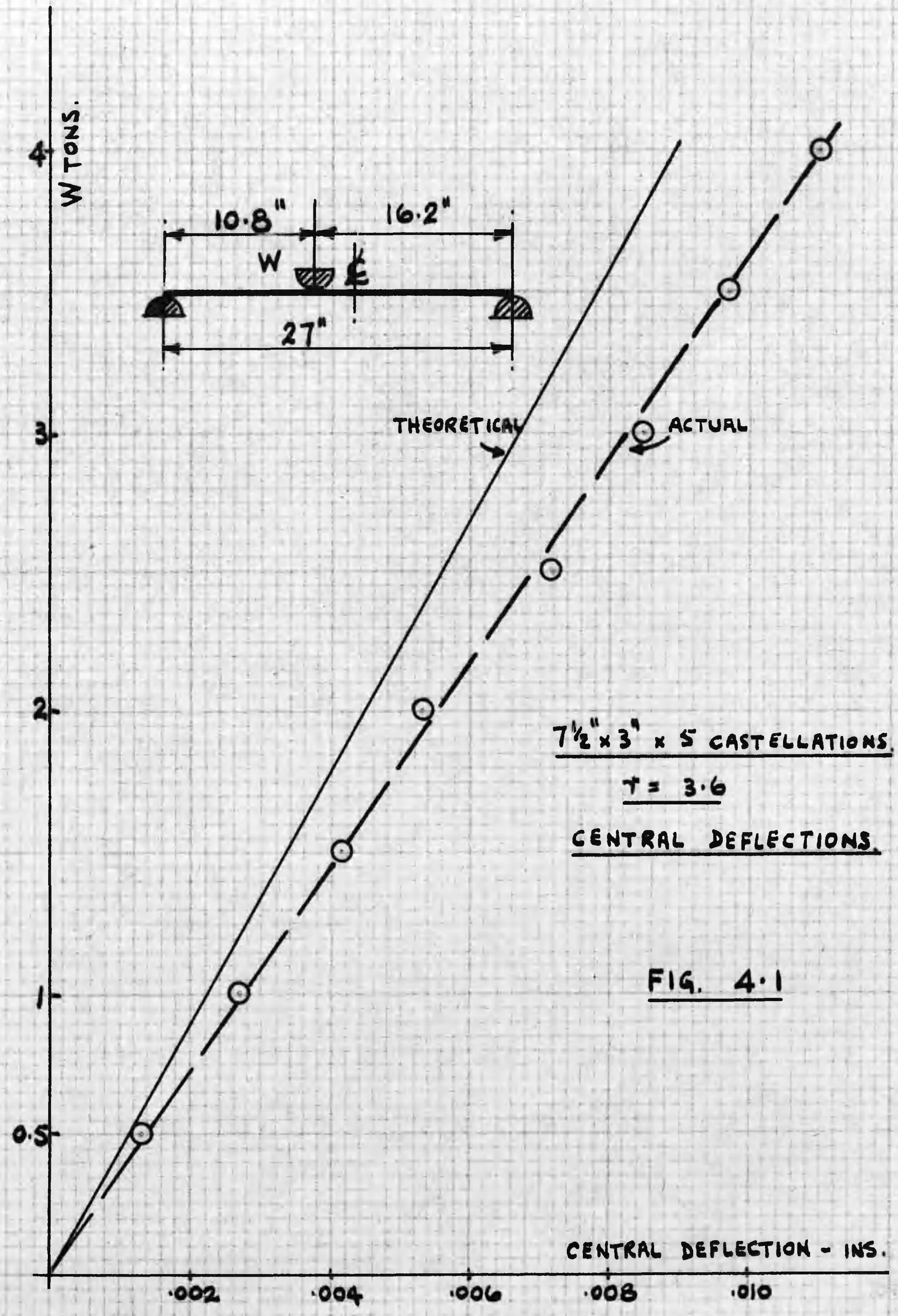

7½" x 3" x 5 CASTELLATIONS.

T = 3·6

CENTRAL DEFLECTIONS.

FIG. 4·1

Fig. 4.2

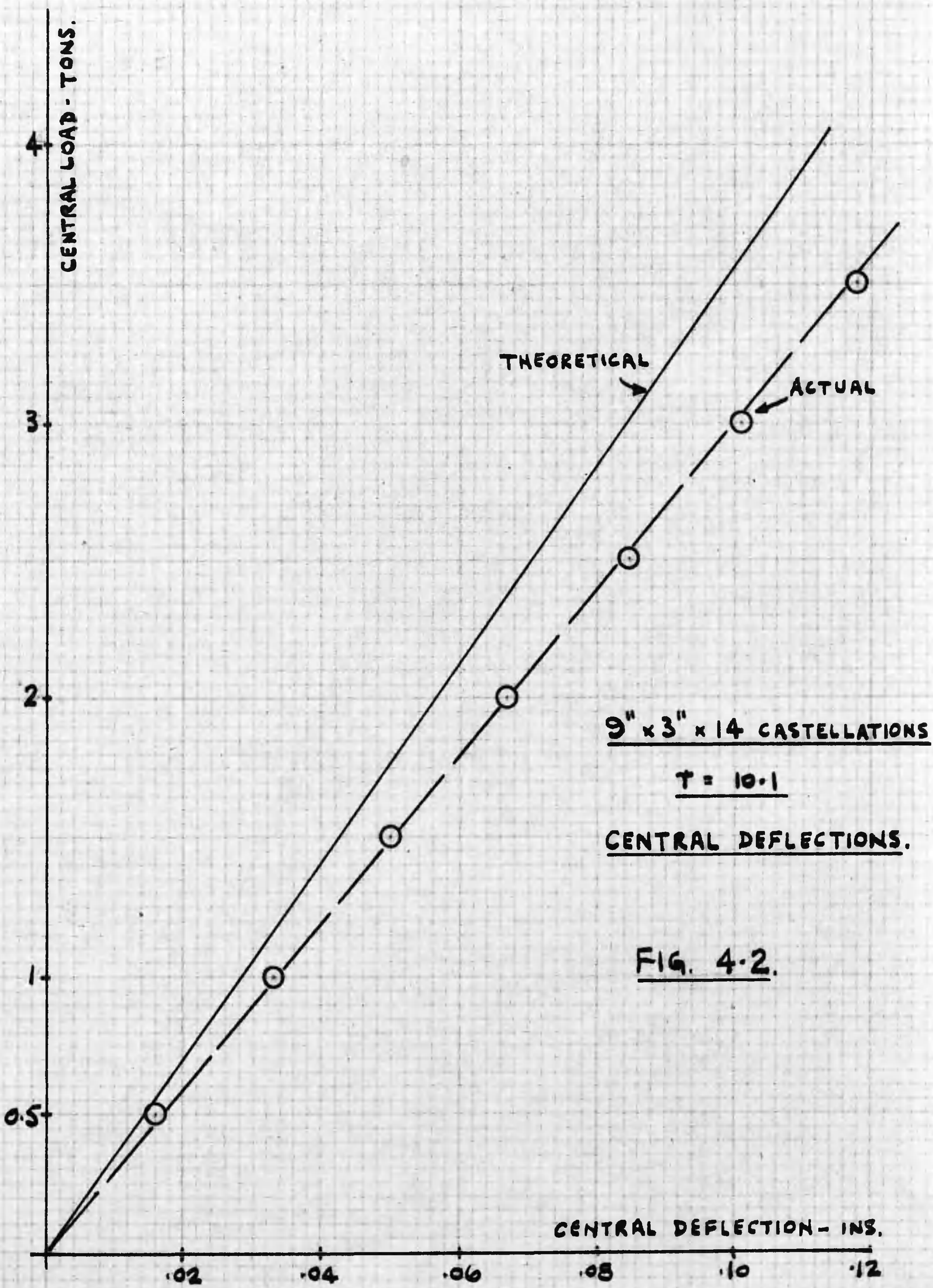
CENTRAL LOAD - TONS.
4
3
2
1
0.5
THEORETICAL
ACTUAL
9" x 3" x 14 CASTELLATIONS
T = 10·1
CENTRAL DEFLECTIONS.
CENTRAL DEFLECTION - INS.
·02
·04
·06
·08
·10
·12

FIG. 4·2.

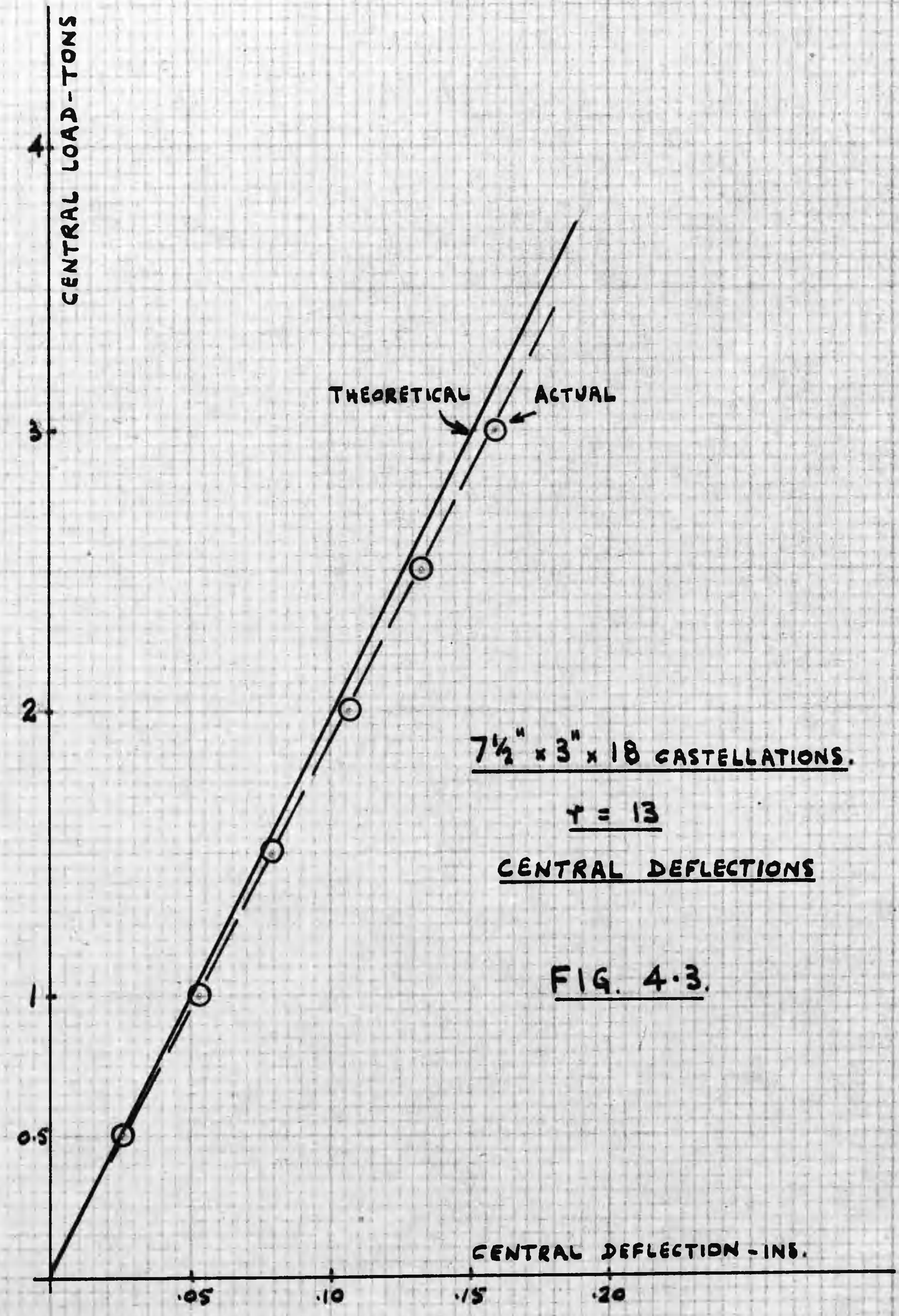
CENTRAL LOAD - TONS
4
3
2
1
0.5
THEORETICAL
ACTUAL
7½" x 3" x 18 CASTELLATIONS.
t = 13
CENTRAL DEFLECTIONS
CENTRAL DEFLECTION - INS.
·05
·10
·15
·20

FIG. 4·3.

Fig. 4.4

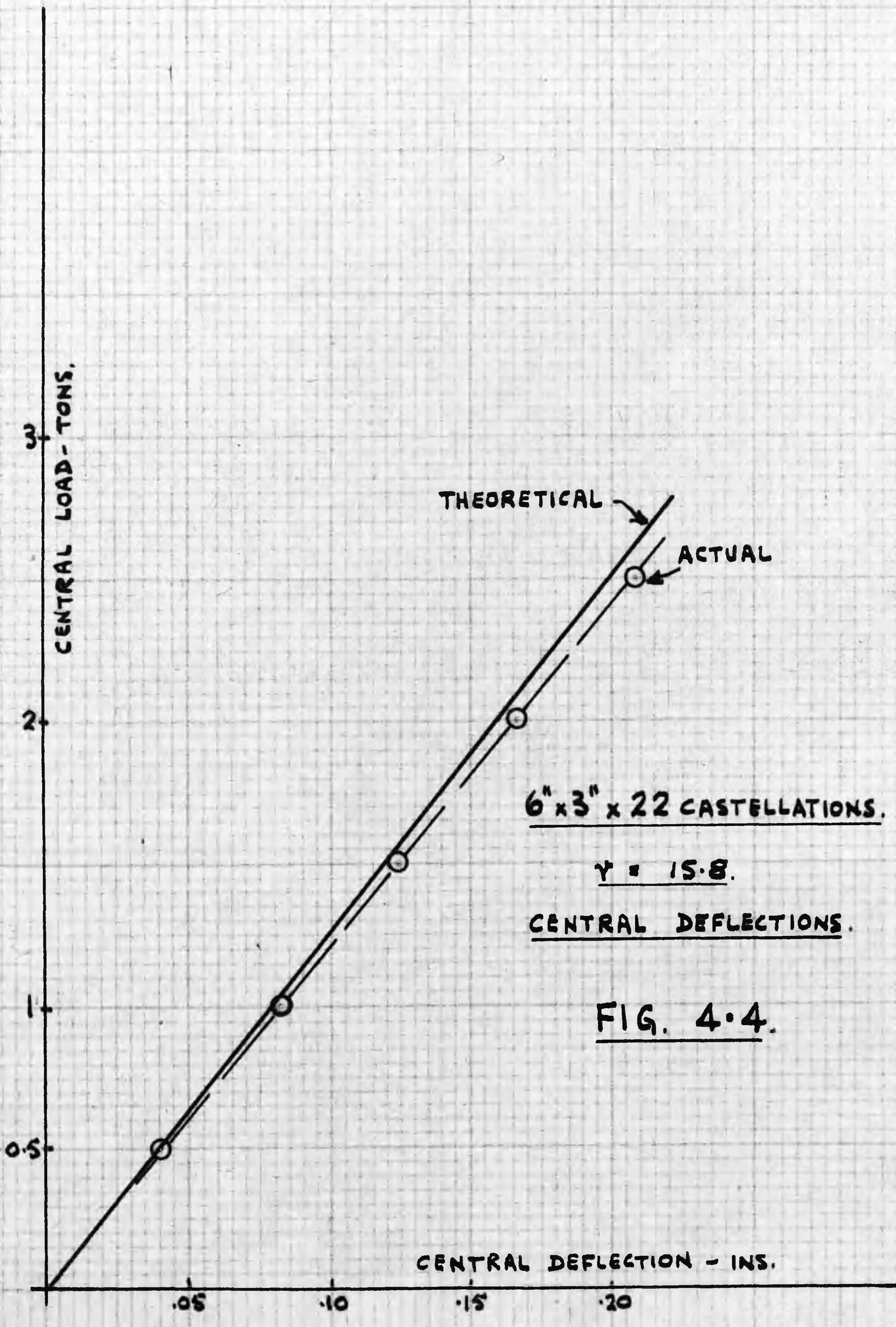

6" x 3" x 22 CASTELLATIONS.

γ = 15·8.

CENTRAL DEFLECTIONS.

FIG. 4·4.

Fig. 4.5

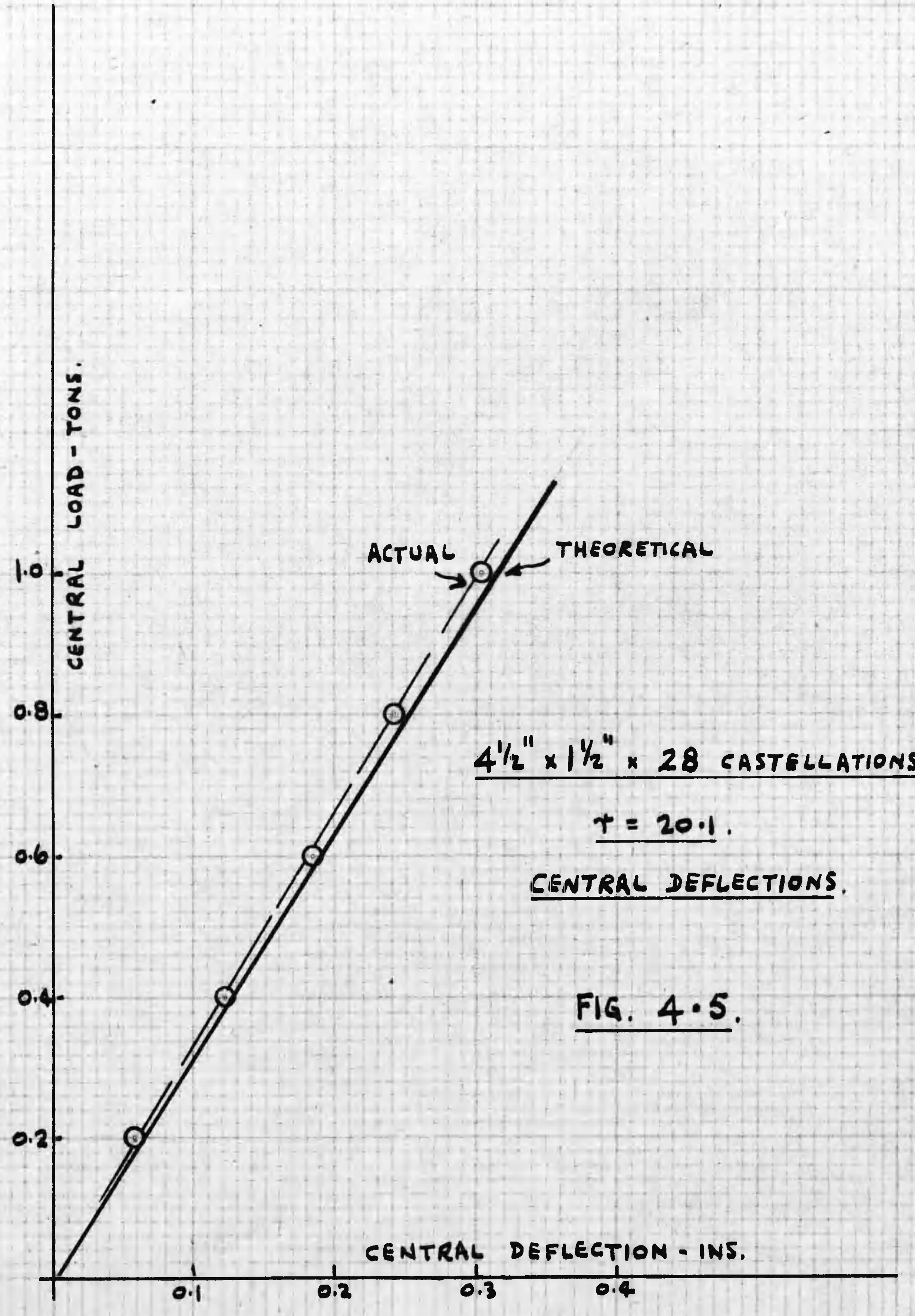

CENTRAL LOAD - TONS.
CENTRAL DEFLECTION - INS.
ACTUAL
THEORETICAL
1.0
0.8
0.6
0.4
0.2
0.1
0.2
0.3
0.4
4½" x 1½" x 28 CASTELLATIONS
τ = 20.1.
CENTRAL DEFLECTIONS.
FIG. 4.5.

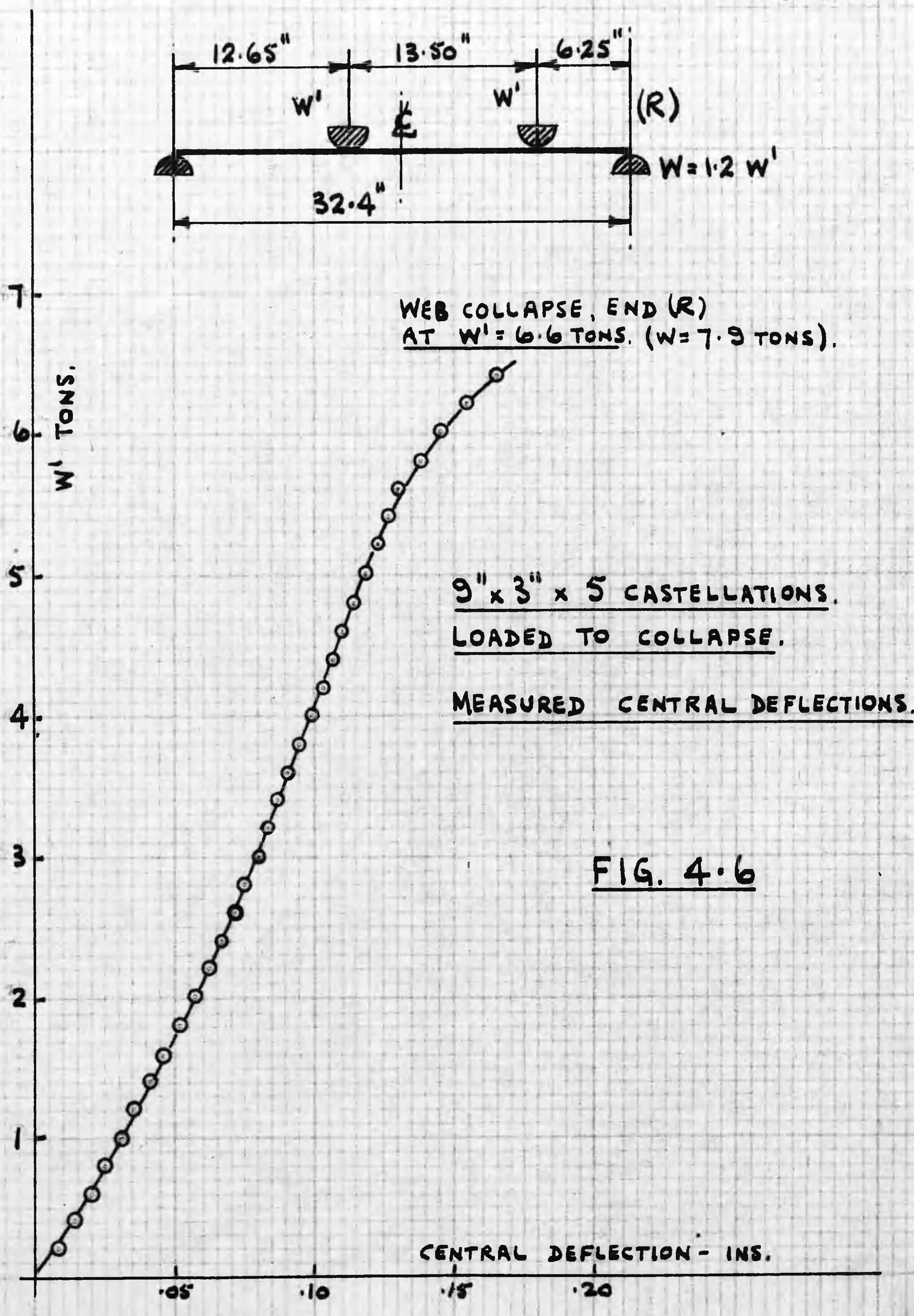
12·65"
13·50"
6·25"
W'
W'
(R)
W=1·2 W'
32·4"
WEB COLLAPSE, END (R)
AT W' = 6·6 TONS. (W=7·9 TONS).
W' TONS.
9" x 3" x 5 CASTELLATIONS.
LOADED TO COLLAPSE.
MEASURED CENTRAL DEFLECTIONS.
CENTRAL DEFLECTION - INS.
·05
·10
·15
·20
1
2
3
4
5
6
7

FIG. 4·6

Fig. 4.7

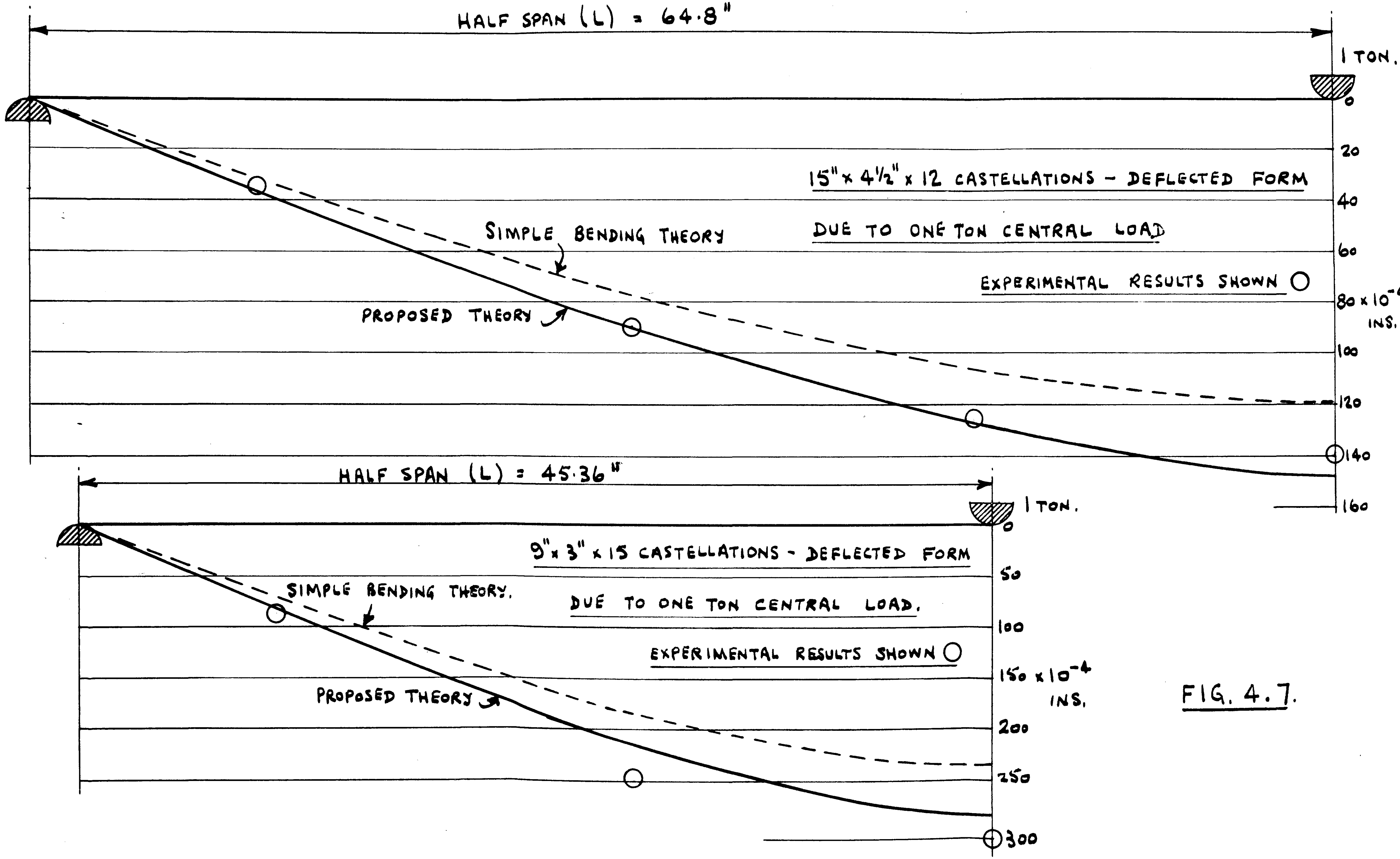

HALF SPAN (L) = 64.8"
1 TON.
0
20
40
60
80 x 10^-4 INS.
100
120
140
160
15" x 4½" x 12 CASTELLATIONS - DEFLECTED FORM
DUE TO ONE TON CENTRAL LOAD
SIMPLE BENDING THEORY
EXPERIMENTAL RESULTS SHOWN ○
PROPOSED THEORY
HALF SPAN (L) = 45.36"
1 TON.
0
50
100
150 x 10^-4 INS.
200
250
300
9" x 3" x 15 CASTELLATIONS - DEFLECTED FORM
SIMPLE BENDING THEORY.
DUE TO ONE TON CENTRAL LOAD.
EXPERIMENTAL RESULTS SHOWN ○
PROPOSED THEORY

FIG. 4.7.

expression for central deflection based on simple bending theory is easily shown to be, $y_c = 0.300$ W ins. (W = central load in tons) and if this is plotted on fig. 4.5 the result is indistinguishable from the curve of measured deflections.

It would appear that at a span/depth ratio of the order of 20 the simple bending theory gives good results, but for ratios of the order of 10 (fig. 4.7) the simple theory underestimates the deflections by about 15%.

Some variation is apparent in the measured deflections for span/depth ratios of the order of 10 as shown by figs. 4.2, 4.3 and 4.7. Fig. 4.2 shows a difference of about 16% between theoretical and measured deflections (r = 10.1) whereas figs. 4.3 and 4.7 show better agreement (5% for r = 13 and 7% for r = 10.8).

One of the deflection tests was continued until web buckling occured at one end of the beam. This test was part of the web buckling test 9" x 3" No. 1 of table 5.1 chapter 5.
The measured central deflections for this test are plotted in fig. 4.6 which also shows the loading arrangement adopted.

Stress distribution

A summary of the tests conducted on stress distribution appears in table 4.3 below along with references to the figures in which the results appear.

TABLE 4.3. Tests on stress distribution.

Section	Results shown in figure,	tests carried out.
15"x 4½"x 12 castellations. Test I	4.8, 4.9 and 4.10	Web and flange stresses
15"x 4½"x 12 castellations. Test II	4.11 and 4.12	Web and flange stresses.
9"x 3"x 14 castellations.	4.13	Flange stresses.
7½"x 3"x 5 castellations.	4.14	Flange stresses.
15"x 6"x 7 castellations. With and without Stiffeners.	4.15	Web and stiffener stresses.

Readings of strain along the boundaries of the holes in the web were taken with the gauges positioned as near as their width would allow to the edge of the hole. As a result the stresses measured are applicable to points some ⅛" away from the boundary but it is not thought that this will involve serious differences.

Theoretical results are also shown in the figures, generally as a series of curves, whilst the experimental results are plotted as point readings.

The theoretical results are all based on the simple analysis which assumes points of inflexion at the mid-points of both the chord and web members. On this basis the stress analysis of any beam is relatively straight forward involving statical principles alone. Two examples will suffice to show this.

Fig. 4.8

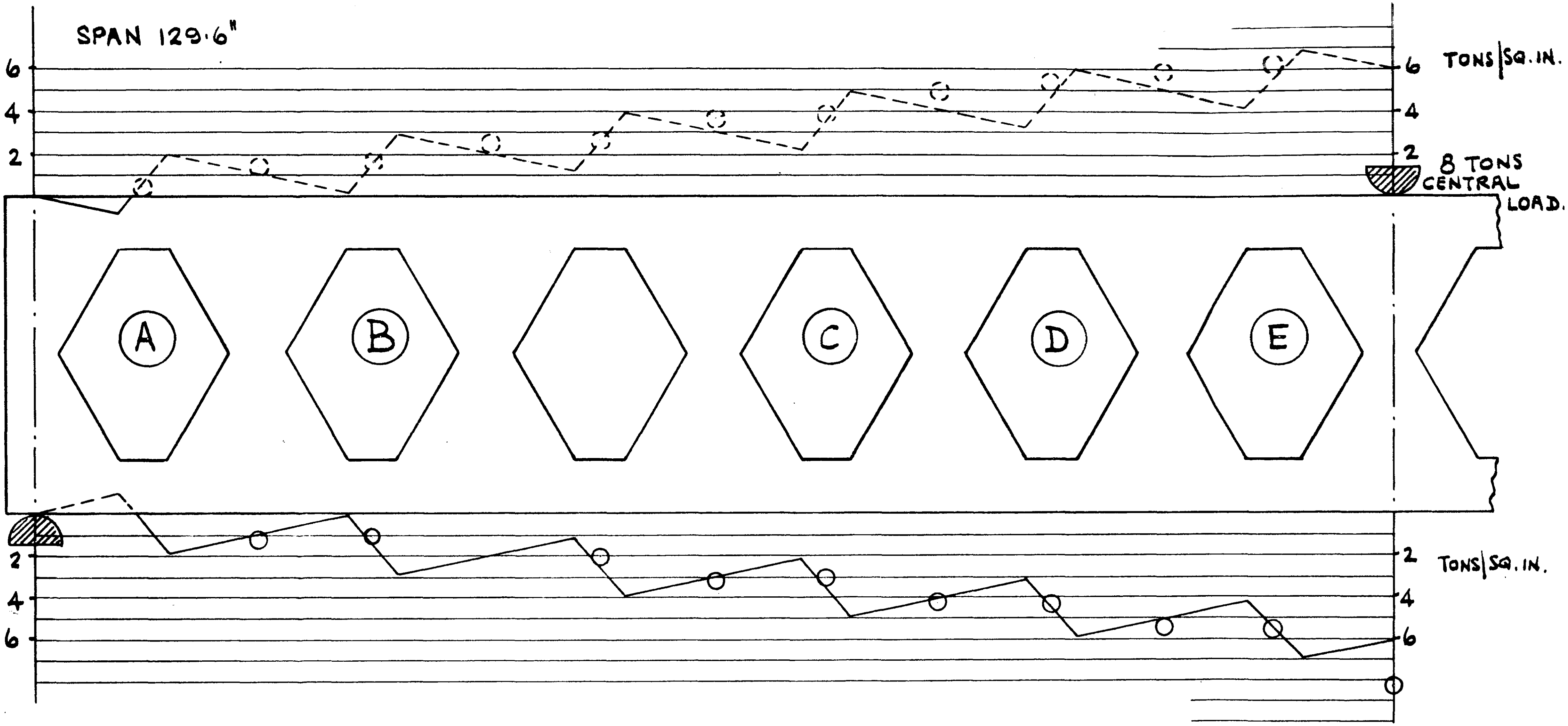

15" x 4½" x 12 CASTELLATIONS (TEST I).
FLANGE STRESSES (OUTER FIBRE).

———	THEORETICAL	TENSILE STRESS.
- - - -	"	COMPRESSIVE "
○	MEASURED	TENSILE "
◌	"	COMPRESSIVE "

FIG. 4.8.

Fig. 4.9

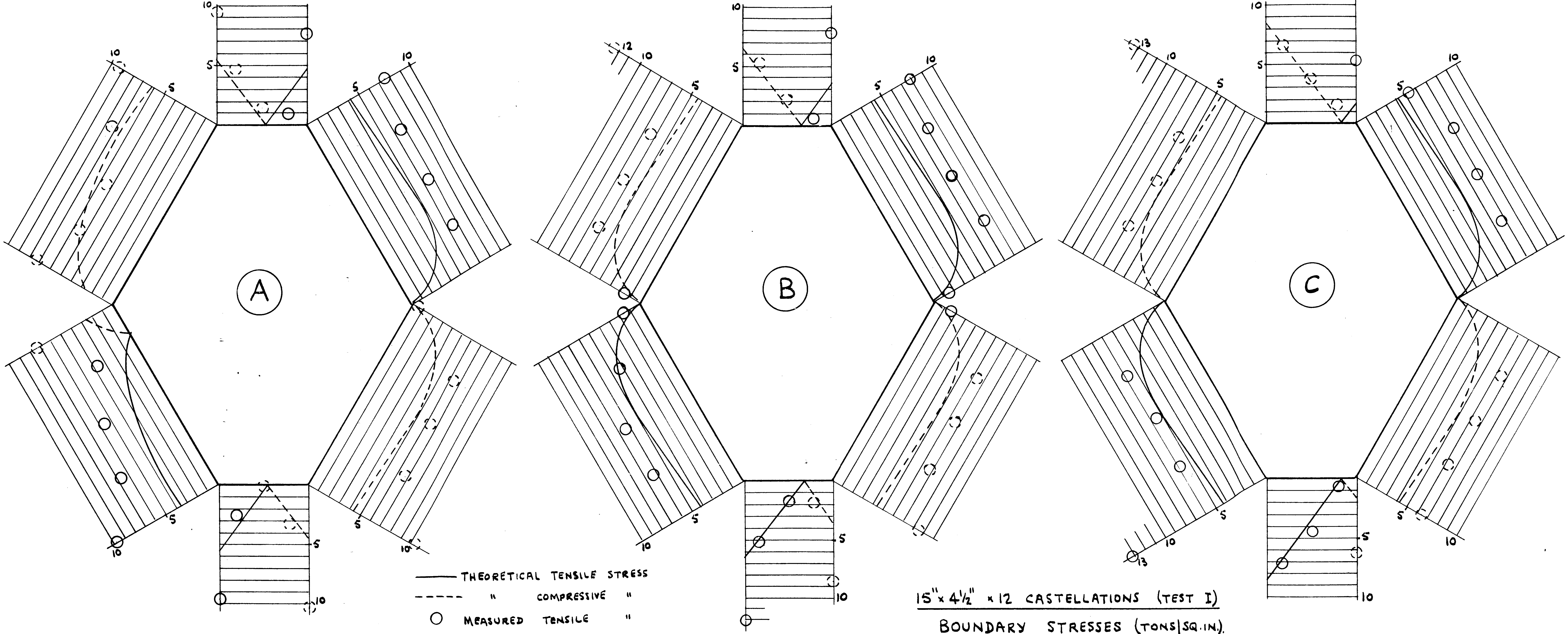

——— THEORETICAL TENSILE STRESS
- - - - " COMPRESSIVE "
○ MEASURED TENSILE "
◌ " COMPRESSIVE "

15" × 4½" × 12 CASTELLATIONS (TEST I)
BOUNDARY STRESSES (TONS/SQ.IN.)

FIG. 4.9.

Fig. 4.10

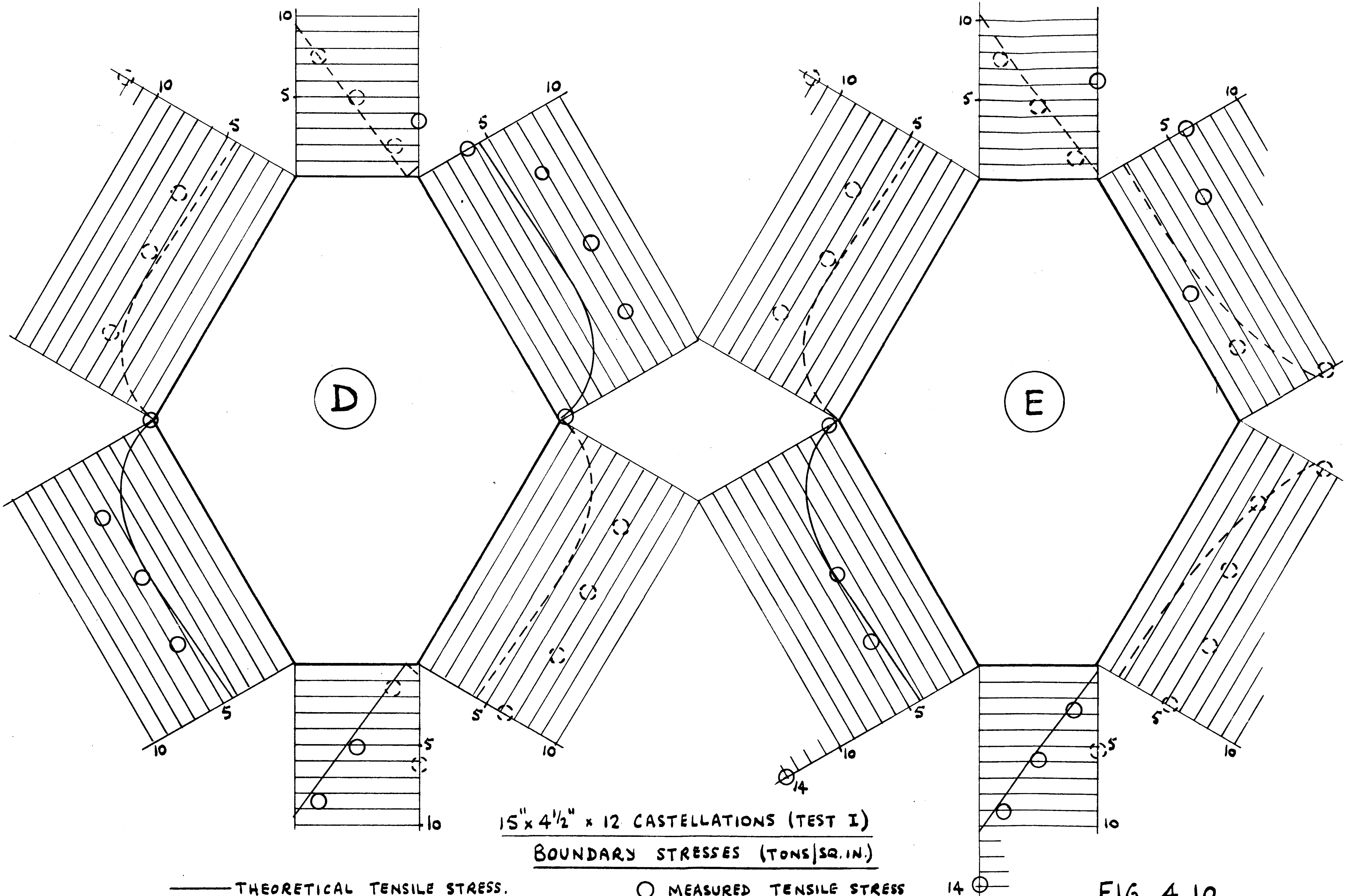

15" x 4½" x 12 CASTELLATIONS (TEST I)

BOUNDARY STRESSES (TONS/SQ.IN.)

——— THEORETICAL TENSILE STRESS.
- - - - " COMPRESSIVE "
○ MEASURED TENSILE STRESS
◌ " COMPRESSIVE "

FIG. 4.10.

FIG. 4.11

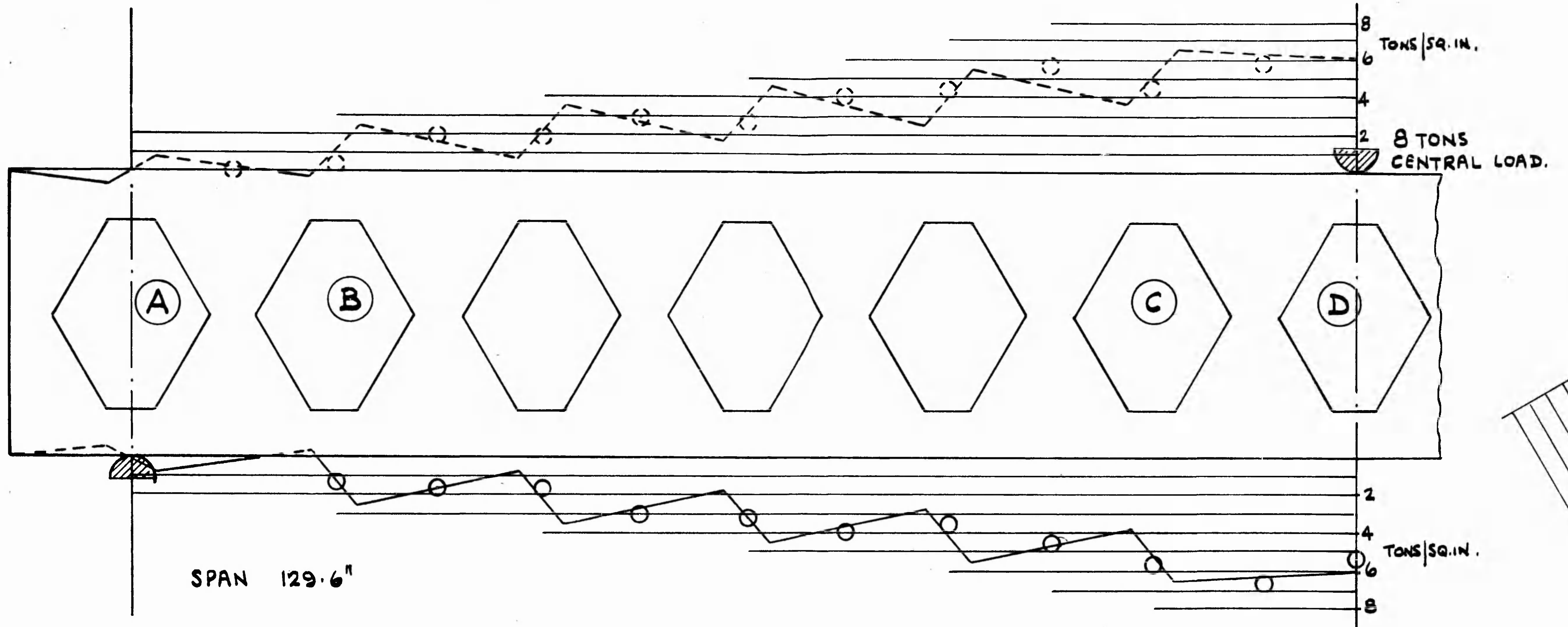

FLANGE STRESSES.

——— THEORETICAL TENSILE STRESS
- - - - " COMPRESSIVE "
○ MEASURED TENSILE "
◌ " COMPRESSIVE "

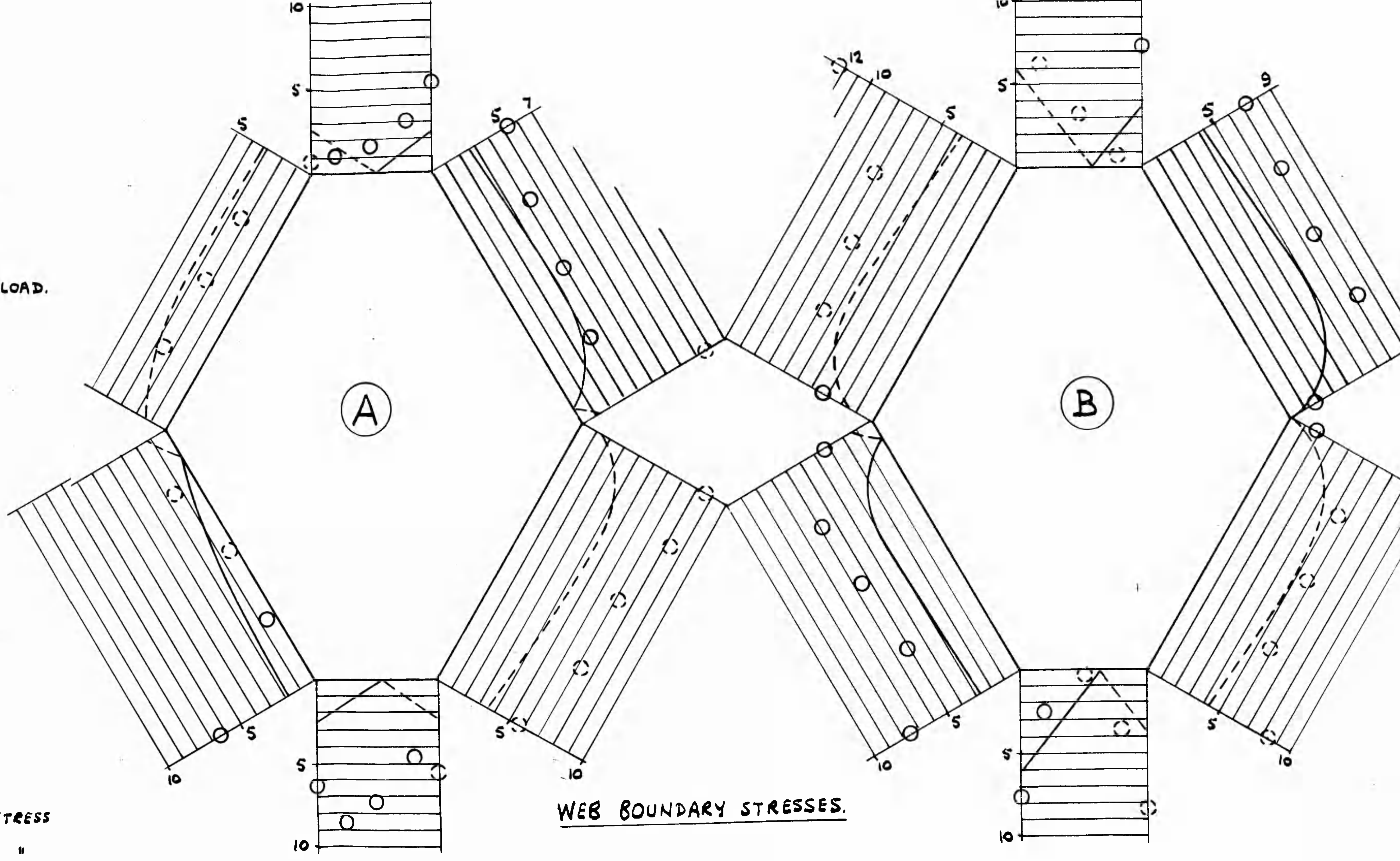

WEB BOUNDARY STRESSES.

15" × 4½" × 12 CASTELLATIONS (TEST II). FIG. 4.11.

FIG. 4.12

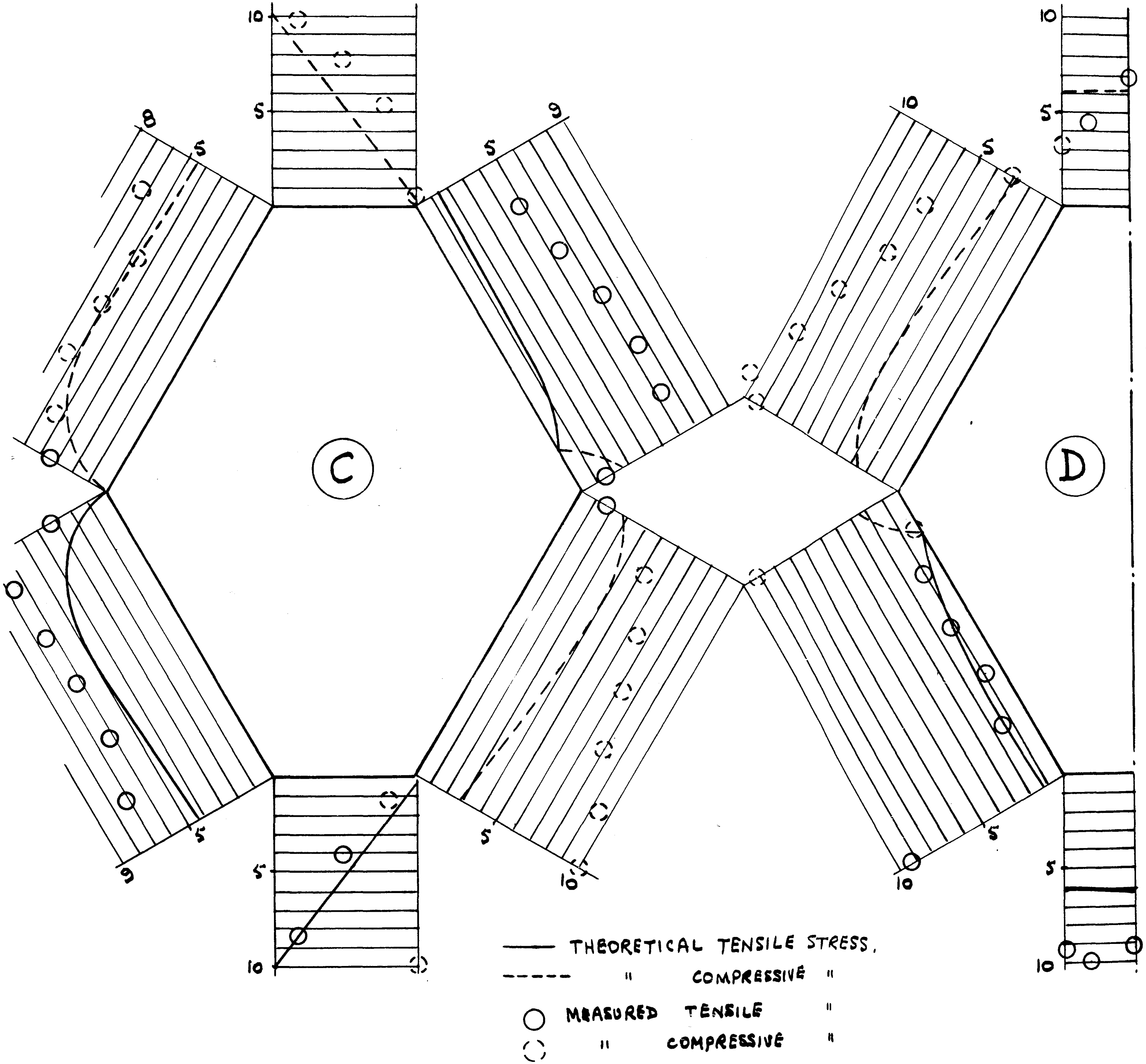

15" x 4½" x 12 CASTELLATIONS

(TEST II)

BOUNDARY STRESSES

TONS|SQ. IN.

FIG. 4.12.

FIGS. 4.13 & 4.14.

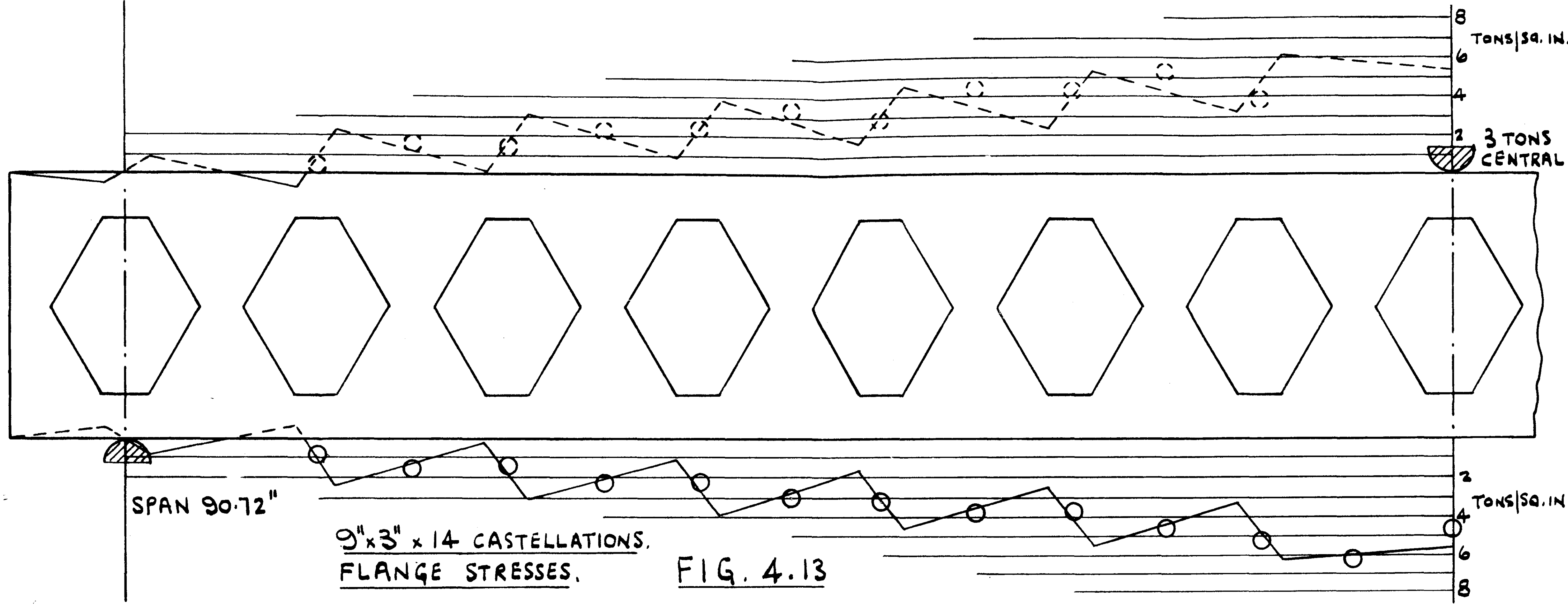

9" x 3" x 14 CASTELLATIONS.
FLANGE STRESSES.

FIG. 4.13

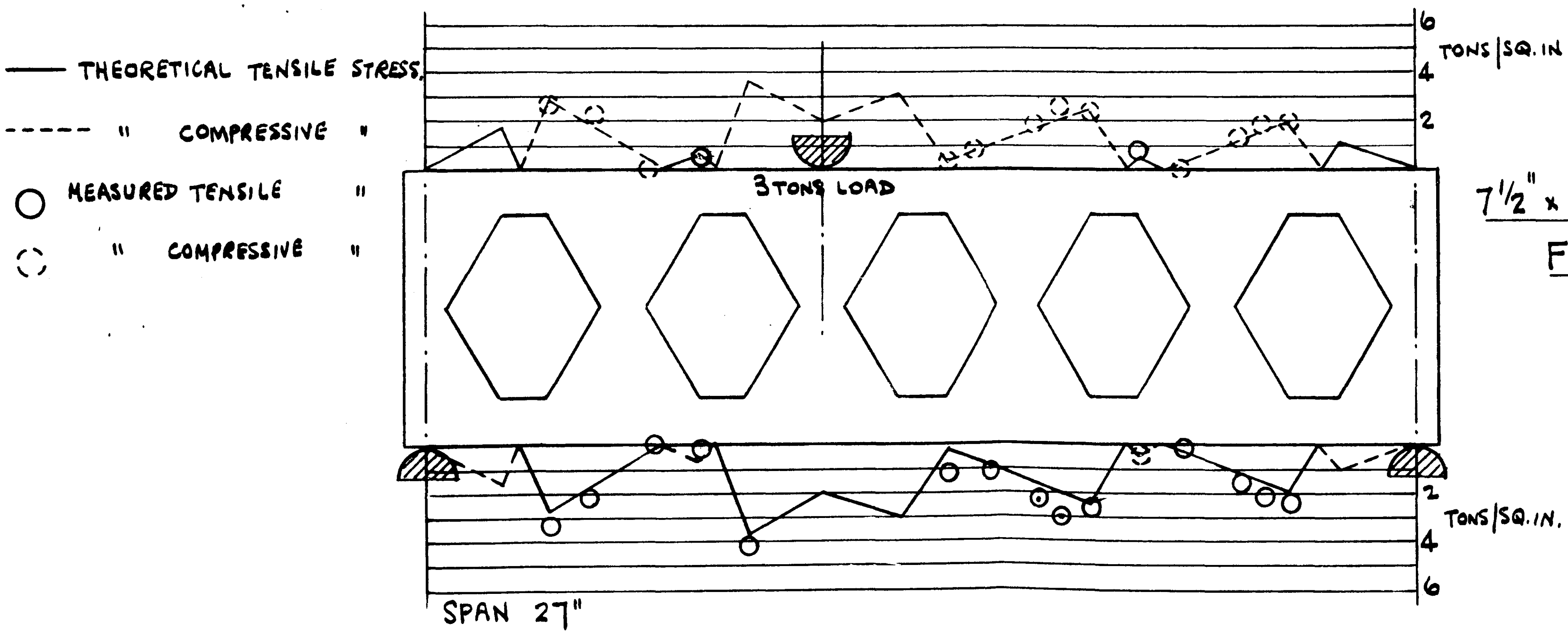

7½" x 3" x 5 CASTELLATIONS.
FLANGE STRESSES

FIG. 4.14.

FIG. 4.15

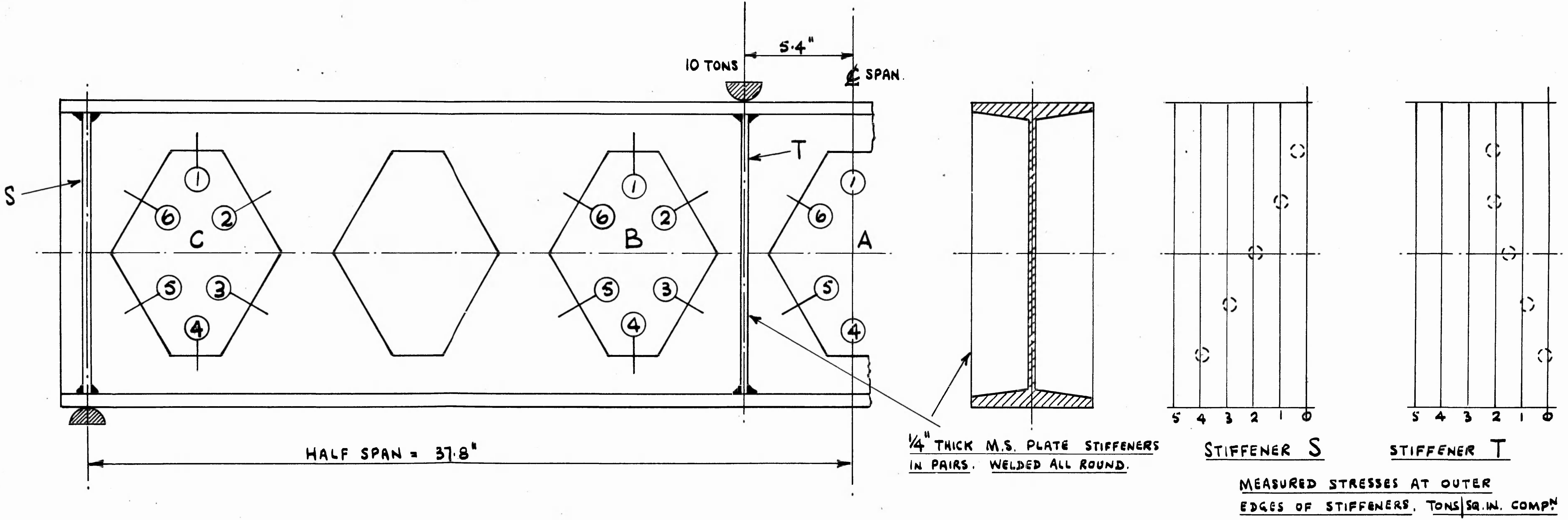

MEASURED STRESSES ON BOUNDARIES OF HOLES.

TONS/SQ.IN. TENSION +ve.

HOLE	POSITION	WITH STIFFENERS	WITHOUT STIFFENERS.
A	1	− 3·22	− 3·70
	4	+ 2·51	+ 2·72
	5	+ 1·87	+ 1·95
	6	− 3·76	− 6·00
B	1	− 4·24	− 4·00
	2	+ 8·20	+ 7·90
	3	− 9·60	− 10·10
	4	+ 2·40	+ 2·97
	5	+ 11·90	+ 11·80
	6	− 12·10	− 12·10
C	1	− 1·23	− 2·33
	2	+ 11·90	+ 12·90
	3	− 12·20	− 12·80
	4	+ 1·19	− 0·14
	5	+ 10·00	+ 11·10
	6	− 11·15	− 12·40

15" x 6" (EX. 15"x 6" R.S.J.) x 7 CASTELLATIONS.

SYMMETRICALLY LOADED WITH TWO 10 TONS. LOADS. FIG. 4.15.

Example 1. Consider the case of the $7\frac{1}{2}$" x 3" x 5 castellations beam (fig. 4.14) with concentrated load not at the centre. The force analysis for the members of this beam is as shown in fig. 2.6. Referring to fig. 4.14, for a load of 3 tons positioned as shown, the left hand reaction is 1.8 tons and the right hand 1.2 tons. The direct stress in the chord to the left of the load is given by, equation (2.34),

$$f_{dl} = \frac{1.8\ x}{d\ A} = \pm\ 0.182\ x \text{ tons/sq.in. (x inches)}$$

Similarly to the right of the load,

$$f_{dr} = \frac{1.2\ x}{d\ A} = \pm\ 0.121\ x \text{ tons/sq.in.}$$

The bending moments in the chords at the critical points (the top and bottom corners of the holes) are,

$$M_{cl} = \text{Shear at panel centre} \times D/12$$

$$= 0.9 \times \frac{7.5}{12} = 0.563 \text{ ton.ins.}$$

The corresponding outer fibre bending stress is,

$$f_{bl} = \frac{0.563 \times 0.376}{0.102} = \pm\ 2.08 \text{ tons/sq.in.}$$

(using t_2 and I_c from table 4.1)

Similarly, $M_{cr} = 0.6 \times \frac{7.5}{12} = 0.375$ ton.in.

and, $f_{br} = \frac{0.375 \times 0.376}{0.102} = 1.38$ tons/sq.in.

These stresses, when appropriately combined, are shown plotted in fig. 4.14 along with those obtained by experiment.

Example 2. Consider now the case of the 15" x $4\frac{1}{2}$" x 12 castellations beam (test I) shown in figs. 4.8, 4.9 and 4.10.

The direct stress in the chord is (eqn. 2.34),

$$f_d = \frac{W\ x}{2\ d\ A} = \frac{4\ x}{15\ .\ 2.85} = 0.0935\ x \text{ tons/sq.in.}$$

The vertical shear at the centre of each chord member is W/4 hence the bending moment at the critical sections in the chords is,

$$W/4\ .\ D/12 = 2.5 \text{ tons.ins.}$$

The bending stress at the outer face of the flange is,

$$f_{bo} = \frac{2.5 \times 0.505}{1} = \pm 1.26 \text{ tons/sq.in.},$$

and the bending stress at the inner face of the chord (the top and bottom edges of the holes) is,

$$f_{bi} = \frac{2.5 \times 1.991}{1} = \pm 4.97 \text{ tons/sq.in.}$$

The web stresses are best obtained in tabular form,

a) end members.

$$M_w = \frac{W\ell}{2 \times 4} = 10.8 \text{ tons. ins.}$$

Measuring x (ins) from the mid-height of the vertical the direct stress is,

$$f_{xd} = \frac{W/\cancel{2}4}{t_1 (D/6 + \frac{x}{\sqrt{3}})} = \frac{2}{0.3\ (2.5 + \frac{x}{\sqrt{3}})}$$

and the bending stress is,

$$f_{xb} = \frac{12\ M_w\ x}{t_1\ d\ (D/6 + \frac{x}{\sqrt{3}})^2} = \frac{28.8\ x}{(2.5 + \frac{x}{\sqrt{3}})^2}$$

Thus table 4.4 can be written down,

TABLE 4.4

x inches	f_{xd} tons/sq.in.	f_{xb} tons/sq.in.
0	2.68	0
1	2.17	3.03
2	1.83	4.30
3	1.58	4.85
4	1.39	5.02
5	1.24	4.97

b) Intermediate members (other than central member)

$f_{xd} = 0$ and, $M_w = Wl/24$

In a similar way to that above,

$$f_{xb} = \frac{57.6\,x}{\left(2.5 + \frac{2x}{\sqrt{3}}\right)^2}$$ hence table 4.5 below,

TABLE 4.5

x inches	0	1	2	3	4	5
f_{xb} tons/sq.in.	0	4.30	5.00	4.88	4.56	4.24

c) Central vertical $M_w = 0$ (by symmetry) and $T_w = 4$ tons.

Hence, $$f_{xd} = \frac{4}{t_1\left(D/6 + \frac{2x}{\sqrt{3}}\right)}$$, hence table 4.6 below,

TABLE 4.6.

x inches	0	1	2	3	4	5
f_{xd} tons/sq.in.	5.35	3.66	2.78	2.24	1.90	1.62

Again the above stresses, when appropriately combined, are shown plotted in figs. 4.8, 4.9 and 4.10 along with those obtained by experiment.

Test 15" x 4½" x 12 castellations No. II was designed to be compared with test I on the same beam to show the differences in stress distribution obtained by loading and supporting the beam at the centres of the holes instead of at the centres of the verticals. The results show the purely local nature of this effect.

The tests on the 15" x 4½" beams were the first to be carried out and it is evident that the critical stresses in the flanges have been missed by the practice of taking readings at the mid-points of each panel. This omission was rectified when the $7\frac{1}{2}$" x 3" beam was tested (fig. 4.14) and it is clear that these critical stresses do in fact occur as anticipated.

In general the agreement between actual and predicted stresses in the flanges is good. The differences are never serious and the agreement shown in fig. 4.14 is particularly good.

The same cannot be said for the web stresses however. Although the general distribution of stress is as anticipated there are some serious differences in the magnitudes of the stresses. This is generally most evident at the top and bottom corners of the holes where the theory completely fails to predict the stress concentrations occuring there. It should be borne in mind that a radius is left in these corners (in the case of the 15" deep beam the radius is $\frac{1}{2}$") and that the strain readings were taken with the gauges located, as nearly as possible, parallel to the boundary. No doubt these stress concentrations could be reduced if this radius were increased but it should be remembered that this would mean a sacrifice of some material at the mid-heights of the verticals.

Away from the top and bottom corners of the holes the agreement between measured and predicted stresses is better except in regions near concentrated loads where local disturbances of the stress distributions are evident.

The 15" x $4\frac{1}{2}$" x 12 castellations beam, loaded as for test II, was taken up to collapse load after the elastic tests had been carried out and at a central load of 15.7 tons local crushing of the top flange under the load was evident accompanied by pronounced lateral instability. Figure 4.16 shows the local crushing in the top flange at the load point as does fig. 3.5 also. Fig 4.17 shows the permanent set of the beam due to lateral buckling. This measured 0.35" at the centre of the beam on removal of the load.

The 9" x 3" x 14 castellations beam was also loaded to collapse. In this case lateral instability was evident at a central load of 7.9 tons and again a permanent set remained on removal of the load. Fig. 4.18 shows this beam after test.

It is not intended to pursue the matter of lateral instability of the beams in this thesis. The testing frame used would have required further modification if such an investigation was required and it was felt that the problem was big enough to warrant a separate investigation.

Web stiffeners.

Two beams were tested in an attempt to assess the efficiency of stiffeners for castellated beams. Both beams were made of 15" x 6" x 45 lb. R.S.Js. the holes being flame-cut in the web without expanding the beams. One beam had welded ¼" plate stiffeners at the supports and under the loads. This beam is shown in fig. 4.15 (and later in fig. 5.19). The other beam was identical except for the lack of stiffeners.

Both beams were subjected to two-point symmetrical loading of 20 tons total on a span of 75.6" and strain readings were taken at intervals along the outside edges of the stiffeners and at points on the boundaries of the holes. The results are shown in fig. 4.15. The stiffener stresses were measured on both sides of each stiffener

Fig. 4.16

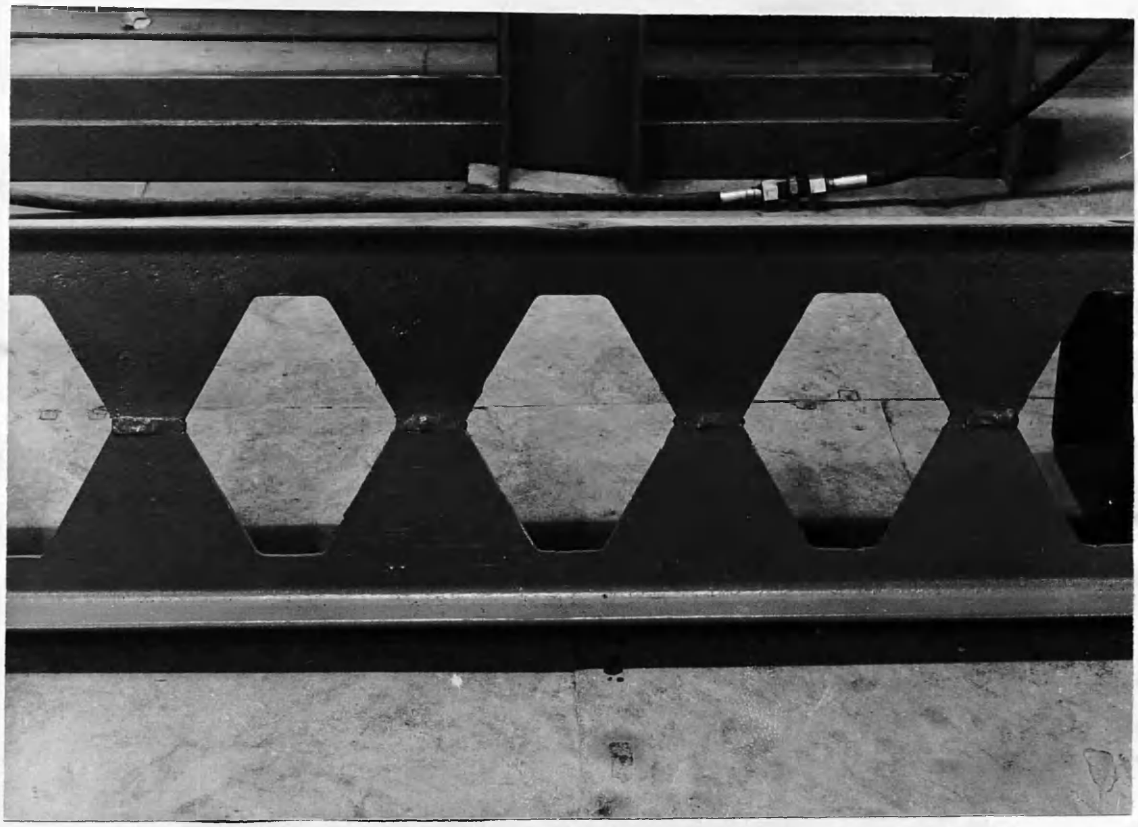

Figure 4.16

Showing local crippling of top flange at load point.

Fig. 4.17

Figure 4.17

15" x $4\frac{1}{2}$" beam after test showing permanent set due to lateral buckling.

Figure 4.18

9" x 3" beam after test showing
permanent set due to lateral buckling.

and both back and front and to left and right of the centre of the beam. Thus the stresses shown are in each case the mean of eight readings. The points on the boundaries of the holes at which stress readings were made are also shown in fig. 4.15 and the values of stress recorded are given in the table in the same figure.

It is seen that the presence of the stiffeners makes very little difference to the stresses in the web of the beam. Further, the stresses in the stiffeners themselves are relatively small. These two beams were later tested to collapse and the results of these tests will be given in chapter 5 when dealing with the subject of web stability.

CHAPTER 5

Web stability. Analytical and experimental treatment of the web problem.

The problem of web stability comes into prominence when comparatively heavy loads are applied to short spans. In order to be able to assess the behaviour of the beams over the whole working range of span/depth ratios it is necessary to be able to predict the critical loading condition which will produce instability or plastic deformation in the web.

Consider a simply-supported beam. The geometry of the beam at one of the supports is shown in fig. 5.1., in general this will be the critical portion of the web (the beams being supported at their ends) and the considerations of this chapter will be restricted to the behaviour of this part of the beam.

It is proposed to reduce the problem of web stability to that of a member subjected to axial thrust and major axis bending moments. The work of chapter 2 has shown that points of inflexion may be taken to occur at the mid-points of the members forming each panel. This being so the force actions on the portion of the web at a support can be resolved into a thrust of W/2 and equal major axis, double curvature, bending moments of Wl/4 at the ends of the member, where W is the reaction due to the imposed loading on the beam and l the spacing of the panels. These typical force actions are shown in fig. 5.2.

The shape of the member will be approximated to that shown in fig. 5.3 in order to give a condition of symmetry about the longitudinal axis.

The problem is complicated by,

a) the varying breadth of section.

b) The fact that the end moments are applied about the major axis (in the plane of the web) since this will produce torsional effects.

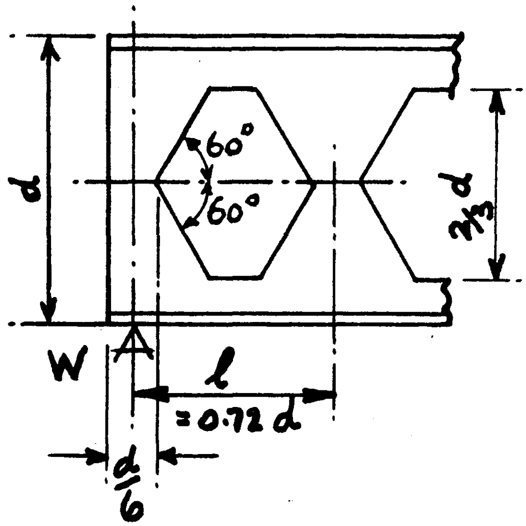

FIG. 5.1.

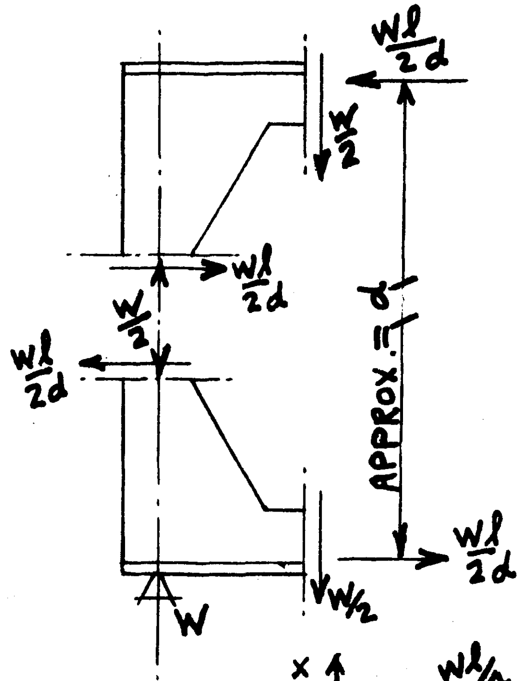

FIG. 5.2

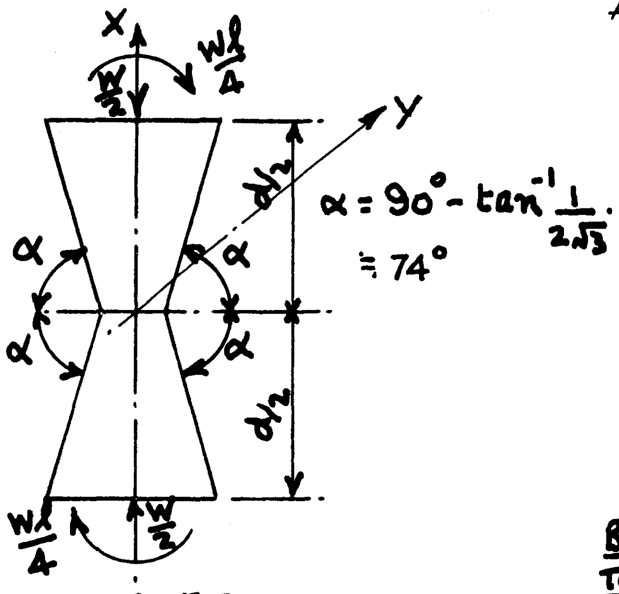

FIG. 5.3

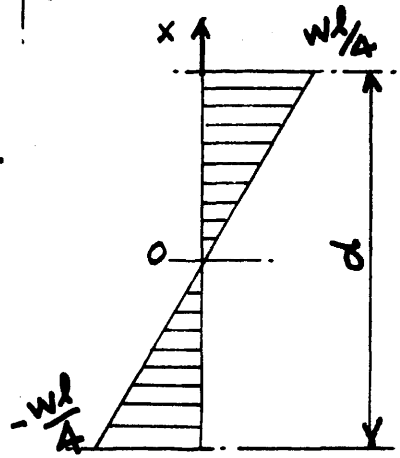

FIG. 5.4.

BENDING MOMENT DIAGRAM DUE TO APPLIED END MOMENTS IN THE PLANE OF THE WEB.

c) The uncertain nature of the support provided by the flanges.

d) The possibility of plasticity developing before the critical load for elastic instability is reached.

e) The presence of initial lack of straightness. Owing to the method of manufacture of the beams it would appear that some unavoidable lack of straightness will result.

f) The presence of residual stresses from rolling and particularly from the welding process.

In view of the foregoing complications it would be difficult to obtain a rigorous solution of the problem. The experimental results, which will be presented and discussed at a later stage, have all shown evidence of yield occuring at loads less than half the ultimate buckling loads. An elastic stability analysis would thus seem to be inappropriate and, bearing in mind the difficulties already mentioned, an elastic-plastic stability treatment would be intractable. The elastic behaviour only of the web will be considered here and an attempt will be made to find a simple approximate answer which can be compared with the experimental results. As far as possible the solution will be kept within the scope of B.S. 449 (1948) "The use of Structural Steel in Building". Referring to clause 22(a) of this specification it is stated that members subjected to both axial compression and bending stresses shall be so proportioned that the following condition is satisfied,

$$\frac{f_a}{F_a} + \frac{f_{bc}}{F_{bc}} \ngtr 1 \qquad \text{..................(5.1)}$$

where, f_a = the axial compressive stress,

F_a = the permissible axial compressive stress in the absence of applied bending moments,

f_{bc} = the sum of the compressive stresses due to bending about both rectangular axes, and,

F_{bc} = the permissible compressive bending stress in the absence of thrust.

For members of uniform section values of F_a are given in the specification in terms of the slenderness ratio of the member. These values are based on the Perry-Robertson strut formula (17) which gives the mean axial stress at which the yield point is just reached in a pin-ended strut with an initial lack of straightness. The value of F_{bc} to be used is also prescribed in the specification as the lesser of,

$$F_{bc} = \frac{1000}{L/r} \times K_1 \quad \text{tons/sq. in.} \quad \ldots\ldots\ldots\ldots\ldots\ldots (5.2)$$

where, L = length between effective lateral restraints which will be taken as d in this case. (ins)

r = radius of gyration of the section perpendicular to the plane of bending. (ins)

K_1 = a factor varying from 1.00 to 1.50 which is related to the shape of the cross-section and will always take the value 1.00 for castellated beams.

and, F_{bc} = 10 tons/sq. in. ....(5.3)

Equation (5.3) gives the upper limit on the allowable compressive bending stress and equation (5.2) relates to lateral instability and is based on the critical stress for a beam subjected to a uniform bending moment. In the case of a member of varying cross-section such as the web member of a castellated beam the value of F_a given in the specification (if based on the minimum cross-section) would err on the safe side almost to the point of being unrealistic and in order to obtain a more rational value for this particular problem the behaviour of the member will be investigated in a little more detail. Consider first the action of the axial thrust alone.

Effect of axial thrust in the absence of applied bending moments.

The following assumptions or simplifications are made,

1) Full lateral restraint is provided to the compression flange of the beam. This would seem a reasonable assumption since it is generally made when dealing with the other criteria of design i.e., limiting stress and deflection.

2) The ends of the web member are fully fixed in direction. The extent of direction fixing in an actual beam will be difficult to assess, it will depend on, among other things, the torsional rigidity of the flanges. In the short span cases where the subject of web stability is of importance it is probable that the extent of direction fixing will be considerable.

3) The applied thrust is given by W/2 at all stages of loading.

4) The initial deviations from straightness can be adequately represented by a cosine curve.

5) The additional deflections caused by the application of the axial thrust can also be represented by a cosine curve.

The initial lack of straightness is taken to be given by,

$$y_0 = \frac{b_0}{2}\left(1 + \cos\frac{2\pi x}{d}\right) \qquad \text{................(5.4)}$$

with co-ordinate axes directed as shown in fig. 5.3, and the additional deflections take the form,

$$y = \frac{b}{2}\left(1 + \cos\frac{2\pi x}{d}\right) \qquad \text{................(5.5)}$$

The strain energy stored in the member will be taken as that due to bending alone and is given by,

$$U = \frac{1}{2}\int_{-d/2}^{+d/2} EI\left(d^2y/dx^2\right)^2 dx \qquad \ldots\ldots\ldots\ldots\ldots\ldots(5.6)$$

where, $EI = EI_0\left(1 \pm \frac{2\sqrt{3}x}{d}\right)$ from $x = 0$ to $x = \pm d/2$ $\qquad \ldots\ldots\ldots\ldots\ldots\ldots(5.7)$

and, $I_0 = \frac{dt^3}{72}$ $\qquad \ldots\ldots\ldots\ldots\ldots\ldots\ldots\ldots\ldots\ldots\ldots\ldots(5.8)$

the second moment of area of the cross-section at the centre.

The work done by the axial load in the case of a member with initial curvature is derived by Hoff (18) as,

$$V = \frac{P}{2}\int_{-d/2}^{+d/2}\left\{2\,dy/dx\cdot\frac{dy_0}{dx} + \left(dy/dx\right)^2\right\}dx \qquad \ldots\ldots\ldots(5.9)$$

where P represents the axial thrust, in this case equal to W/2.

Carrying out the necessary integrations,

$$U = \frac{\pi^2 P_e}{2d}\left(2b^2 + c\frac{b^2 d}{2}\right) \qquad \ldots\ldots\ldots(5.10)$$

where, $P_e = \frac{\pi^2 EI_0}{d^2}$ $\qquad \ldots\ldots\ldots\ldots\ldots\ldots\ldots\ldots\ldots\ldots(5.11)$

i.e. the first Euler load for the minimum cross-section,

and, $c = \frac{2\sqrt{3}}{d}$ $\qquad \ldots\ldots\ldots\ldots\ldots\ldots\ldots\ldots\ldots\ldots\ldots(5.12)$

Also, $V = \frac{\pi^2 P}{4d}\left(2bb_0 + b^2\right)$ $\qquad \ldots\ldots\ldots\ldots\ldots\ldots(5.13)$

The condition of equilibrium is represented by,

$$U = V \qquad \ldots\ldots\ldots\ldots\ldots(5.14)$$

whence, $P = P_e\frac{(4b^2 + cb^2 d)}{(2bb_0 + b^2)}$ $\qquad \ldots\ldots\ldots\ldots\ldots(5.15)$

In the case of an initially straight member the load producing elastic instability becomes,

$$P = 7.5\,P_e \qquad \ldots\ldots\ldots\ldots\ldots\ldots(5.16)$$

This is to be compared with $P = 4\ P_e$ for a member of uniform cross-section equal to the minimum section at the centre of the web member and gives an indication of the extra strength available.

The value of P given by equation (5.16) was checked using the Lagrangian Multiplier method (19) and virtually the same result was obtained.

Now Δ = the total central displacement = $b + b_o$

whence from (5.15),

$$P = 7.5\,P_e\left(\frac{\Delta - b_o}{\Delta + b_o}\right) \qquad \text{................(5.17)}$$

or, $$\Delta = \left(\frac{7.5\,P_e + P}{7.5\,P_e - P}\right) b_o \qquad \text{................(5.18)}$$

Now the critical stresses will occur at the central section (in the absence of applied bending moment) where the bending moment M_c is given by, $M_c = -EI\,d^2y/dx^2 = EI_o\left(\frac{2b\pi^2}{d^2}\right)$ from (5.5)

Hence the maximum compressive stress is,

$$f_{max} = \frac{3W}{dt} + \frac{\pi^2 Et}{d^2}(\Delta - b_o)$$ where t = web thickness.

Substituting for Δ from (5.18),

$$f_{max} = \frac{3W}{dt} + \frac{2\pi^2 E t b_o}{d^2}\left(\frac{P}{7.5\,P_e - P}\right)$$

A simplification may be made at this stage if it is observed that $7.5\ P_e$ will always be considerably greater than P, and f_{max} then becomes,

$$f_{max} = \frac{3W}{dt} + \frac{\pi^2 E t b_o W}{7.5\,d^2\,P_e} \qquad \text{..............(5.19)}$$

The mean value of all the measurements of b_o made (see results later) can be taken as $b_o = 0.003\ d$ and giving f_{max} the usual value of yield stress for mild steel i.e. 15.25 tons/sq.in. the following results

$$p = \frac{15.25}{1 + 0.0096\,(d/t)} \qquad \ldots\ldots\ldots\ldots\ldots(5.20)$$

The value of p in equation (5.20) is the mean intensity of longitudinal stress which produces yield in compression at the centre of the member. Applying a load factor of 2 to this,

$$F_a = \frac{7.625}{1 + 0.0096\,(d/t)} \qquad \ldots\ldots\ldots\ldots\ldots(5.21)$$

This is the value of F_a which will be used in equation (5.1).

The value of f_a the actual longitudinal stress is given by,

$$f_a = \frac{3\,W}{d\ t} \qquad \ldots\ldots\ldots\ldots\ldots(5.22)$$

Effect of applied bending moments in the absence of axial thrust.

A separate investigation of the critical stresses occuring under the actions of the applied bending moments alone would be much more complex and is hardly justified in view of the previous simplifications and the fact that a simple, practical solution is sought.

The provisions of B.S. 449 will therefore be followed as closely as possible. Using equation (5.2) with $r = \sqrt{\frac{t^2}{12}} = \frac{t}{3.46}$

where t is the web thickness, $F_{bc} = 289\ t/d$, with the provision that, $F_{bc} \not> 10$ tons /sq.in.

Whence for values of $d/t \geqslant 28.9$

$$F_{bc} = \frac{289}{d/t}$$

and for values of $d/t \leqslant 28.9$

$$F_{bc} = 10 \text{ tons/sq.in.} \qquad \ldots\ldots\ldots\ldots\ldots(5.23)$$

Now referring to fig. 5.4 the bending moment at point x is,

$$M_x = 0.36\ W\ x$$

and the outer fibre bending stress is,

$$f_{bc} = \frac{2.16\ W\ x}{t(d/6 + x/\sqrt{3})^2}$$

The maximum value of f_{bc} is given by $df_{bc} / dx = 0$

i.e., $x = \pm\ d/2\sqrt{3}$

whence, $f_{bc\ max.} = 5.6 \dfrac{W}{dt}$ ....(5.24)

Substituting the values of F_a, f_a, F_{bc} and f_{bc} from (5.21),(5.22), (5.23) and (5.24) in equation (5.1) maximum safe values of W (the reaction at the support) are given by,

$$\left.\begin{array}{l} \underline{\text{for } d/t \leq 28.9}, \\ \quad W = \dfrac{dt}{3\left(\dfrac{1 + 0.0096\, d/t}{7.625}\right) + 0.56} \\ \underline{\text{for } d/t \geq 28.9}, \\ \quad W = \dfrac{dt}{3\left(\dfrac{1 + 0.0096\, d/t}{7.625}\right) + \dfrac{5.6\, d/t}{28.9}} \end{array}\right) \quad ......(5.25)$$

Alternatively the maximum safe values of mean longitudinal stress are given by,

$$\left.\begin{array}{l} \underline{\text{for } d/t \leq 28.9} \\ \quad p = \dfrac{1000}{318 + 1.26\, d/t} \\ \underline{\text{for } d/t \geq 28.9} \quad p = \dfrac{1000}{131 + 7.71\, d/t} \end{array}\right) \quad ......(5.26)$$

The relationships given by equations (5.26) are plotted in fig. 5.6 along with the expression for F_a from equation (5.21) and values of F_a obtained from table 7 pf B.S. 449. In using table 7 B.S. 449 the effective length of the member was taken as 0.7 d and the radius of gyration as $t/\sqrt{12}$.

This concludes the theoretical treatment of the problem but before proceeding to the experimental work the shear stresses existing in the weld at the mid-height of the member will be considered briefly.

Shear stress at weld.

Referring to fig. 5.2 the horizontal shear force acting on the weld at the centre of the web member is equal to $\frac{W\,l}{2\,d}$. Providing complete penetration of the weld is achieved in accordance with B.S. 449 clause 44 (c) the area resisting shear is dt/6.

In addition the weld is subjected to a thrust of W/2 and the resultant stress is given by,

$$f_s = \sqrt{\left\{\left(\frac{Wl}{2d}\cdot\frac{6}{dt}\right)^2 + \left(\frac{3W}{dt}\right)^2\right\}} = 3.69\ W/dt$$

The allowable maximum shearing stress is obtained from B.S. 449 clause 20 as 6.5 tons/sq.in. Whence the maximum shearing stress limit on the value of W is given by, $W \leqslant 1.76\ d\,t$

and the maximum permissible value of mean longitudinal stress is,

$$p = 3 \times 1.76 = 5.28 \text{ tons/sq. in.}$$

The welds in the intermediate members (other than under load points) carry no axial thrust but a value of horizontal shear of Wl/d. By a similar reasoning to that used above it is readily shown that the maximum permissible value of mean longitudinal stress is

$p = 3.53$ tons/sq. in. which is less than that above and hence the more critical of the two, however, the values of p given by equation (5.26) are seen to be less than this for all values of d/t. It may be concluded that shear stress at the weld is not critical and it is significant that of all the tests conducted by the author in no case did any sign of weld failure occur. In one test carried out by the makers, in a series of six, weld failure occured at a load approaching the buckling load but later examination showed the weld to be faulty.

Experimental work on web stability.

The tests were all conducted on beams in the "as received" condition supplied by the makers, the beams being cut to length by sawing as required.

Figure 5.5 shows diagrammatically the test arrangement. The beams were simply-supported and loaded in all cases with two concentrated loads from hydraulic jacks measured by means of pressure capsules. The disposition of the loads and the span for each test are shown in table 5.1 along with other experimental data. In cases where it was intended to examine the web continuously throughout the loading process up to buckling the loads were asymmetrically disposed about the centre of the span. The two loads were maintained equal for all the measurements and the end of the beam where the reaction was greatest was the end examined.

The two hydraulic jacks were completely independent each having its own pump and pressure capsule.

The tests on the 15" x 6" beams were carried out in the University of Glasgow, in the testing frame already described, and were in the nature of preliminary tests as far as web buckling was concerned. Numbers 1 and 2 of these tests were designed to show the difference, if any, between a welded and an unwelded beam. Both these beams had holes flame cut in the web according to the standard pattern, beam 1 was tested in this condition whilst beam 2 was cut and welded along the centre-line for the whole of its length. The welded beam required a higher load to produce buckling (table 5.1) but it is not intended to attach any significance to this as the

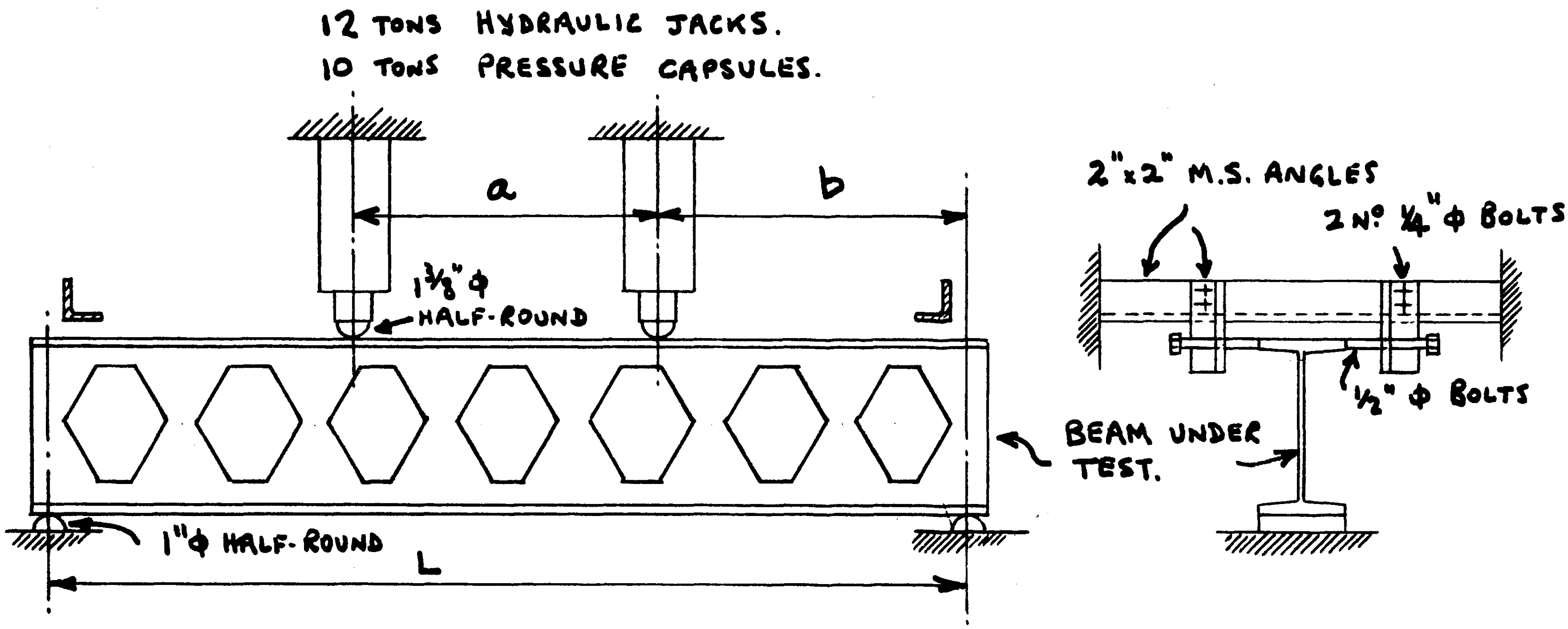

LOADING ARRANGEMENT SHOWING LATERAL RESTRAINING DEVICE.

FIG. 5.5

Table. 5.1

SUMMARY OF TESTS ON WEB STABILITY

TABLE 5.1.

SECTION	TEST.	LOADING ARRANGEMENT FIG. 5.5			MEASURED WEB THICKNESS	MEASURED VALUE OF b_o	LOAD W TONS AT FIRST SIGN OF YIELD.	ULTIMATE LOAD W TONS	MEAN LONGITUDINAL STRESS AT YIELD TONS/SQ.IN.	MEAN LONGITUDINAL STRESS AT BUCKLING TONS/SQ.IN.	$\frac{d}{t}$	COMMENTS.
		a	b	L								
$4\frac{1}{2}" \times 1\frac{1}{2}"$	1	16"	6.4"	29.2"	0.200"	.0022 d	NO RESULT	4.5	NO RESULT	15	22.5	
	2	"	"	"	0.203"	.0033 d	NO RESULT	4.5	NO RESULT	14.8	22.2	
	3	"	"	"	0.195"	.0024 d	3.4	–	11.6	–	23.0	TEST DISCONTINUED AT W = 3.4 TONS. SOME PERMANENT SET REMAINED.
$6" \times 3"$	1	"	7.0"	30.2"	0.210"	.0060 d	NO RESULT	5.0	NO RESULT	12.0	28.6	
	2	"	"	"	0.210"	.0033 d	NO RESULT	5.6	NO RESULT	13.3	28.6	
	3	"	"	"	0.210"	.0050 d	2.6	5.0	6.2	12.0	28.6	
$7\frac{1}{2}" \times 3"$	1	"	4"	27"	0.210"	.0044 d	3.6	7.9	6.9	15.0	35.7	
	2	"	"	"	0.220"	.0013 d	2.3	6.5	4.2	11.8	34.1	
$15" \times 6"$	1	10.8"	32.4"	6'-3½"	0.380"	–	NO RESULT	18.5	NO RESULT	9.75	39.5	HOLES FLAME CUT OUT OF 15"×6" × 45# R.S.J.
	2	"	"	"	0.380"	–	NO RESULT	21.0	NO RESULT	11.1	39.5	DITTO BUT CUT ALONG ℄ OF BEAM AND WELDED.
	3	6'-3½"	"	11'-8½"	0.360"	–	NO RESULT	22.0	NO RESULT	12.2	41.7	
$9" \times 3"$	1	13.5"	6.25"	32.4"	0.225"	.0006 d	2.9	7.9	4.3	11.7	40	
	2	"	"	"	0.225"	.0029 d	NO RESULT	8.25	NO RESULT	12.2	40	

difference in load between the two tests is not greater than that found in other tests on supposedly identical beams.

The remainder of the tests were carried out at King's College in the structural testing space frame shown in fig. 5.16. These tests were more exhaustive in that the behaviour of the web member was observed at all loads up to buckling and in each case an attempt was made to record the load at which yield first developed.

Deflections were measured with Mercer dial gauges reading to 0.0001" and strains with the 20 mm. gauge length Mai-hak vibrating wire gauges already mentioned. Again the clamp shown in fig. 3.4 was used to hold two gauges in position on the specimen.

The Mai-hak equipment permitted a continuous exploration of strain that would not have been possible with fixed resistance gauges. A few readings sufficed to show the region of maximum strain and this could then be studied in more detail.

The lateral restraining device used in the space frame is also shown in fig. 5.5 and again in fig. 5.17. At each end of the beam under test a 2" x 2" M.S. angle was fixed in the frame at right-angles to the beam and on this were bolted, in suitable positions depending on the flange width under test, two short lengths of 2" x 2" angle. These were drilled and tapped to take ½" dia. bolts which were arranged to bear on the top flange of the beam under test. This device provided lateral support and enabled the top flange to be returned to its original position after each load increment so that the position fixing would be virtually 100%. In order to achieve the latter a dial gauge was positioned on the top flange and a constant reading maintained using the half-inch dia. bolts as the test proceeded. The arrangement can be seen in fig. 5.17 which also shows the buckled form of a beam after test.

The following is an outline of a typical test procedure,

1) Check dimensions of beam, i.e. depth, web thickness, dimension d/6 at mid-height of web etc.,

2) Measure lack of straightness at centre with 0.001" depth gauge.

3) Arrange beam in frame and check dimensions a, b and L (fig.5.5)

4) Attach dial gauges, strain gauges etc.,

5) Apply a small load a number of times until uniformity of readings with load is achieved.

6) Carry out the test removing strain gauges before taking beam up to ultimate load.

One difficulty in using the Mai-hak gauges lies in the limitation on the total strain that can be recorded for a single setting of the gauge. This varies from gauge to gauge but for the 20 mm. gauges is always of the order of 7.5×10^{-4}, and with $E = 13,400$ tons/sq.in. this represents a stress of approximately 10 tons/sq.in. If it is required to measure strains larger than this the zero reading of the gauge has to be changed during the test and this introduces a source of possible error. However, if the setting of the gauge is changed well within the limit of elasticity some check is obtained from the continuity of the readings. This method was found to work quite satisfactorily providing reasonable care was taken with the gauges.

The experimental results are summarized in table 5.1 which gives the reactions W at which first yield and buckling occured with the corresponding values of mean longitudinal stress. These results are also shown plotted in fig. 5.6.

A selection of the results of strain and deflection readings is shown in figs. 5.7 to 5.15. These are sufficient to give a fairly complete picture of the behaviour of the beams. Figs. 5.7 and 5.13 show the variation in longitudinal stress along the length of the web member and the maximum mean compressive stress is seen to occur at a depth below the centre approximately equal to 0.25 d which agrees fairly well with the theoretical value of 0.29 d.

Fig. 5.10 shows the variation in longitudinal stress at the mid-height of the member for test 6" x 3" No.1 showing reasonable agreement between theoretical and actual values. The agreement is better in the case of test $4\frac{1}{2}$" x $1\frac{1}{2}$" No. 1 shown in fig. 5.12. In the first case the effect of bending in a plane normal to that of the web has been overestimated and in the second case it is seen to be underestimated.

In studying the buckled form of the web it was observed that in all cases the centre of the node occured at a point about 0.16 d below mid-height. In testing 6" x 3" No. 3 strains were measured at this point and the results are plotted in fig. 5.10 so that a comparison may be made with stresses occuring at the centre of the member in a similar beam.

A typical buckled form is shown by fig. 5.17 and fig. 5.18.

In all cases the strain measurements were made at points as near as the width of the gauges allowed to the straight boundary of the member. In fact these measurements were made at points distant approximately $\frac{1}{8}$" from the boundary. In consequence the actual boundary stresses will be generally somewhat higher than those recorded but it is not thought that the differences will be serious.

Agreement between predicted and measured stresses is generally

FIG. 5.6

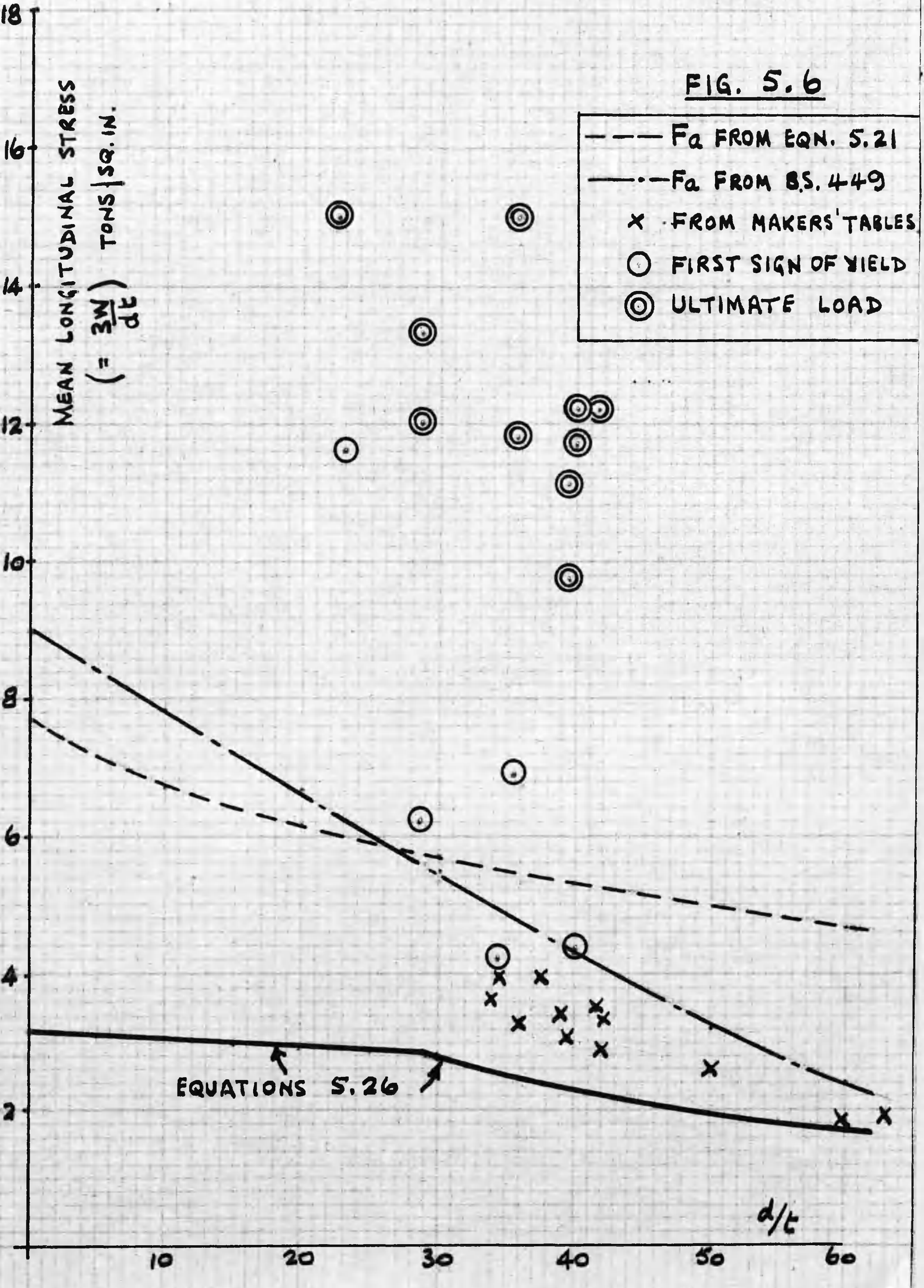
Fa FROM EQN. 5.21
Fa FROM B.S. 449
FROM MAKERS' TABLES
FIRST SIGN OF YIELD
ULTIMATE LOAD
MEAN LONGITUDINAL STRESS
(= 3W/dt) TONS/SQ. IN.
EQUATIONS 5.26
d/t
18
16
14
12
10
8
6
4
2
10
20
30
40
50
60

Fig. 5.7

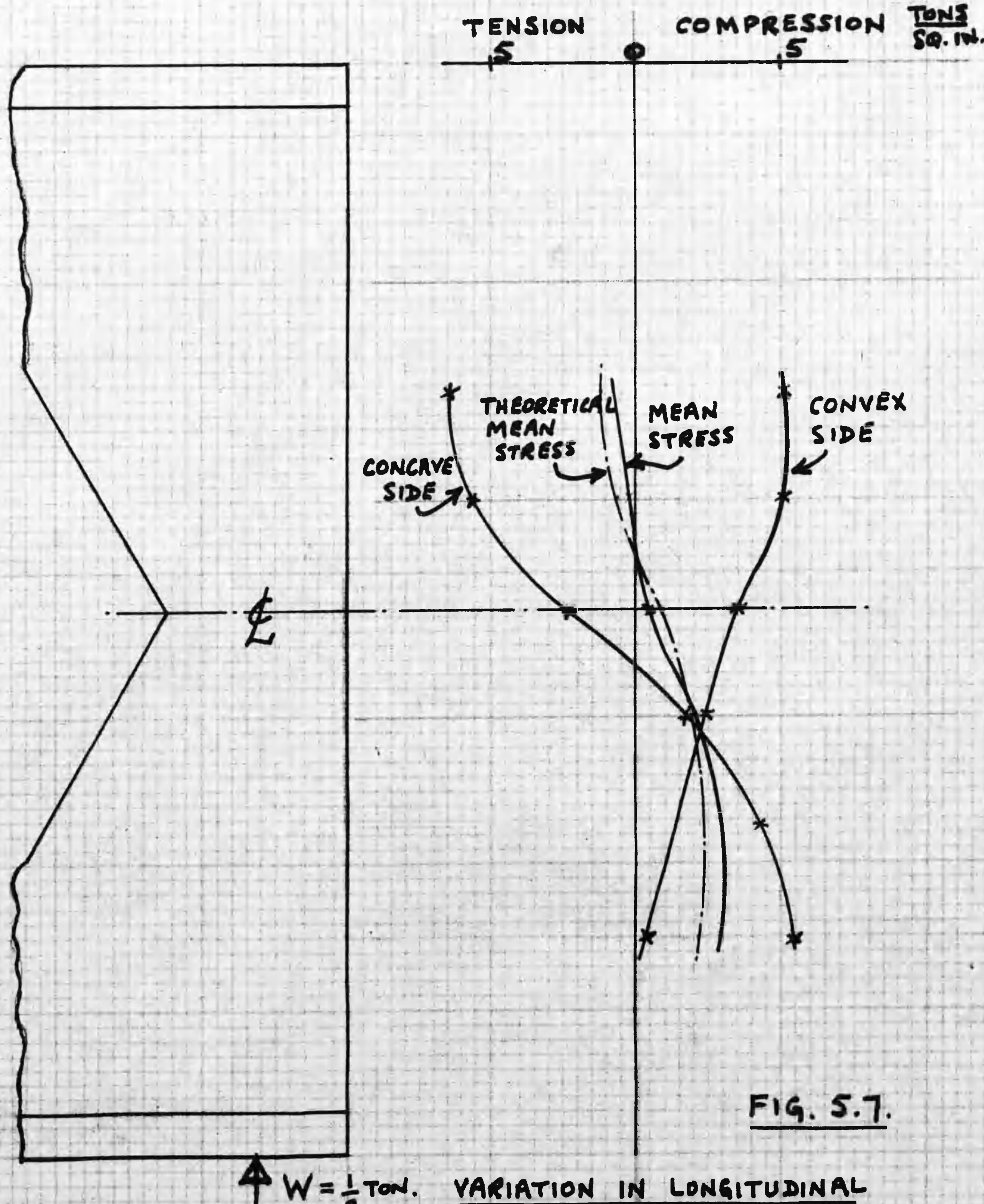

FIG. 5.7.

VARIATION IN LONGITUDINAL STRESS. TEST 7½" x 3" Nº 2.

Fig. 5.8

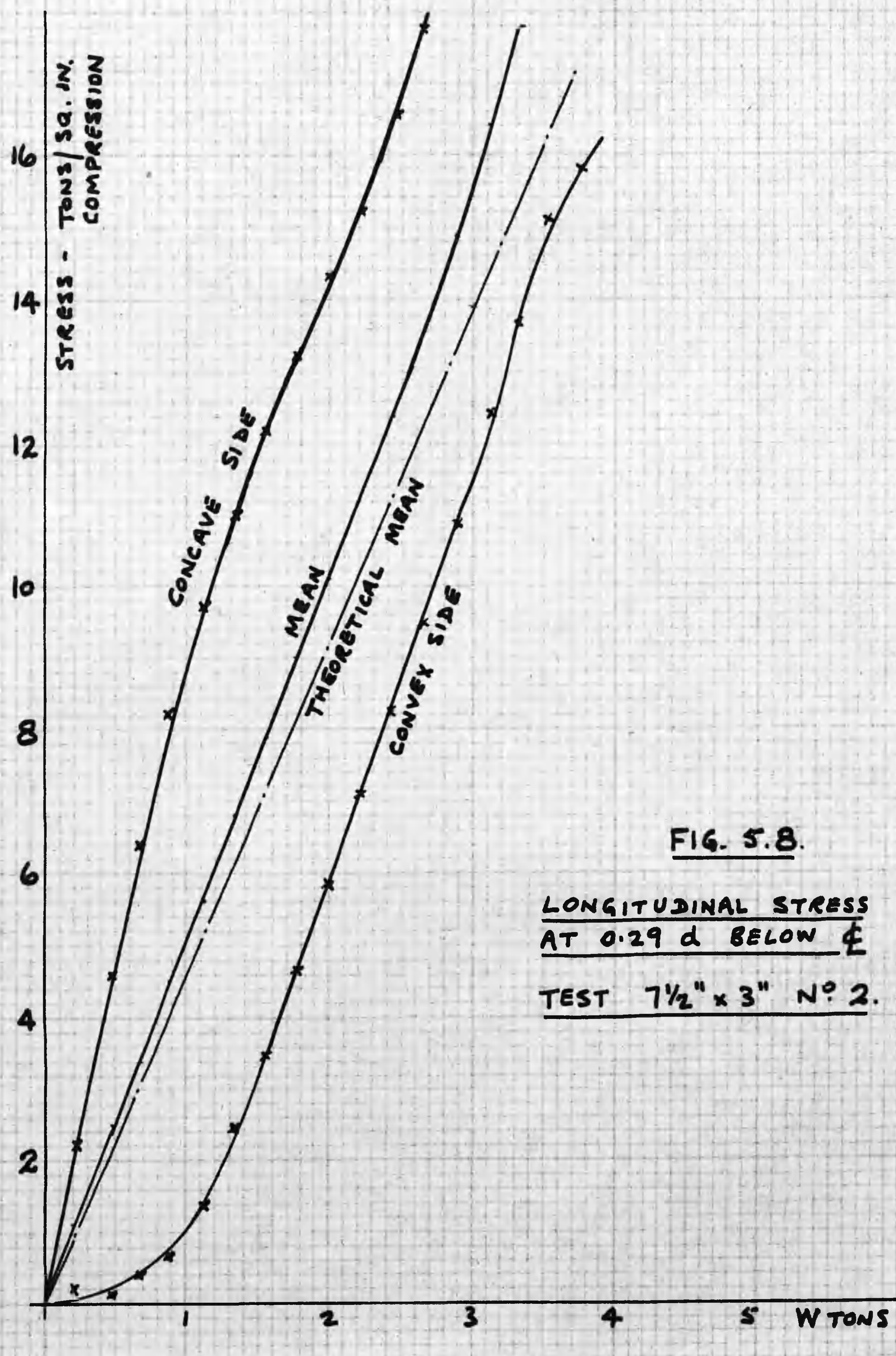

FIG. 5.8.

LONGITUDINAL STRESS AT 0·29 d BELOW ℄

TEST 7½" x 3" Nº 2.

Fig. 5.9

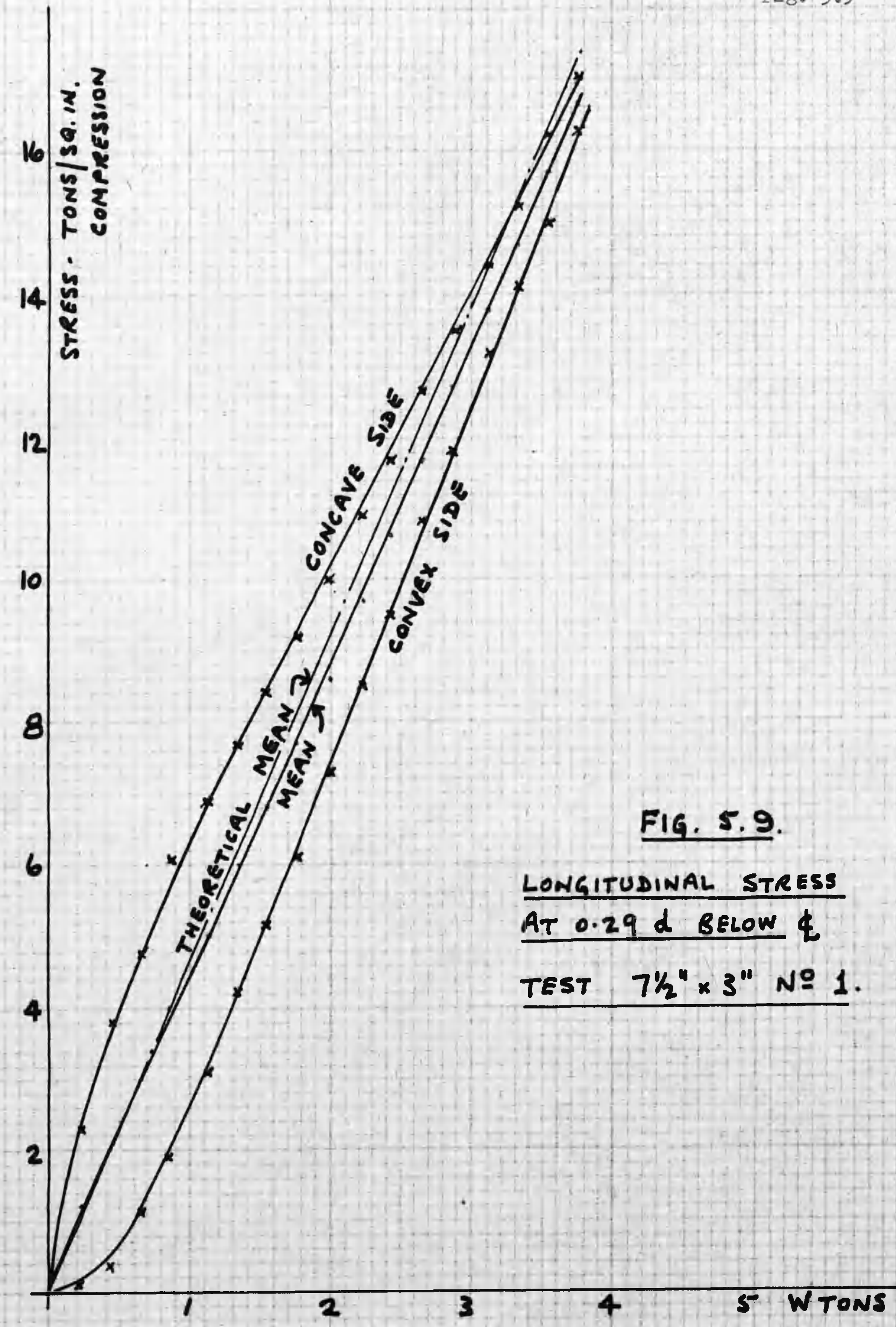
STRESS - TONS/SQ. IN. COMPRESSION
16
14
12
10
8
6
4
2
1
2
3
4
5 W TONS
CONCAVE SIDE
THEORETICAL MEAN
MEAN
CONVEX SIDE
FIG. 5.9.
LONGITUDINAL STRESS
AT 0·29 d BELOW ℄
TEST 7½" × 3" Nº 1.

Fig. 5.10

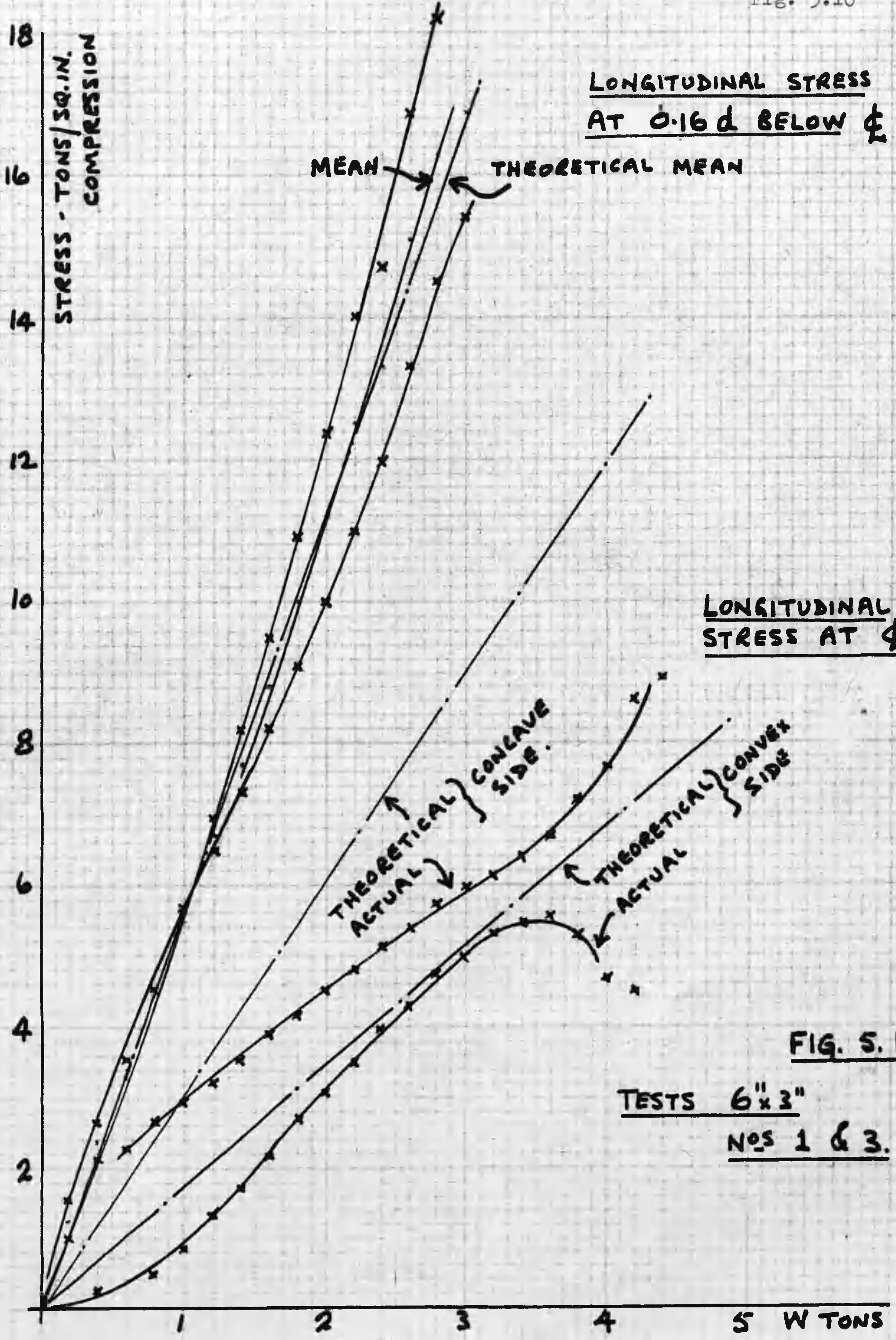

FIG. 5. 10.

TESTS 6" x 3"
Nos 1 & 3.

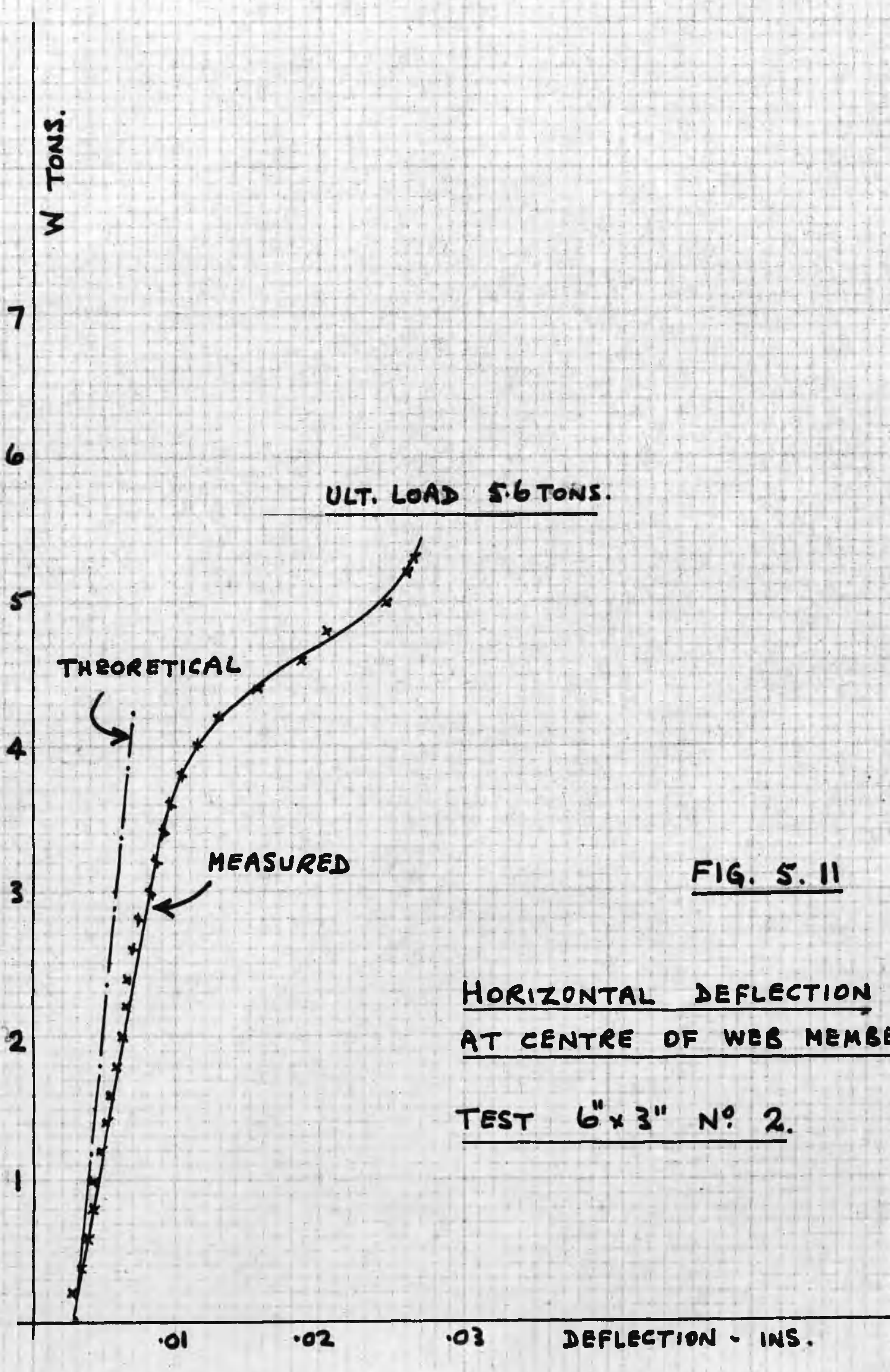

FIG. 5. 11

HORIZONTAL DEFLECTION AT CENTRE OF WEB MEMBER.

TEST 6" x 3" No. 2.

Fig. 5.12

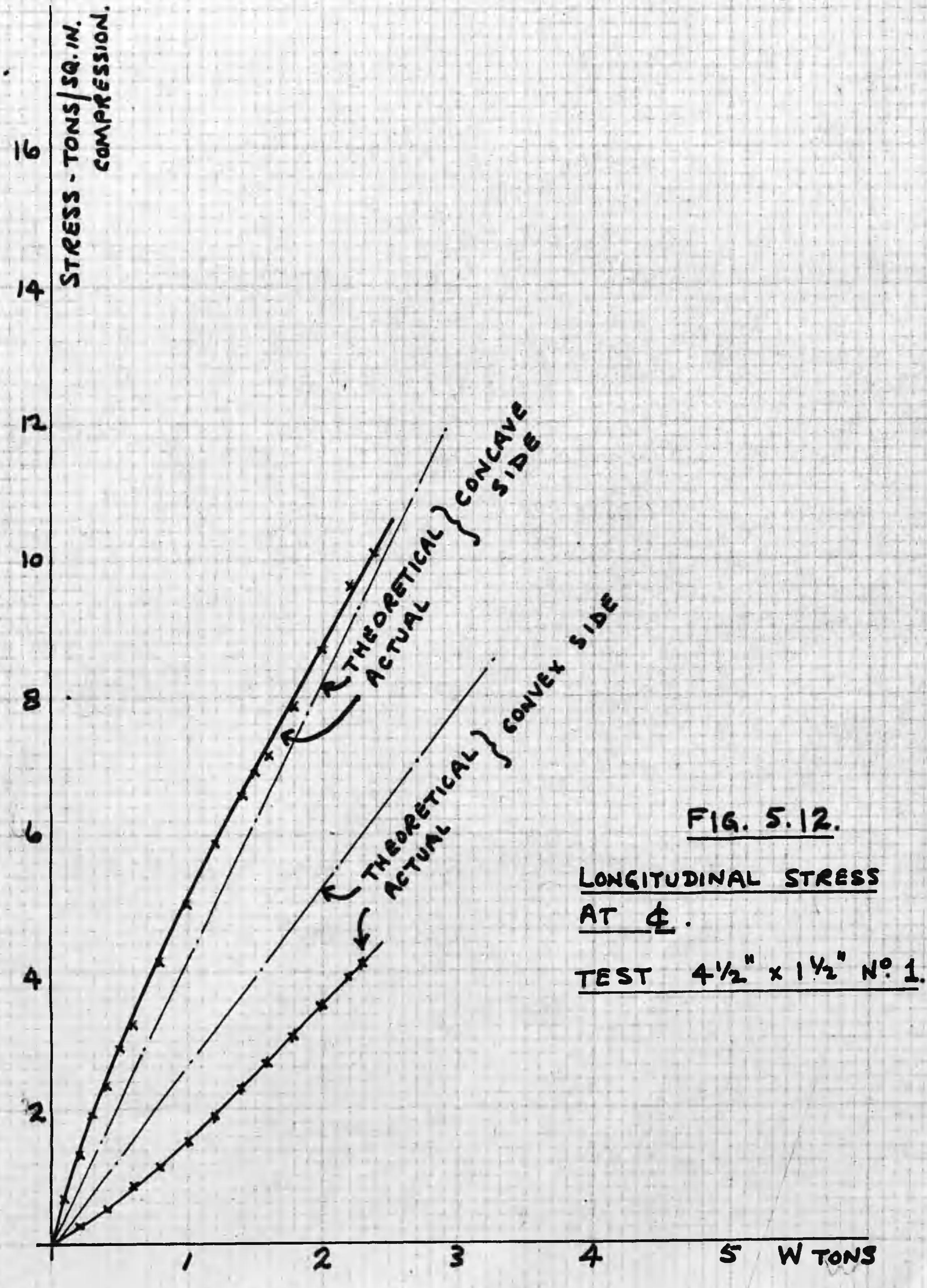

FIG. 5.12.

LONGITUDINAL STRESS AT ℄.

TEST 4½" x 1½" No. 1.

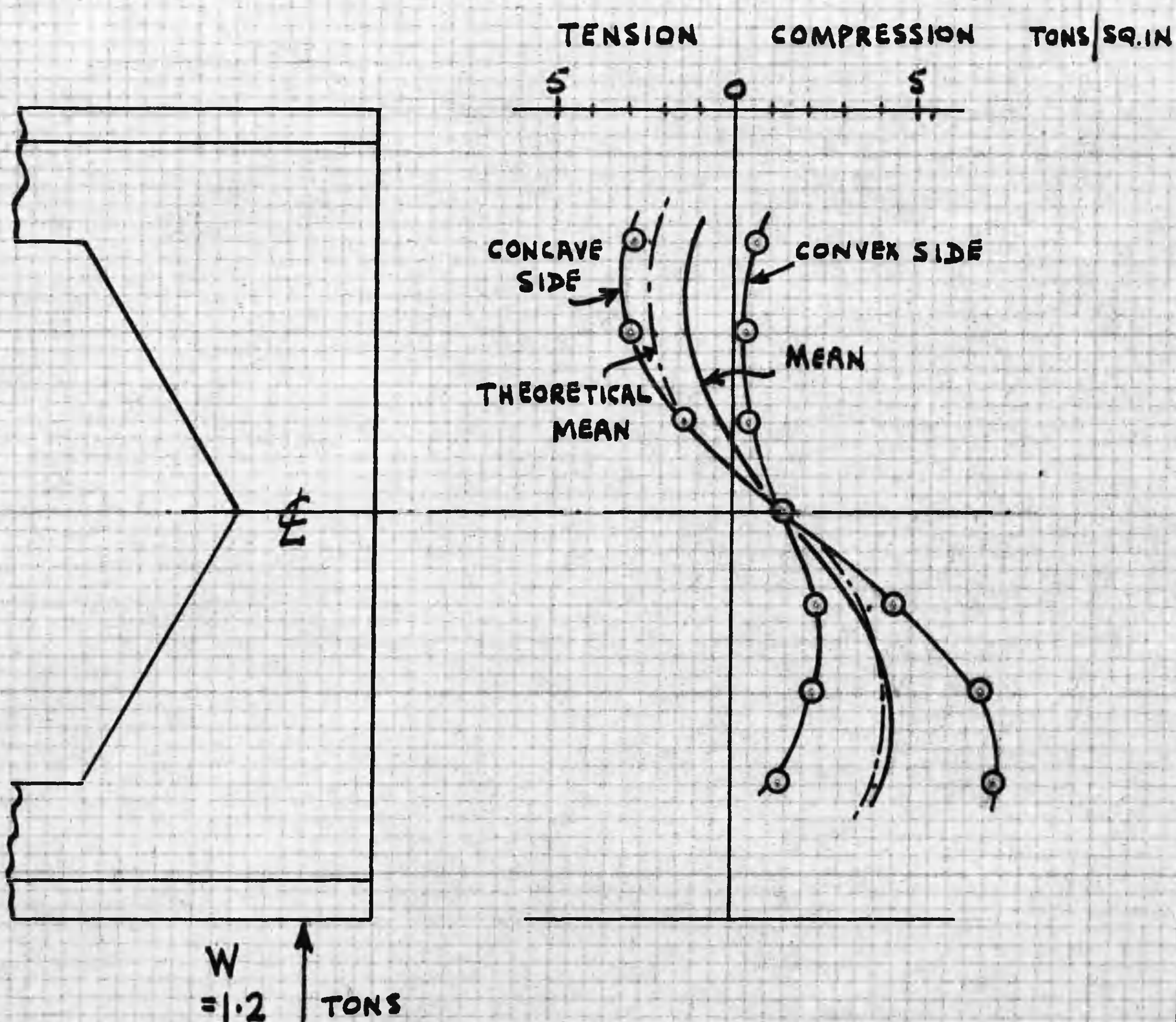

VARIATION IN LONGITUDINAL STRESS. TEST 9"x3" No. 1.

FIG. 5.13.

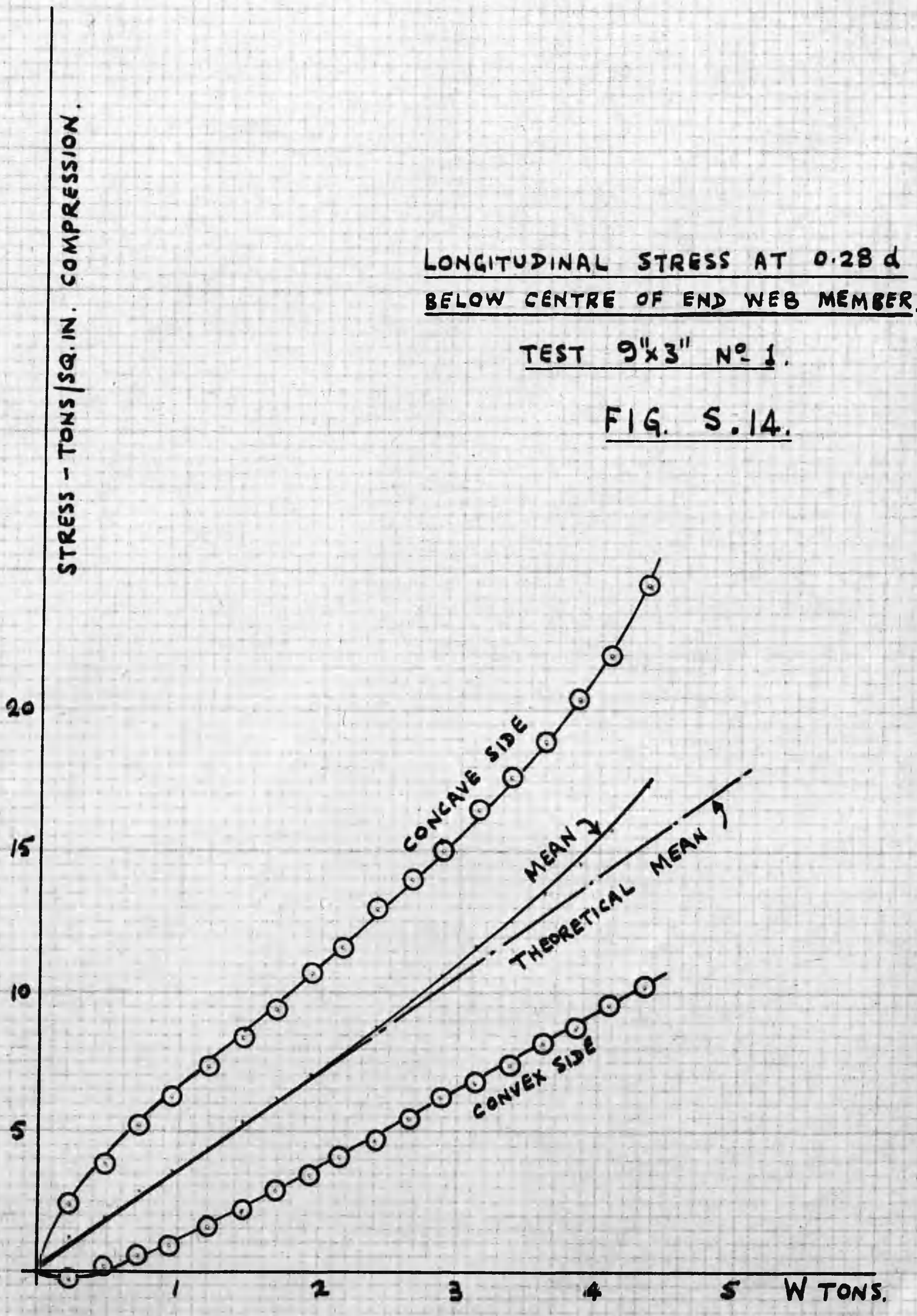
LONGITUDINAL STRESS AT 0.28 d
BELOW CENTRE OF END WEB MEMBER.
TEST 9"x3" No. 1.
STRESS - TONS/SQ.IN. COMPRESSION.
20
15
10
5
1
2
3
4
5
W TONS.
CONCAVE SIDE
MEAN
THEORETICAL MEAN
CONVEX SIDE

FIG. 5.14.

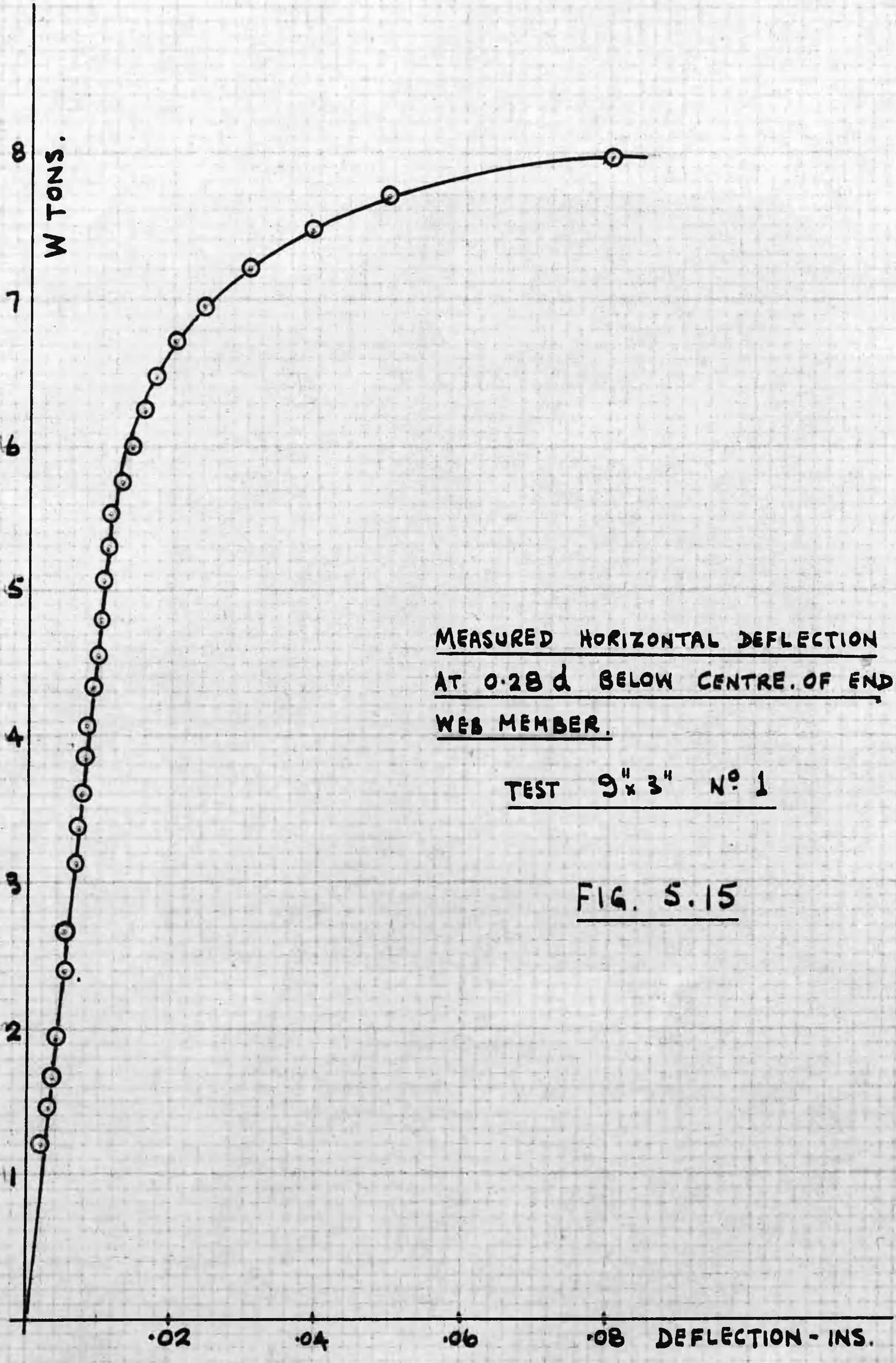
W TONS.
8
7
6
5
4
3
2
1
·02
·04
·06
·08
DEFLECTION - INS.
MEASURED HORIZONTAL DEFLECTION
AT 0·28 d BELOW CENTRE. OF END
WEB MEMBER.
TEST 9" x 3" No 1

FIG. 5.15

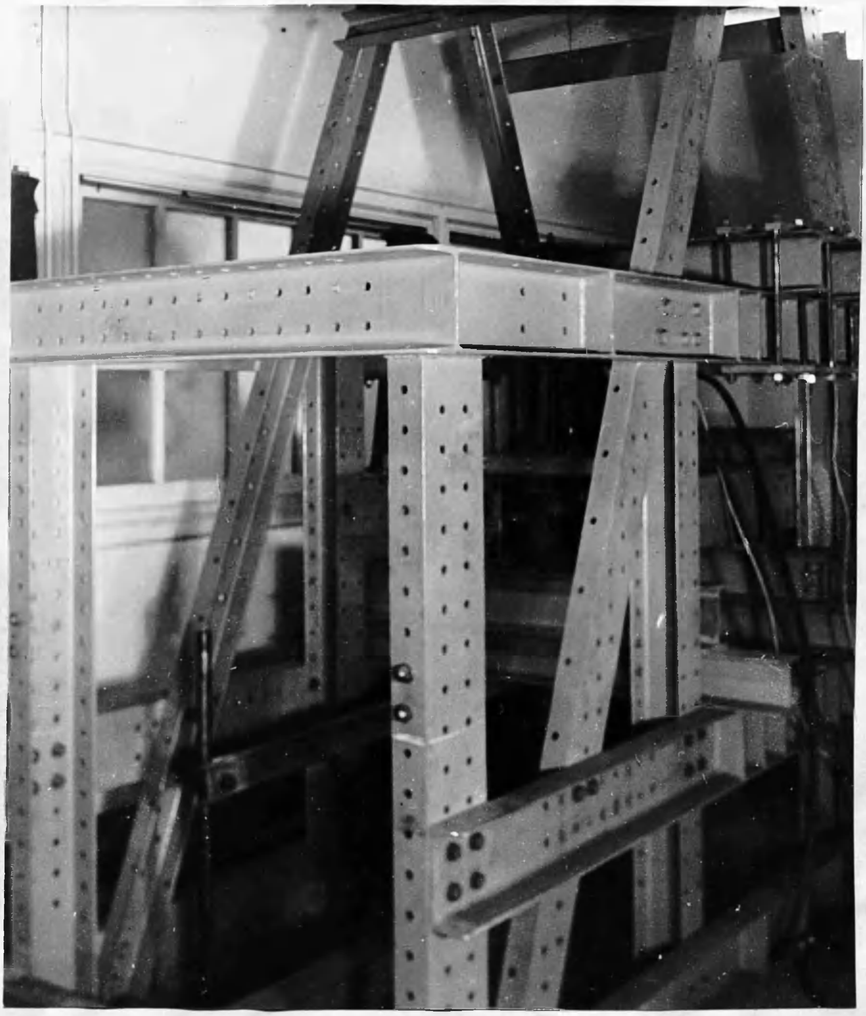

Figure 5.16

Space frame, Structures Laboratory, King's College.

Fig. 5.17

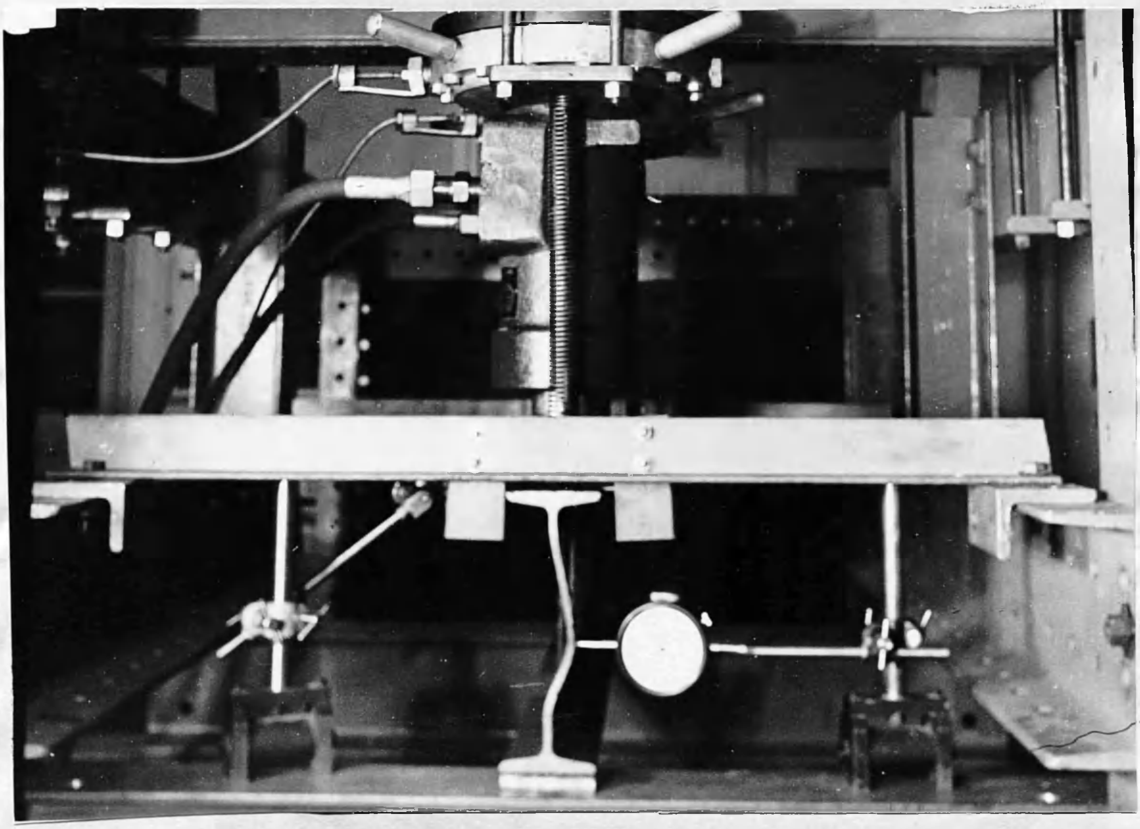

Figure 5.17

Showing space frame, lateral restraining device and beam after test.

Fig. 5.18

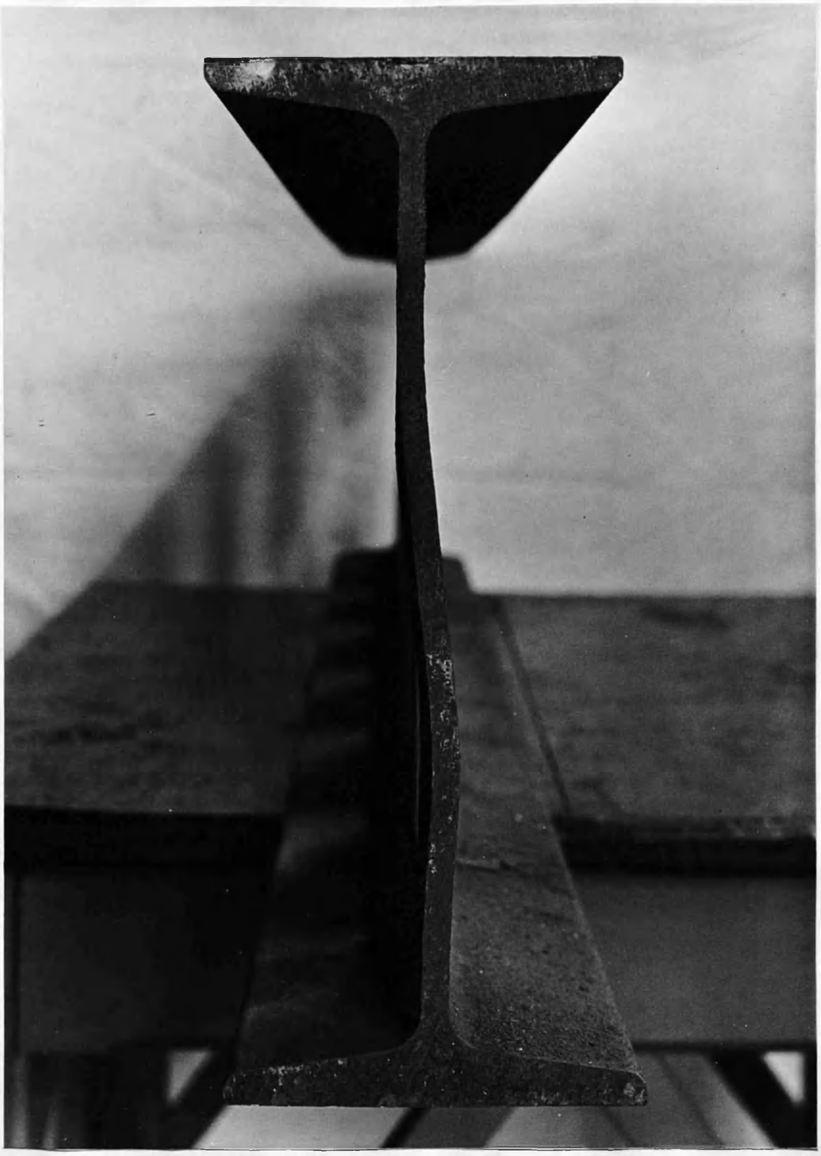

Figure 5.18

A typical web buckling failure.

good, in fact better than would be expected in view of the far reaching simplifications made in the theory. The approximation in the shape of the member to that of fig. 5.3 does not seem to have invalidated the theory and would thus appear to be acceptable.

The theoretical deflection at the centre of the member as obtained from equation (5.18) is sustantially below that obtained by experiment, see fig. 5.11. This is probably due to relative rotation of the flanges. An attempt was made in developing the theory to take some account of this but the solution rapidly became difficult to manipulate and, in view of the difficulty in assigning a suitable value to the torsional stiffness of the flanges, it was discarded. The comparison between the actual and predicted stresses is somewhat better, figs. 5.10, 5.12 and 5.14.

Referring now to the results shown in fig. 5.6 and using safe values of mean longitudinal stress as given by equations(5.26) the following table of load factors (table 5.2) can be deduced.

TABLE 5.2

Test		Load factor based on first yield.	Load factor based on collapse.
$4\frac{1}{2}$" x $1\frac{1}{2}$"	1	No result	5.17
	2	Do.	5.11
	3	3.87	no result
6" x 3"	1	no result	4.28
	2	Do	4.75
	3	2.22	4.28
$7\frac{1}{2}$" x 3"	1	2.76	6.00
	2	1.68	4.72
9" x 3"	1	1.87	5.10
	2	no result	5.30
15" x 6"	1	no result	4.24
	2	Do.	4.83
	3	Do.	5.54

The lowest load factor based on first yield is 1.68 and the highest 3.87 the average being 2.48. The theory is thus conservative since it is based on yield occuring at a load factor of 2.00.

The lowest load factor based on collapse is 4.24 and the highest 6.00 the average being 4.9 which shows the high reserve of strength possessed by the beams.

All the "first yield" load factors in table 5.2 are based on the load at which a stress of 15.25 tons/sq.in. was recorded. In some of the cases where "no result" is quoted central deflection curves were constructed for the end web members and if load factors are based on the departure of this curve from the straight line the following table (5.3) results.

TABLE 5.3

Test		load factor based on sudden change in curvature of load-deflection diagram.
$4\frac{1}{2}$" x $1\frac{1}{2}$"	1	3.45
	2	2.82
6" x 3"	2	2.89
9" x 3"	1	3.48

These load factors are generally higher than those from table 5.2 based on a yield stress of 15.25 tons/sq.in. which might indicate that the use of this value of yield stress tends to be rather cautious.

It was observed that some of the beams had an initial twist in the flanges and in testing them no attempt was made to eliminate this by packing either under the jacks or over the supports it being felt that the beams should be tested as near the "as received" condition as possible. It was necessary however to file off the proud weld at the centre in order to be able to take strain measurements there. Beam $7\frac{1}{2}$" x 3" No.2 had a marked twist in the flanges prior to testing and this probably accounts for the low loads carried by this specimen at failure.

In spite of the high load factors obtained it is necessary to proceed with caution when the theory is extended to beams with a d/t ratio greater than 40. Beams within this category could not be tested in the frame available as the loads would have exceeded the capacity of the frame. For a more complete investigation it would be necessary to test some of these deeper beams.

A yield stress of 15.25 tons/sq.in has been used throughout as this is the generally accepted value for mild steel. It is known however that mild steel exhibits a yield stress in compression somewhat higher than this, whilst there is a tendency for the stress to rise continuously during plastic deformation (20). This would appear to be borne out in some of the tests conducted particularly the 9" x 3" No 1. Referring to fig. 5.14 it is seen that stresses of up to 20 tons/sq.in are recorded at a load of 4 tons and fig. 5.15 shows no sign of distress in the member at this load.

The work of this chapter concludes with some notes and test results on the use of web stiffeners.

<u>Web stiffeners.</u>

The two beams tested in the web stiffener investigation of chapter 4 (see fig. 4.15) were loaded to collapse after the elastic measurements had been made. These results are given in table 5.4 below.

TABLE 5.4

Test	Max. load carried	Mode of collapse.
Beam with stiffeners	2 x 20 = 40 tons	local buckling in the web between loads and supports away from stiffeners. Test discontinued when this became evident.
Beam without stiffeners	2 x $18\frac{1}{2}$ = 37 tons	Web buckling at one end.

One further beam tested having the same section as those above, loaded in the same way, and having no stiffeners sustained a load of 2 x 21 = 42 tons before web buckling occured at one end.

A more thorough investigation of the use of stiffeners would be needed before any conclusions could be definitely drawn but the above, along with the corresponding results from chapter 4, would seem to indicate that stiffeners are not of very great utility in these beams.

The stiffened beam is shown in fig. 5.19 and again after test in fig. 5.20. The latter shows the permanent set due to vertical bending. A string line was stretched tightly between the ends of the top flange and this is seen clearly in the figure.

Two further tests were carried out on 15" x 6" beams on the subject of stiffened webs. Each beam was of 11' $8\frac{1}{2}$" span and carried two-point loading symmetrically placed at 6' $3\frac{1}{4}$" centres about the centre of the beam. One beam had the end castellations open and the other had the end holes filled in with welded plate. The results of testing these beams to collapse are shown in table 5.5.

Figure 5.19

The 15" x 6" beam with welded stiffeners.

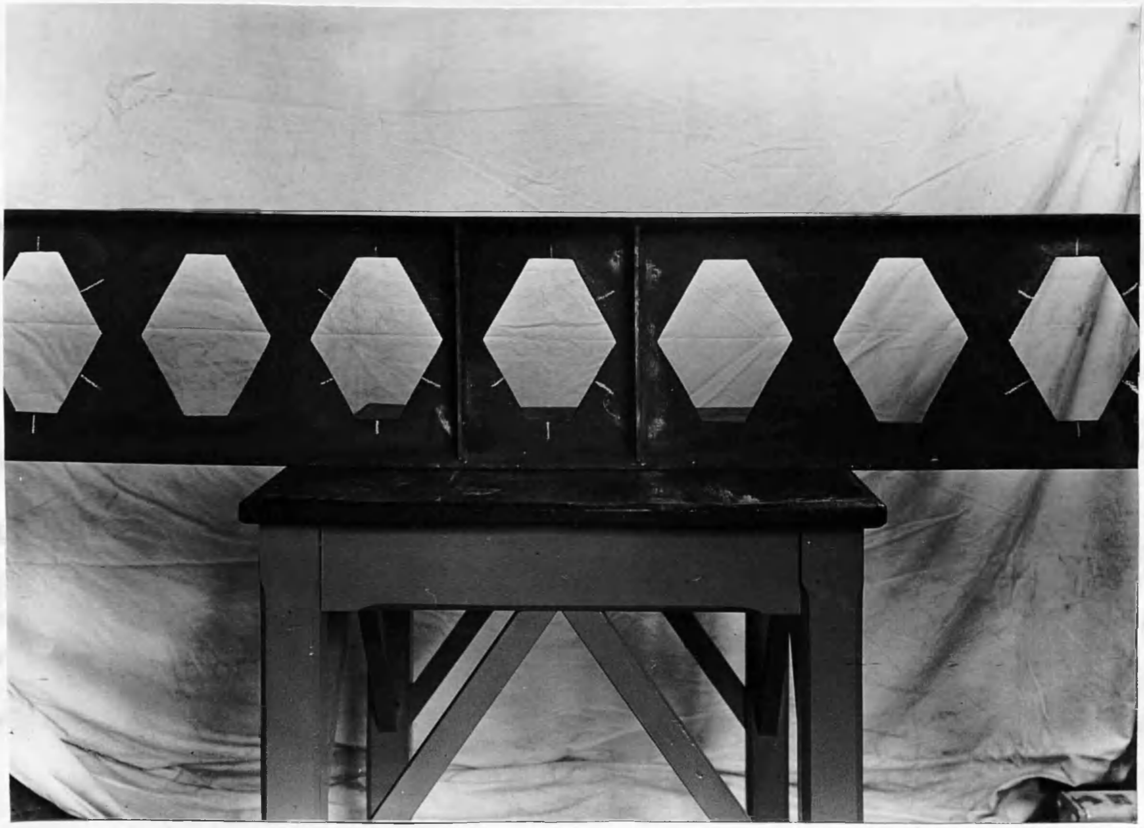

Figure 5.20

The stiffened beam after test showing
permanent set due to vertical bending.

TABLE 5.5

Test	max. load carried	Mode of collapse
Beam, open end castellations	2 x 22 = 44 tons	Web buckling at one end over support.
Beam with end castellations filled-in	2 x 24 = 48 tons	Some sign of local crippling in top flange under one load. No visible signs of buckling in the beam.

Again these results could not be taken as conclusive without a more thorough investigation but the indication is that the filling-in of the end castellations increases the ultimate strength of the beams by a small, but measurable, margin.

CHAPTER 6

Discussion. Recommendations for design.
Mention of related problems not investigated.

Bibliography and references.

It has been the purpose of this work to attempt to give a fairly complete picture of the behaviour of castellated beams over a range of spans and loading conditions wide enough to cover the more critical cases. The central concentrated load has been extensively employed as it is possibly the most critical loading condition of all and is the one most easily manipulated in the theoretical work. The alternative two-point loading condition was adopted where it was desired to produce high shears at the ends of the beams and a region of uniform bending between the loads. Other loading arrangements may be desirable in order to illustrate other features but it was felt that these were of a secondary nature.

Throughout the work on stress distribution the emphasis has been on the determination of boundary stresses. In this connection it is felt that the vibrating wire strain gauge was the best gauge to use. Once a suitable clamp was designed to hold the gauges the measuring of strains was both quickly and easily accomplished. The gauges have the distinct advantage of permitting a less extensive preparation of the surface than with other gauges, and a freedom for the operator to explore the stress distribution at will. An equivalent exploration using electrical resistance gauges would have been much more time consuming.

The use of the gauges to measure internal stress distributions is not so convenient however. An attempt was made to design a clamp which would enable internal strains to be measured but this was not successful. Some measurements of this kind were made with electrical resistance strain gauge rosettes but the results were not very illuminating and have not been included in this thesis.

Some discussion of the test results and their relation to theoretical values has already been included at the ends of chapters 4 and 5, but it would seem convenient to restate some of these remarks here in order that an overall impression of the results may be obtained.

The subject of deflection, an important one from the point of view of design, has been treated in a fairly comprehensive way. As expected the deflections of the beams for short and intermediate spans are considerably greater than those predicted by simple bending theory. This is due to two main factors; the deformation of the chords due to secondary bending and that due to the bending of the web members. These factors are taken into account in the deflection theory based on the concept of a continuous web medium and the result is that deflections for intermediate and long spans can be more closely predicted using this theory. For short spans even this theory is inadequate but deflections in these cases are generally unimportant, considerations of maximum stress and buckling coming into prominence.

It is seen that the simple vierendeel theory based on the assumed location of points of inflexion is adequate for the determination of flange stresses. The disturbances of the flange stress distribution due to secondary bending of the chords is seen to be small for intermediate and long spans. In these cases the simple bending theory gives flange stresses comparable with the vierendeel theory. For shorter spans it would seem necessary to take account of these secondary stresses.

In the case of the web the vierendeel theory is seen to predict the type of stress distribution which occurs but it is inadequate in a number of respects. The magnitudes of the stresses are usually somewhat greater than those anticipated, particularly at the top and bottom corners of the holes and in regions near concentrated loads or reactions. Over the greater part of the web however, away from the corners and the immediate influence of concentrated loads, the differences are not nearly so serious. Generally the measured stresses are of the order of 10 to 15 % higher than the theoretical values.

Further it is seen that the stress concentrations at the top and bottom corners of the holes are of a purely local nature and for this reason may not necessarily be critical.

The theory of the behaviour of the end web member at a support is shown to be conservative although the variation in experimental results is such that some of the load factors obtained are less than the one adopted in the development of the theory.

The experimental work on web stability was limited to beams with a d/t ratio of 41.7 or less. Many castellated sections have d/t ratios greater than this, for example a 36" x 7½" beam has a d/t ratio of 63 and a 30" x 6½" beam a ratio of 67. The testing of these deeper beams would have required a much larger capacity testing frame than the one used. Although the results show a certain uniformity throughout the tests the extension of the theory to deeper beams should be practised with caution.

The ratio of the average load factors based on collapse and first yield of the end web member is seen to be of the order of two. It may be possible to utilise some of this reserve of strength but it is thought that this matter warrants further investigation before this is done.

The subject of the most economical profile for castellation has not been dealt with but is naturally an interesting one in the light of the results obtained and will be briefly mentioned here.

The major variables in the selection of the profile are: a, b and θ of figure 6.1.

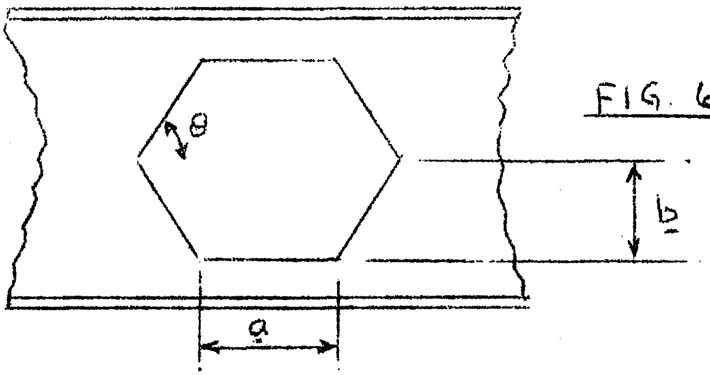

FIG. 6.1.

The dimension b controls the gain in depth by expansion from the original section, a and θ control the geometry of the resulting hole. An increase in b for a given original section produces a deeper beam but weakens the section of the chord. An increase in a gives more material at the mid-height of the web member but lengthens the "bridge" of the castellation and would tend to increase the secondary bending stresses there and produce larger deflections.

It is clear that the variables must be handled jointly and a compromise must be made. If the value of b is chosen such that the increase in depth is 50 % (as for the beams tested in this work) then a and θ can be fixed from considerations of deflection, stress and web buckling. If it is decided that the extra work involved in stiffening the web is justified then a can be kept short and the deflections reduced.

Referring back to chapter 1. fig. 1.3 it is clear that, for the unstiffened beam, the important criteria are deflection and web buckling as defined by point C and curve B D of the figure. An increase in the dimension a gives a higher load at point C but lower loads along the deflection curve BD.

For a given span it would not be difficult to choose the most economical profile but for a general profile to cover all spans for a given initial section a decision has to be made first of all on the question of whether to stiffen the web.
Clearly an answer is not immediately available as to the best profile. The only statement which can be made in this respect in the light of the present experimental evidence, is that for beams with stiffened webs (where necessary) the existing profile as used in this country is perhaps as good as any.

Related problems not investigated.

Apart from the question of the most economical profile certain related problems not investigated in the present work will be briefly mentioned.

The lateral stability of the beams probably deserves a separate investigation. The torsional rigidity of the castellated beam will be reduced by the presence of the holes. Generally the design is based on lateral support being provided to the compression flange of the beam and in these cases lateral instability need not be considered.

The use of castellated sections as columns is another topic of lesser importance. The advantages of expanding rolled sections are less in evidence for columns than for beams and this probably accounts for the tendency to restrict their use almost exclusively to beams.

In a work of this kind many results both theoretical and experimental are naturally excluded in order to keep the presentation as concise as possible. The author hopes that by so doing nothing of importance has been omitted.

BIBLIOGRAPHY AND REFERENCES.

1) "An investigation of welded open-web expanded beams" Altfillisch, Cooke and Toprac. The Welding Journal" (American Welding Society) Vol.XX11 No.2. February 1957.

2) Appleby-Frodingham Castellated Construction - illustrative brochure produced by the Company.

3) The Engineer. Vol 188 p. 352. September 23rd 1949.

4) Engineering. Vol. 168 p. 391. October 14th 1949.

5) Castellated Construction - handbook prepared by the United Steel Structural Co., Scunthorpe, Lincs.

6) Steelwork in Building. A commentary on B.S. 449 by W. Basil Scott. Spon 1952. p.94.

7) Tuzi - "The effect of a circular hole on the stress distribution in a beam under uniform bending moment". Phil. Mag. 1930. Vol.IX.

8) Gibson and Jenkins, "The stress distribution in a simply-supported beam with a circular hole". The Structural Engineer, Vol. XXXIV No. 12. December 1956.

9) Howland R.C.J. - "Biharmonic analysis in a perforated strip" Phil. Trans. Roy. Soc. A232. 1933. pp. 155-222.

10) Heller S.R. (Jnr.) - "The stresses around a small opening in a beam subjected to bending with shear". Proc. 1st U.S. National Congress of Applied Mechanics. p. 239.

11) Letitia Chitty - "On the cantilever composed of a number of parallel beams interconnected by cross-bars". Phil. Mag. XXXVIII pp. 685-699. October 1947.

12) A.J.S. Pippard - Studies in Elastic Structures. Arnold 1952. Chap[illegible] 8 - "Analysis of open-panel structures".

13) M. Smolira. Analysis of Structures. Concrete Publications Ltd., 1955. Example 51. pp. 119, 120.

14) Allen. Relaxation Methods. McGraw-Hill 1954. Chapter 4.

15) L.A. Beaufoy. "Vierendeel Truss Analysis using equivalent elastic systems". International Association for Bridge and Structural Engineering Vol. 11. 1951.

16) Salmon. Materials and Structures. Vol. II. Longmans 1948. Chapter. XV. para. 249.

17) A. Robertson, "The Strength of Struts". Selected Engineering paper No. 28. Institution of Civil Engineers 1925.

18) Hoff. The Analysis of Engineering Structures. Wiley 1956. chapter 3.

19) Bleich. Buckling Strength of Metal Structures. McGraw-Hill 1952. Chapter 2.

20) G. Cook. "Some factors affecting the yield point in mild steel". Institution of Engineers and Shipbuilders in Scotland. Paper 986. 1938.